Appendix of Chapter 2

Table of Figures

List of Tables

Table 4.1 Crystal Data, Collection, and Refinement Parameters for complexes 2.32-2.34.....9

Table 4.2 Crystal Data, Collection, and Refinement Parameters for complexes 2.35-2.37.....11

Table 4.3 Crystal Data, Collection, and Refinement Parameters for complexes 2.38-2.40.....13

Table 4.4 Crystal Data, Collection, and Refinement Parameters for complexes 2.41-2.43.....15

Table 4.5 Crystal Data, Collection, and Refinement Parameters for the ligands L2.3, L2.4 and L2.6 17

Table 4.6 Redox potentials for L2.3 and L2.4.....68

Table 4.7 Parameters used for EPR experiments.....77

4.1 X-ray diffraction studies

Table 4.1 Crystal Data, Collection, and Refinement Parameters for complexes **2.32**-**2.34**.

	2.32	**2.33**	**2.34**
Identification code	JK618	JK446	JK481
Empirical formula	$C_{23}H_{43}Br_2NNiP_2$	$C_{23}H_{45}Cl_2NNiOP_2$	$C_{30}H_{57}Br_2NNiOP_2$
Formula weight	614.05	543.15	728.23
Temperature	90(2) K	97(2) K	101(2) K
Wavelength	0.71073 Å	0.71073 Å	0.71073 Å
Crystal system	Monoclinic	Monoclinic	Trigonal
Space group	$P2_1/c$	$P2_1/c$	$P3_2$
Unit cell dimensions	a = 15.39442(19) Å; α = 90°.	a = 15.2072(2) Å; α = 90°	a = 14.24818(12) Å; α= 90°
	b = 15.59589(16) Å; β = 109.9727(13)°.	b = 15.46619(19) Å; β = 109.4377(18)°	b = 14.24818(12) Å; β = 90°
	c = 12.21507(14) Å; γ = 90°.	c = 12.0823(2) Å; γ = 90°	c = 14.79711(14) Å; γ = 120°.
Volume	2756.32(6) Å^3	2679.77(8) Å^3	2601.51(5) Å^3
Z	4	4	3
Density (calculated)	1.480 g cm^{-3}	1.346 g cm^{-3}	1.394 g cm^{-3}
Absorption coefficient	3.730 mm^{-1}	1.058 mm^{-1}	2.978 mm^{-1}
F(000)	1264	1160	1140
Crystal size	0.159 x 0.086 x 0.030 mm^3	0.096 x 0.079 x 0.053 mm^3	0.297 x 0.221 x 0.188 mm^3
Theta range for data collection	2.203 to 31.497°.	1.937 to 32.272°.	2.859 to 30.034°.
Index ranges	$-22 \le h \le 22$, $-22 \le k \le 22$, $-17 \le l \le 17$	$-22 \le h \le 22$, $-23 \le k \le 23$, $-17 \le l \le 17$	$-20 \le h \le 20$, $-20 \le k \le 20$, $-20 \le l \le 20$
Reflections collected	129018	100345	123185
Independent reflections	9098 [R(int) = 0.0422]	9069 [R(int) = 0.0524]	10128 [R(int) = 0.0669]
Observed Data [$I > 2\sigma(I)$]	7909	8266	9717

Table 4.1 continued

	2.32	**2.33**	**2.34**
R_σ	0.0188	0.0236	0.0267
Completeness to theta = 25.242°	99.8%	99.9%	99.9%
Max. and min. transmission	1.000 and 0.526	1.000 and 0.754	1.000 and 0.255
Data / restraints / parameters	9098 / 0 / 284	9069 / 0 / 302	10128 / 1 / 352
Goodness-of-fit on F^2	1.070	1.037	1.072
Final R indices [$I > 2\sigma(I)$]	$R1$ = 0.0374, $wR2$ = 0.1172	$R1$ = 0.0230, $wR2$ = 0.0567	$R1$ = 0.0222, $wR2$ = 0.0532
R indices (all data)	$R1$ = 0.0449, $wR2$ = 0.1214	$R1$ = 0.0271, $wR2$ = 0.0580	$R1$ = 0.0234, $wR2$ = 0.0534
Largest diff. peak and hole	2.183 and –1.613 e Å^{-3}	0.498 and –0.294 e Å^{-3}	1.068 and –0.605 e Å^{-3}

Table 4.2 Crystal Data, Collection, and Refinement Parameters for complexes **2.35**-**2.37**.

	2.35	**2.36**	**2.37**
Identification code	JK463	JK310	JK496
Empirical formula	$C_{27}H_{53}Cl_2NNiOP_2$	$C_{55}H_{55}BBrF_{24}NNiP_2$	$C_{55}H_{55}BClF_{24}NNiP_2$
Formula weight	599.25	1397.37	1352.91
Temperature	97(2) K	93(2) K	99(2) K
Wavelength	0.71073 Å	0.71073 Å	0.71073 Å
Crystal system	Monoclinic	Triclinic	Triclinic
Space group	$P2_1/c$	$P\bar{1}$	$P\bar{1}$
Unit cell dimensions	a = 8.31376(14) Å; α= 90°	a = 12.42798(10) Å; α = 86.7116(6)°	a = 12.40576(9) Å; α = 83.7749(7)°
	b = 33.1097(4) Å; β = 103.4530(15)°	b = 18.64849(15) Å; β = 83.4611(6)°	b = 18.53954(15) Å; β = 85.8779(7)°
	c = 11.36574(16) Å; γ = 90°	c = 26.1742(2) Å; γ = 83.6005(6)°	c = 26.0628(2) Å; γ = 85.9039(6)°
Volume	3042.75(8) Å^3	5983.07(8) Å^3	5931.35(8) Å^3
Z	4	4	4
Density (calculated)	1.308 g cm^{-3}	1.551 g cm^{-3}	1.515 g cm^{-3}
Absorption coefficient	0.939 mm^{-1}	1.158 mm^{-1}	0.539 mm^{-1}
F(000)	1288	2824	2752
Crystal size	0.304 x 0.041 x 0.026 mm^3	0.290 x 0.246 x 0.225 mm^3	0.209 x 0.086 x 0.068 mm^3
Theta range for data collection	2.215 to 31.600°.	2.085 to 30.500°.	1.927 to 31.000°.
Index ranges	$-12 \le h \le 12$, $-48 \le k \le 48$, $-16 \le l \le 16$	$-17 \le h \le 17$, $-26 \le k \le 26$, $-37 \le l \le 37$	$-17 \le h \le 17$, $-26 \le k \le 26$, $-37 \le l \le 37$
Reflections collected	187469	342794	210366
Independent reflections	10167 [R(int) = 0.0719]	36487 [R(int) = 0.0418]	37063 [R(int) = 0.0424]
Observed Data [$I > 2\sigma(I)$]	9232	30694	30882
R_σ	0.0251	0.0232	0.0286

Table 4.2 Continued

	2.35	**2.36**	**2.37**
Completeness to theta = 25.242°	99.9%	99.9%	99.9%
Max. and min. transmission	1.000 and 0.601	1.000 and 0.321	1.000 and 0.577
Data / restraints / parameters	10167 / 2 / 331	36487 / 312 / 1661	37063 / 228 / 1639
Goodness-of-fit on F^2	1.055	1.015	1.030
Final R indices [$I > 2\sigma(I)$]	$R1$ = 0.0262, $wR2$ = 0.0594	$R1$ = 0.0362, $wR2$ = 0.0865	$R1$ = 0.0374, $wR2$ = 0.0966
R indices (all data)	$R1$ = 0.0307, $wR2$ = 0.0607	$R1$ = 0.0472, $wR2$ = 0.0911	$R1$ = 0.0477, $wR2$ = 0.1018
Largest diff. peak and hole	0.460 and –0.305 e Å^{-3}	1.109 and –0.718 e Å^{-3}	0.789 and –0.676 e Å^{-3}

Table 4.3 Crystal Data, Collection, and Refinement Parameters for complexes **2.38**-**2.40**.

	2.38	**2.39**	**2.40**
Identification code	JK616	JK489	JK216
Empirical formula	$C_{59}H_{63}BBrF_{24}NNiP_2$	$C_{59}H_{63}BClF_{24}NNiP_2$	$C_{23}H_{43}BrNNiP_2$
Formula weight	1453.47	1409.01	534.14
Temperature	93(2) K	100(2) K	99(2) K
Wavelength	0.71073 Å	0.71073 Å	0.71073 Å
Crystal system	Monoclinic	Monoclinic	Monoclinic
Space group	$P2_1/c$	$P2_1/c$	$I2/a$
Unit cell dimensions	a = 17.1037(2) Å; α = 90°	a = 17.17068(18) Å; α = 90°.	a = 27.7696(5) Å; α = 90°
	b = 19.09461(19) Å; β = 104.5530(11)°	b = 19.09340(17) Å; β = 104.4857(10)°	b = 8.95195(18) Å; β = 103.394(2)°
	c = 19.96721(19); γ = 90°	c = 19.78604(19) Å; γ = 90°	c = 21.5241(4) Å; γ = 90°
Volume	6311.83(12) Å^3	6280.57(11) Å^3	5205.18(19) Å^3
Z	4	4	8
Density (calculated)	1.530 g cm^{-3}	1.490 g cm^{-3}	1.363 g cm^{-3}
Absorption coefficient	1.101 mm^{-1}	0.513 mm^{-1}	2.413 mm^{-1}
F(000)	2952	2880	2248
Crystal size	0.271 x 0.159 x 0.099 mm^3	0.181 x 0.109 x 0.063 mm^3	0.193 x 0.078 x 0.073 mm^3
Theta range for data collection	2.101 to 33.000°.	2.126 to 31.500°.	2.397 to 30.187°.
Index ranges	$-26 \le h \le 26$, $-29 \le k \le 29$, $-30 \le l \le 30$	$-25 \le h \le 25$, $-28 \le k \le 28$, $-29 \le l \le 29$	$-38 \le h \le 38$, $-12 \le k \le 12$, $-30 \le l \le 30$
Reflections collected	366034	220963	76423
Independent reflections	23787 [R(int) = 0.0539]	20686 [R(int) = 0.0328]	7164 [R(int) = 0.0538]
Observed Data [$I > 2\sigma(I)$]	18951	17779	6320
R_σ	0.0241	0.0175	0.0267

Table 4.3 Continued

	2.38	**2.39**	**2.40**
Completeness to theta = 25.242°	100 %	99.9%	99.9%
Max. and min. transmission	1.000 and 0.292	1.000 and 0.657	1.000 and 0.644
Data / restraints / parameters	23787 / 1100 / 1095	20686 / 300 / 930	7164 / 0 / 265
Goodness-of-fit on F^2	1.031	1.042	1.028
Final R indices [$I > 2\sigma(I)$]	$R1$ = 0.0379, $wR2$ = 0.0949	$R1$ = 0.0356, $wR2$ = 0.0930	$R1$ = 0.0229, $wR2$ = 0.0548
R indices (all data)	$R1$ = 0.0547, $wR2$ = 0.1037	$R1$ = 0.0435, $wR2$ = 0.0975	$R1$ = 0.0293, $wR2$ = 0.0565
Largest diff. peak and hole	0.966 and –0.588 e Å^{-3}	0.929 and –0.469 e Å^{-3}	0.524 and –0.449 e Å^{-3}

Table 4.4 Crystal Data, Collection, and Refinement Parameters for complexes **2.41**-**2.43**.

	2.41	**2.42**	**2.43**
Identification code	JK438	JK323	JK476
Empirical formula	$C_{23}H_{43}ClNNiP_2$	$C_{30}H_{57}BrNNiOP_2$	$C_{30}H_{57}ClNNiOP_2$
Formula weight	489.68	648.32	603.86
Temperature	93(2) K	101(2) K	101(2) K
Wavelength	0.71073 Å	0.71073 Å	0.71073 Å
Crystal system	Monoclinic	Monoclinic	Monoclinic
Space group	*I*2/*a*	$P2_1/c$	$P2_1/c$
Unit cell dimensions	a = 21.5192(3) Å; α = 90°	a = 16.6715(2) Å; α = 90°	a = 16.6701(2) Å; α = 90°
	b = 8.78006(12) Å; β = 102.8956(12)°	b = 11.17710(10) Å; β = 105.136(2)°	b = 11.18478(12) Å; β = 105.0860(12)°
	c = 27.8483(3) Å; γ = 90°	c = 17.9789(3) Å; γ = 90°	c = 17.7347(2) Å; γ = 90°
Volume	5128.95(11) Å^3	3233.95(8) Å^3	3192.70(7) Å^3
Z	8	4	4
Density (calculated)	1.268 g cm^{-3}	1.332 g cm^{-3}	1.256 g cm^{-3}
Absorption coefficient	0.995 mm^{-1}	1.957 mm^{-1}	0.814 mm^{-1}
F(000)	2104	1380	1308
Crystal size	0.114 x 0.077 x 0.052 mm^3	0.281 x 0.210 x 0.172 mm^3	0.165 x 0.127 x 0.075 mm^3
Theta range for data collection	1.942 to 30.988°.	2.167 to 30.996°.	2.668 to 31.499°.
Index ranges	$-30 \le h \le 30$, $-12 \le k \le 12$, $-39 \le l \le 39$	$-24 \le h \le 24$, $-16 \le k \le 16$, $-25 \le l \le 26$	$-24 \le h \le 24$, $-16 \le k \le 16$, $-25 \le l \le 26$
Reflections collected	70541	98945	154040
Independent reflections	7598 [R(int) = 0.0367]	10259 [R(int) = 0.0442]	10562 [R(int) = 0.0437]
Observed Data [$I > 2\sigma(I)$]	6901	9292	9646
R_σ	0.0183	0.0239	0.0177
Completeness to theta = 25.242°	99.9%	99.9%	99.9%

Table 4.4 Continued

	2.41	**2.42**	**2.43**
Max. and min. transmission	1.000 and 0.588	1.000 and 0.310	1.000 and 0.814
Data / restraints / parameters	7598 / 0 / 265	10259 / 0 / 343	10562 / 0 / 343
Goodness-of-fit on F^2	1.066	1.054	1.049
Final R indices [$I > 2\sigma(I)$]	$R1$ = 0.0243, $wR2$ = 0.0602	$R1$ = 0.0243, $wR2$ = 0.0527	$R1$ = 0.0245, $wR2$ = 0.0594
R indices (all data)	$R1$ = 0.0285, $wR2$ = 0.0617	$R1$ = 0.0297, $wR2$ = 0.0541	$R1$ = 0.0283, $wR2$ = 0.0606
Largest diff. peak and hole	0.595 and –0.276 e Å^{-3}	0.476 and –0.310 e Å^{-3}	0.447 and –0.202 e Å^{-3}

Table 4.5 Crystal Data, Collection, and Refinement Parameters for the ligands **L2.3**, **L2.4** and **L2.6**

	L2.3	**L2.4**	**L2.6**
Identification code	JK298	JK296a	JK530
Empirical formula	C_{23} H_{49} B_2 N P_2	C_{27} H_{57} B_2 N P_2	C_{27} H_{51} N P_2
Formula weight	423.19	479.29	451.62
Temperature	93(2) K	93(2) K	93(2) K
Wavelength	0.71073 Å	0.71073 Å	0.71073 Å
Crystal system	Orthorhombic	Monoclinic	Monoclinic
Space group	*Pbca*	$P2_1/c$	$P2_1/c$
Unit cell dimensions	a = 15.1462(3) Å; α = 90°	a = 13.40579(16) Å; α = 90°	a = 8.56285(13) Å; α = 90°
	b = 13.8773(3) Å; β = 90°	b = 13.31814(15) Å; β = 96.0754(11)°	b = 15.3315(2) Å; β = 90.2867(14)°
	c = 25.2869(4) Å; γ = 90°	c = 16.8815(2) Å; γ = 90°	c = 21.0878(3) Å; γ = 90°
Volume	5314.99(16) Å^3	2997.10(6) Å^3	2768.40(7) Å^3
Z	8	4	4
Density (calculated)	1.058 g cm^{-3}	1.062 g cm^{-3}	1.084 g cm^{-3}
Absorption coefficient	0.173 mm^{-1}	0.160 mm^{-1}	0.171 mm^{-1}
F(000)	1872	1064	1000
Crystal size	0.435 x 0.078 x 0.066 mm^3	0.268 x 0.154 x 0.116 mm^3	0.352 x 0.207 x 0.144 mm^3
Theta range for data collection	2.098 to 31.399°.	1.952 to 32.191°.	1.931 to 32.344°.
Index ranges	$-22 \le h \le 22$, $-19 \le k \le 20$, $-37 \le l \le 37$	$-19 \le h \le 19$, $-19 \le k \le 19$, $-24 \le l \le 24$	$-12 \le h \le 12$, $-22 \le k \le 23$, $-31 \le l \le 31$
Reflections collected	183000	93557	81891
Independent reflections	8727 [R(int) = 0.0823]	10091 [R(int) = 0.0361]	9281 [R(int) = 0.0329]
Observed Data [$I > 2\sigma(I)$]	7801	8837	8320
R_σ	0.0279	0.0209	0.0194

Table 4.5 Continued

	L2.3	**L2.4**	**L2.6**
Completeness to theta = 25.242°	100%	99.9%	100%
Max. and min. transmission	1.000 and 0.601	1.000 and 0.403	1.000 and 0.375
Data / restraints / parameters	8727 / 0 / 289	10091 / 0 / 329	9281 / 0 / 287
Goodness-of-fit on F^2	1.049	1.040	1.038
Final R indices [$I > 2\sigma(I)$]	$R1$ = 0.0332, $wR2$ = 0.0832	$R1$ = 0.0304, $wR2$ = 0.0835	$R1$ = 0.0297, $wR2$ = 0.0791
R indices (all data)	$R1$ = 0.0393, $wR2$ = 0.0859	$R1$ = 0.0363, $wR2$ = 0.0864	$R1$ = 0.0343, $wR2$ = 0.0812
Largest diff. peak and hole	0.435 and –0.237 e Å^{-3}	0.434 and –0.247 e Å^{-3}	0.491 and –0.227 e Å^{-3}

4.2 NMR spectra

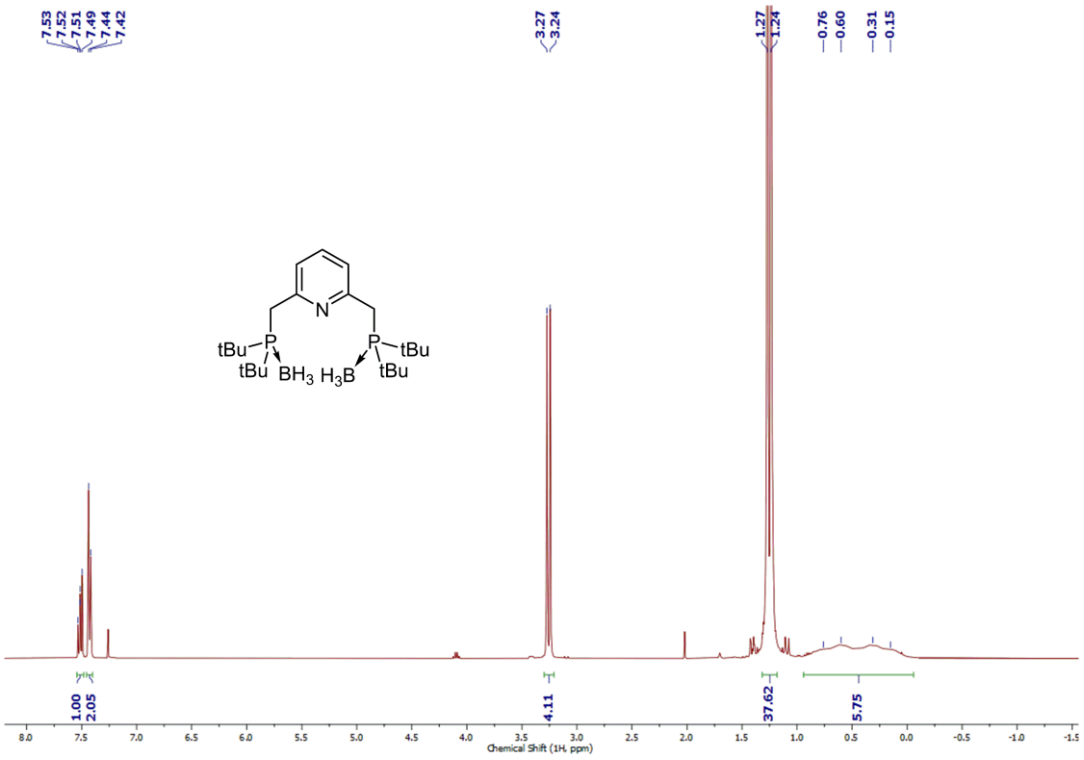

Figure 4.1 ^{1}H NMR spectrum of **L2.2** (400 MHz, $CDCl_3$).

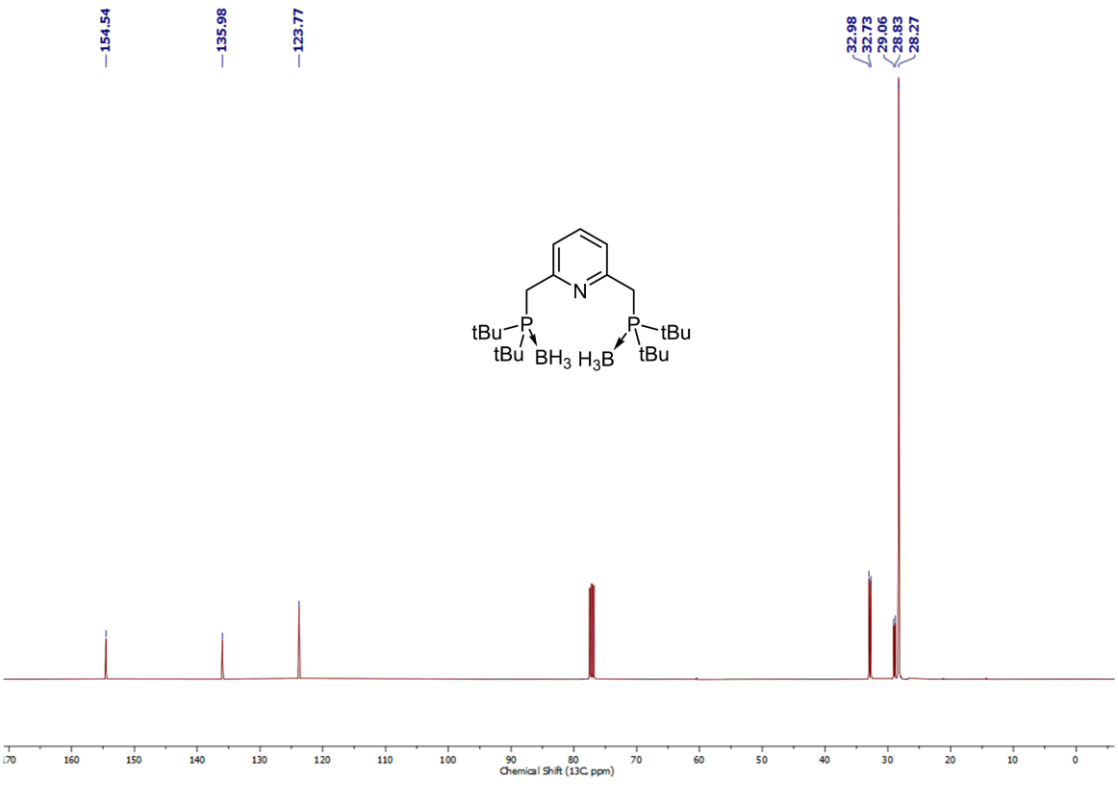

Figure 4.2 $^{13}C\{^{1}H\}$ NMR spectrum of **L2.2** (101 MHz, $CDCl_3$).

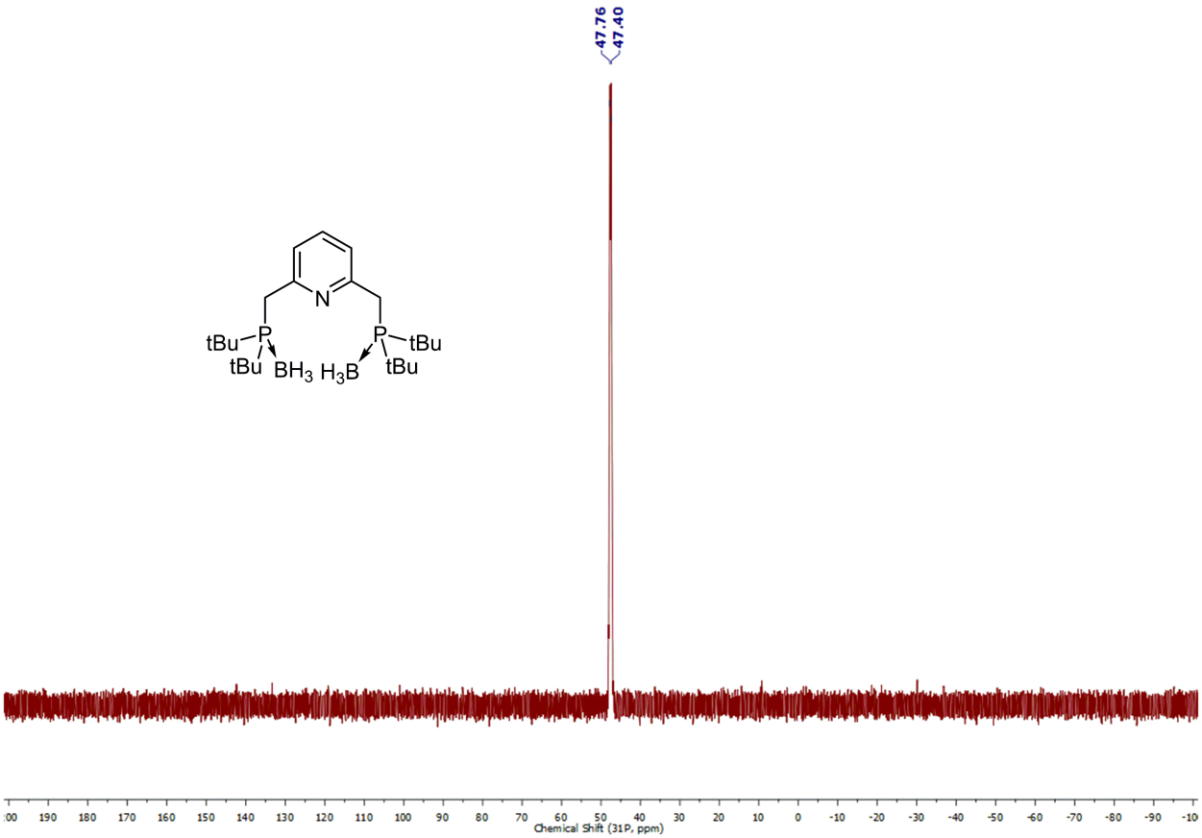

Figure 4.3 $^{31}P\{^{1}H\}$ NMR spectrum of **L2.2** (162 MHz, $CDCl_3$)

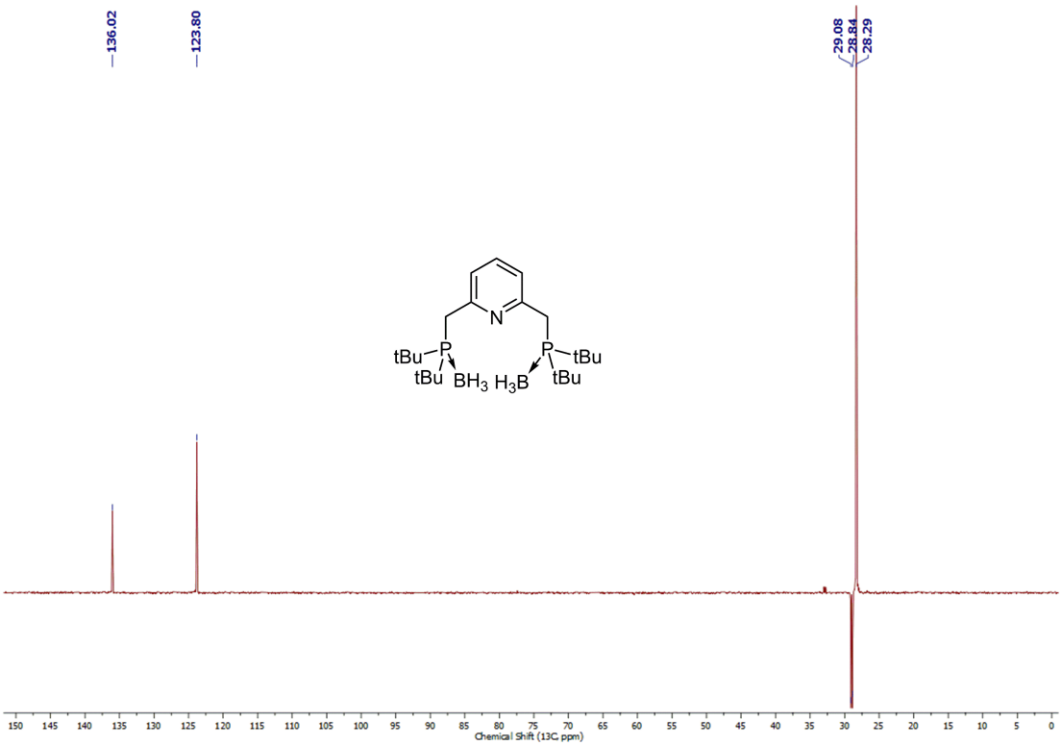

Figure 4.4 DEPT-135 NMR spectrum of **L2.2** (101 MHz, $CDCl_3$)

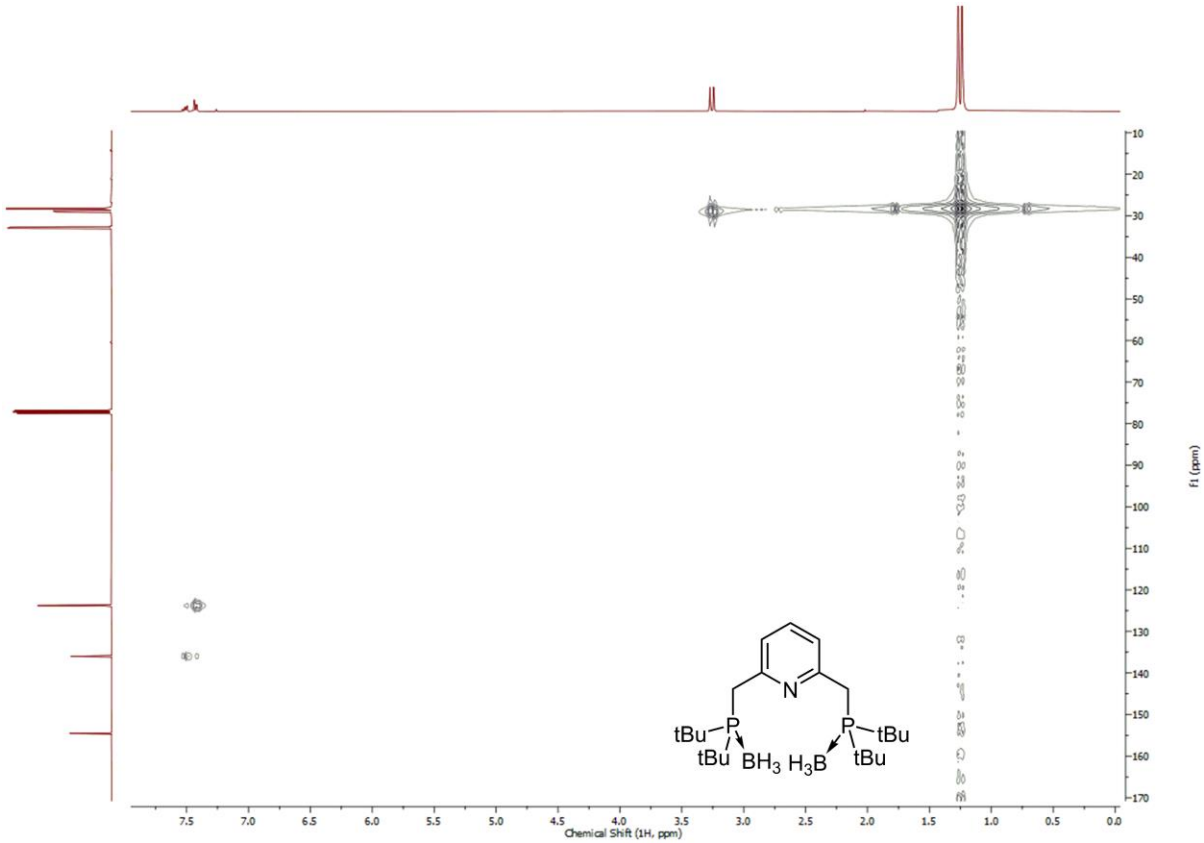

Figure 4.5 HMQC NMR spectra of **L2.2** ($CDCl_3$)

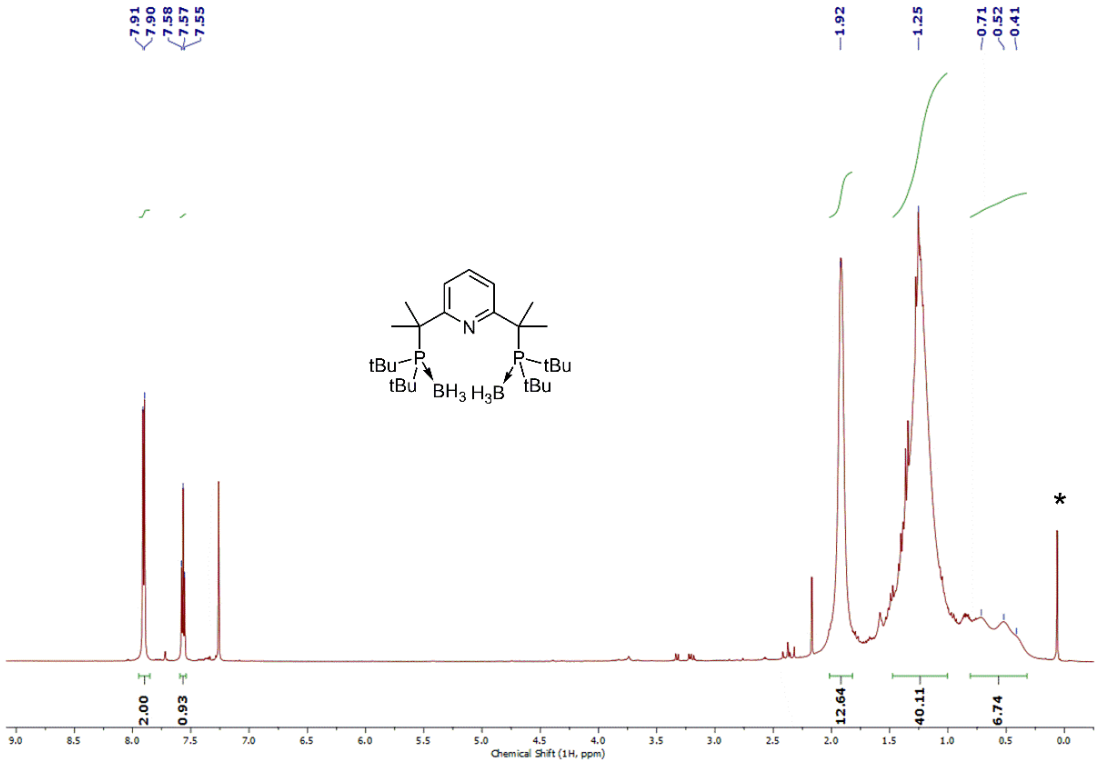

Figure 4.6 ^1H NMR spectrum of **L2.4** (600 MHz, $CDCl_3$).* Traces of silicon grease

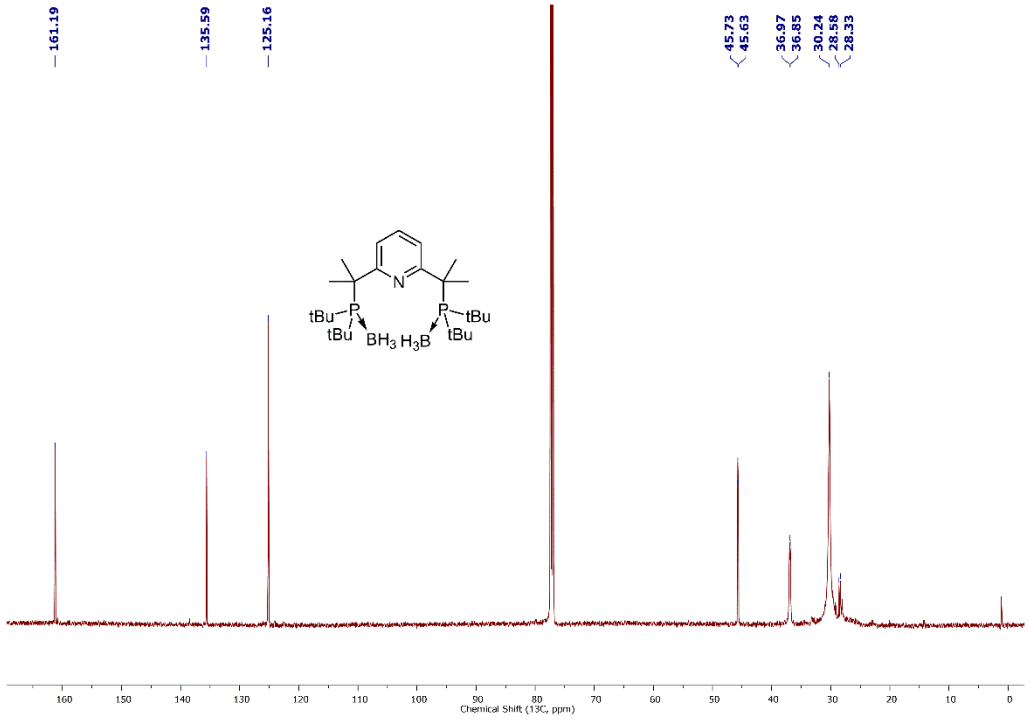

Figure 4.7 $^{13}C\{^{1}H\}$ NMR spectrum of **L2.4** (151 MHz, $CDCl_3$).

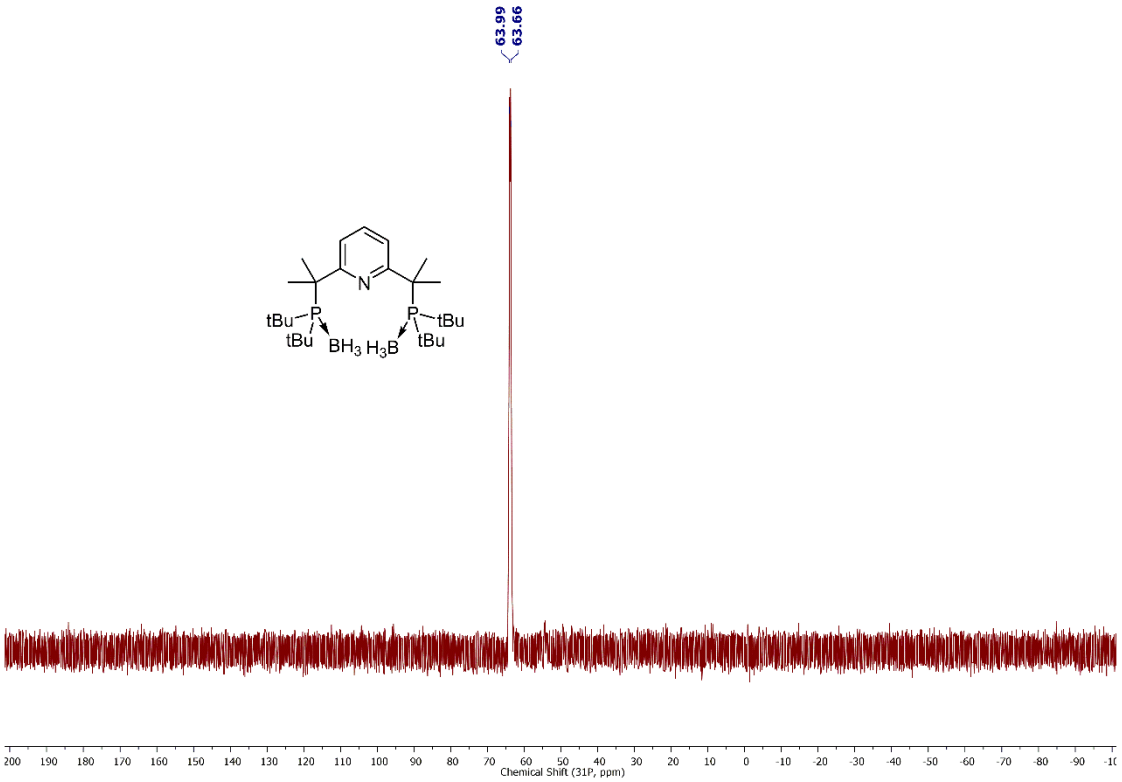

Figure 4.8 $^{31}P\{^{1}H\}$ NMR spectrum of **L2.4** (243 MHz, $CDCl_3$).

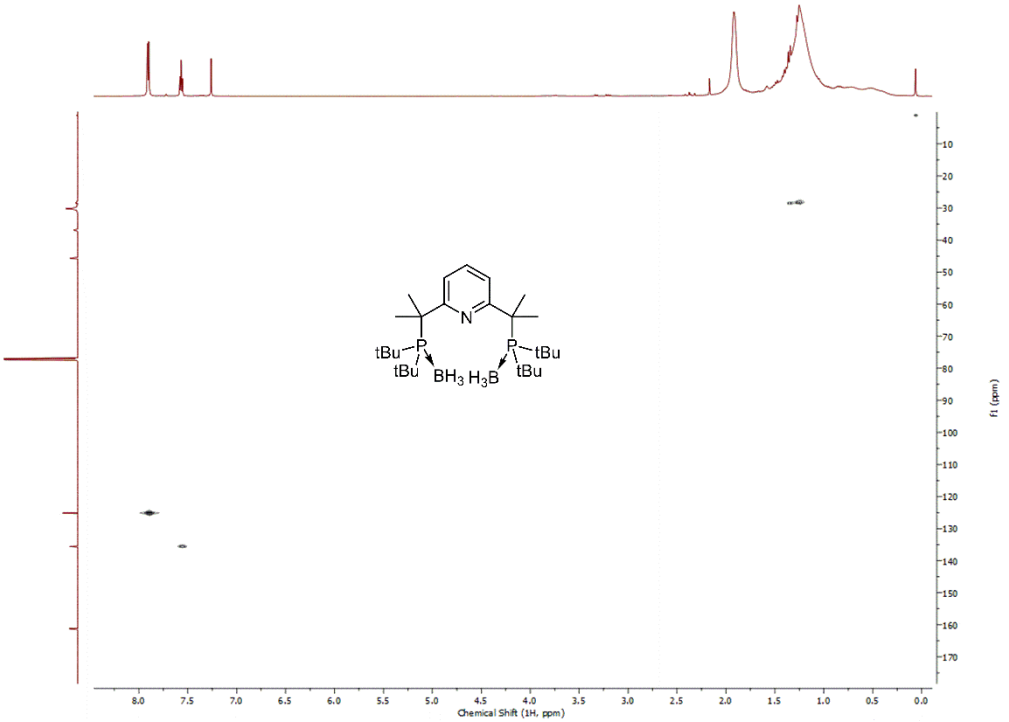

Figure 4.9 ^{1}H-^{13}C HMQC NMR spectrum of **L2.4** ($CDCl_3$).

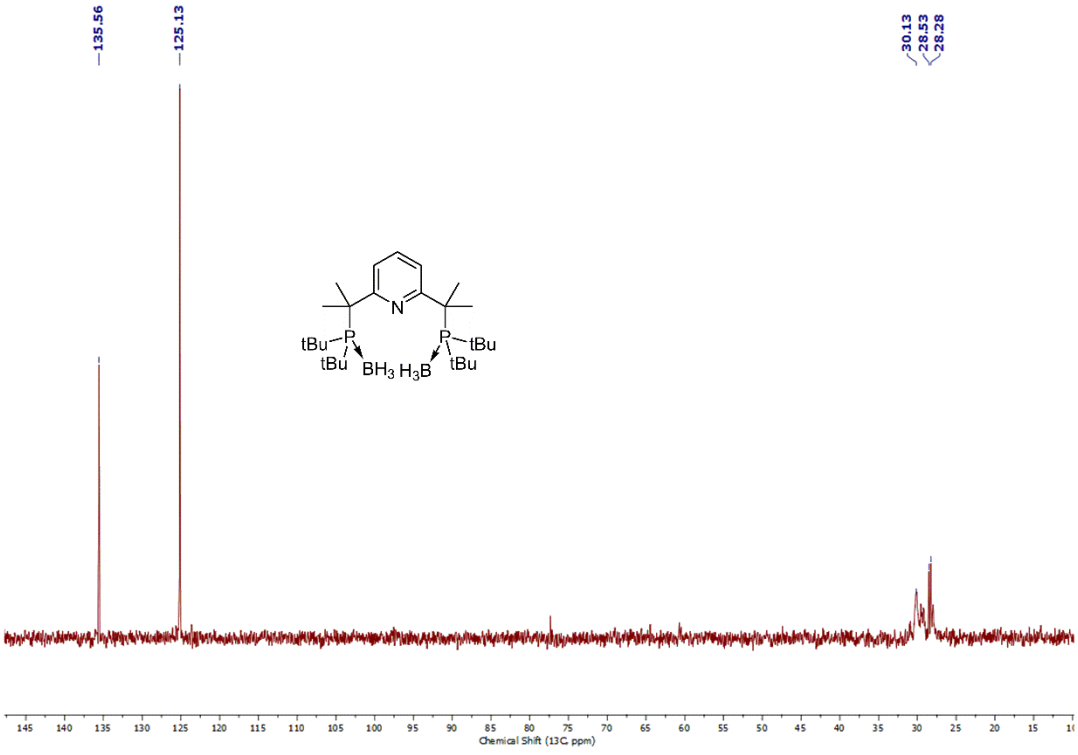

Figure 4.10 DEPT-135 NMR spectrum of **L2.4** (151 MHz, $CDCl_3$).

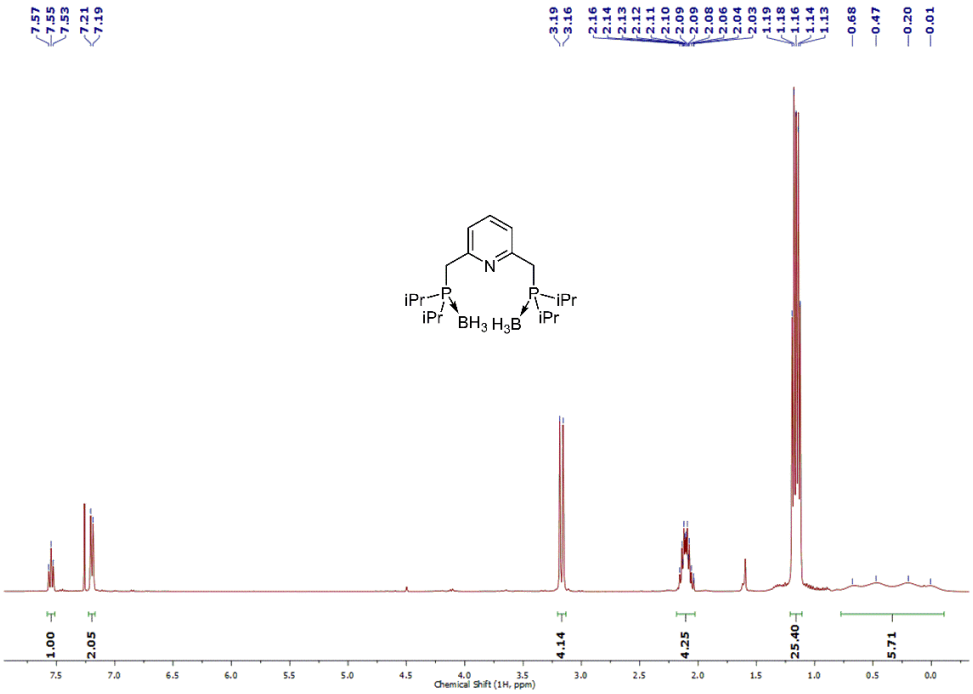

Figure 4.11 ^{1}H NMR spectrum of **L2.1** (400 MHz, $CDCl_3$).

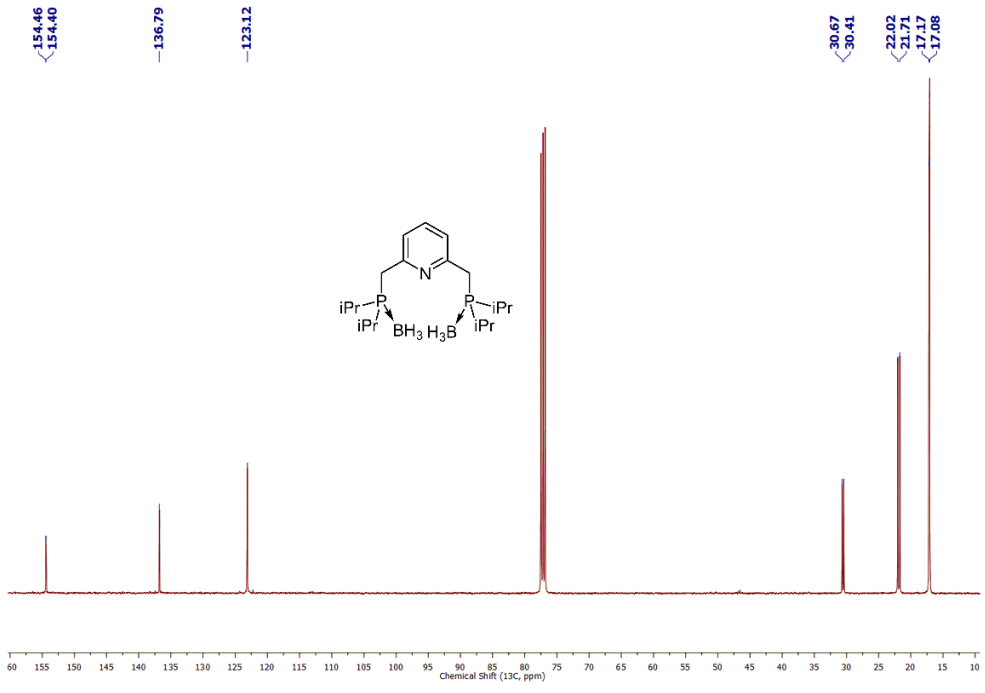

Figure 4.12 $^{13}C\{^{1}H\}$ NMR spectrum of **L2.1** (101 MHz, $CDCl_3$).

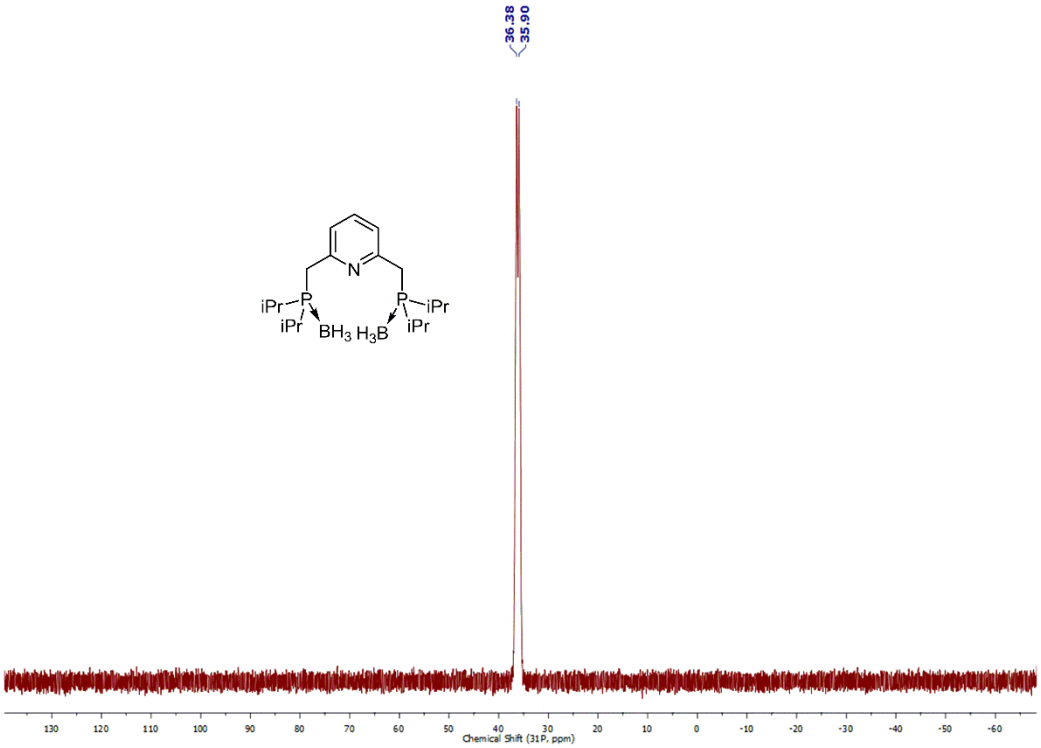

Figure 4.13 $^{31}P\{^{1}H\}$ NMR spectrum of L2.1 (162 MHz, $CDCl_3$).

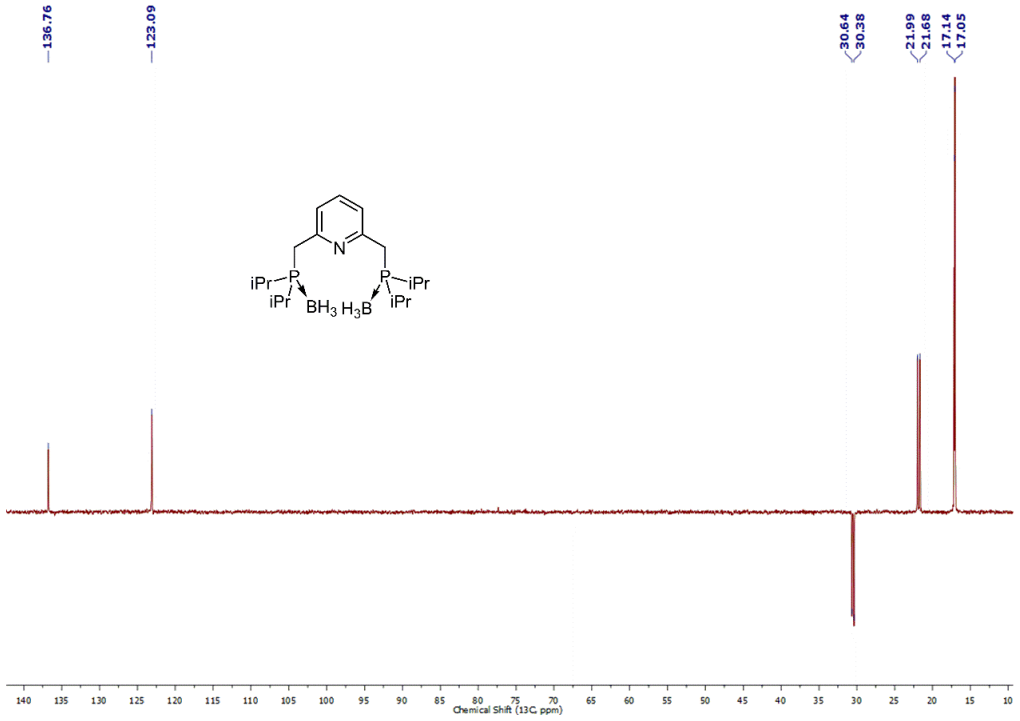

Figure 4.14 DEPT-135 NMR spectrum of **L2.1** (101 MHz, $CDCl_3$).

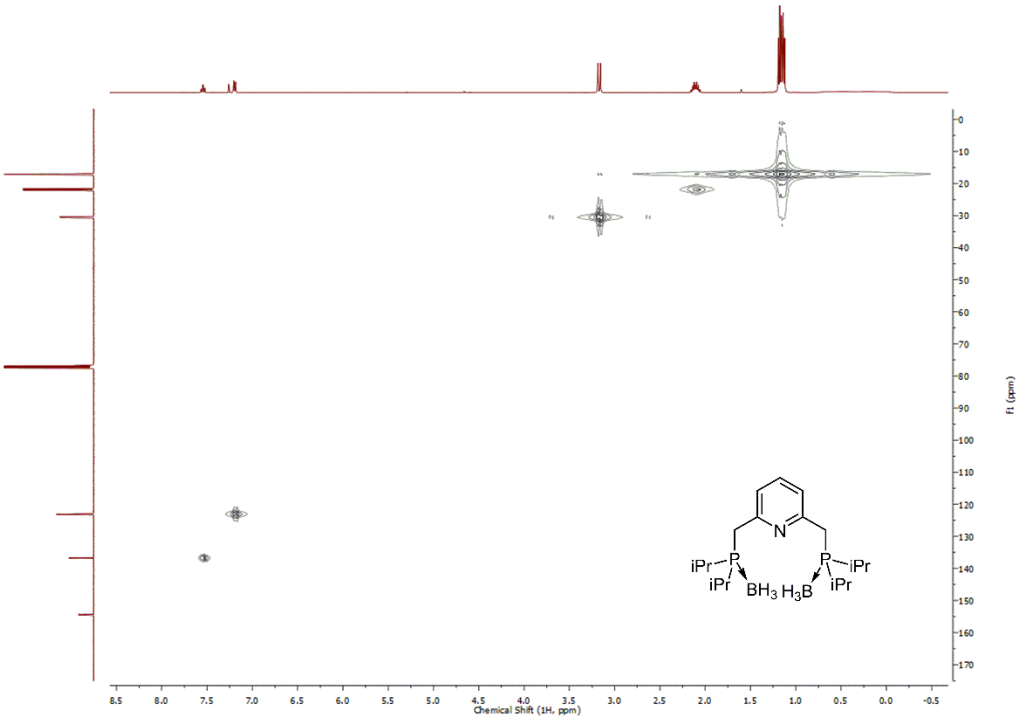

Figure 4.15 ^{1}H-^{13}C HMQC NMR spectrum of **L2.1** ($CDCl_3$).

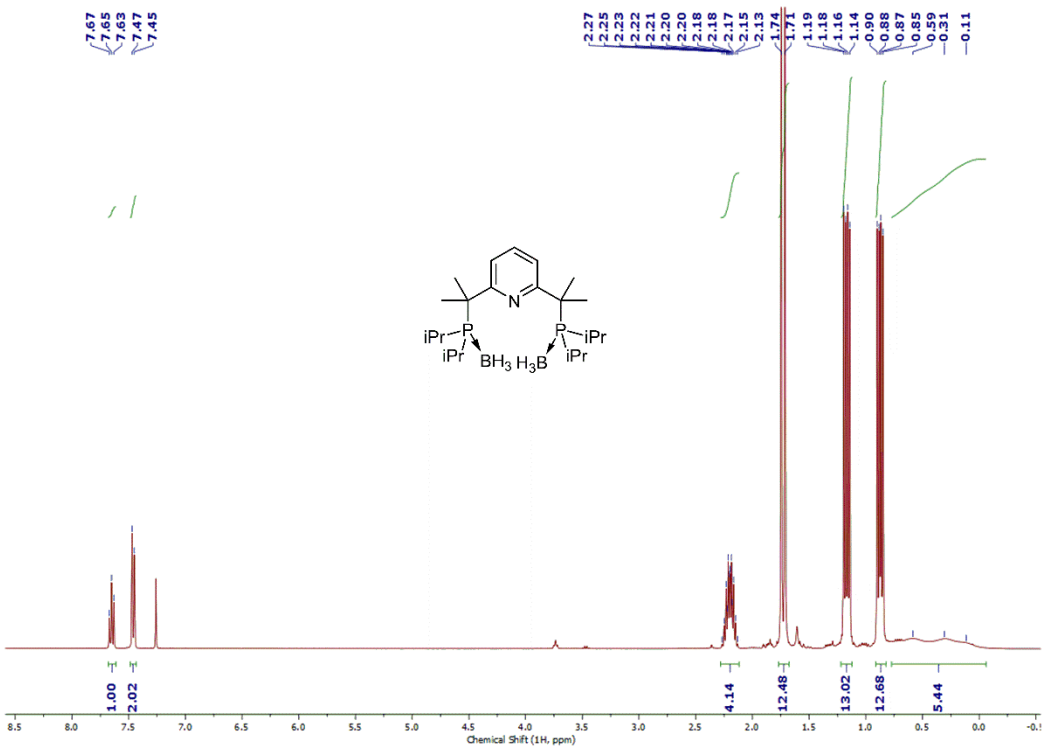

Figure 4.16 ^{1}H NMR spectrum of **L2.3** (400 MHz, $CDCl_3$).

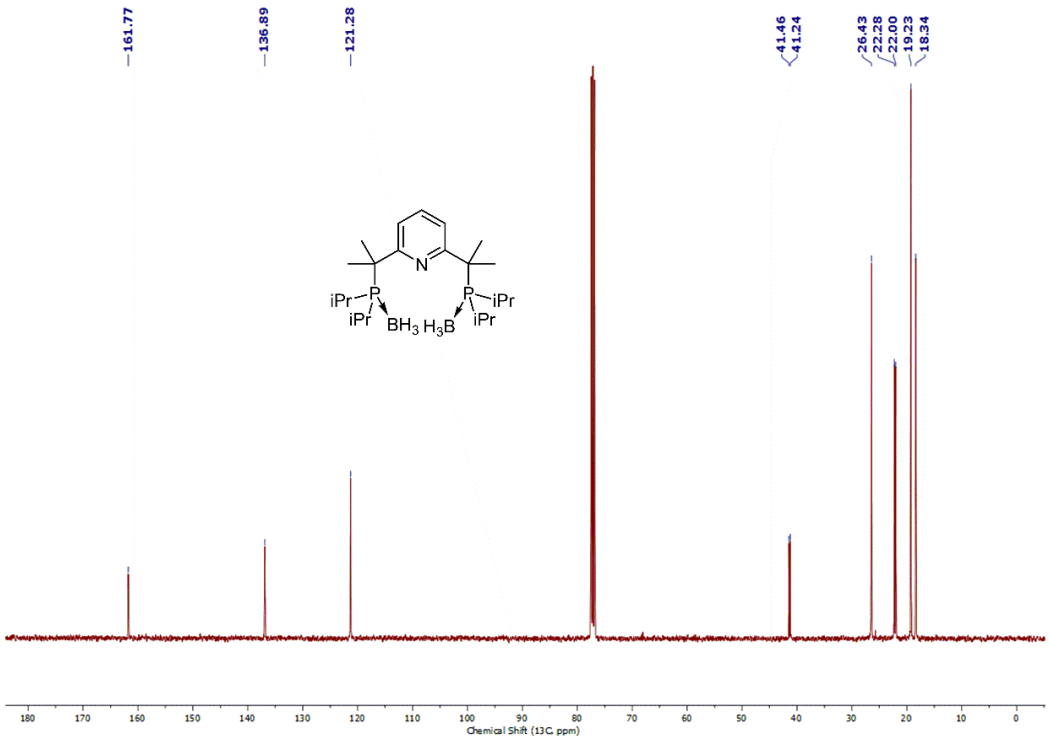

Figure 4.17 $^{13}C\{^{1}H\}$ NMR spectrum of **L2.3** (101 MHz, $CDCl_3$).

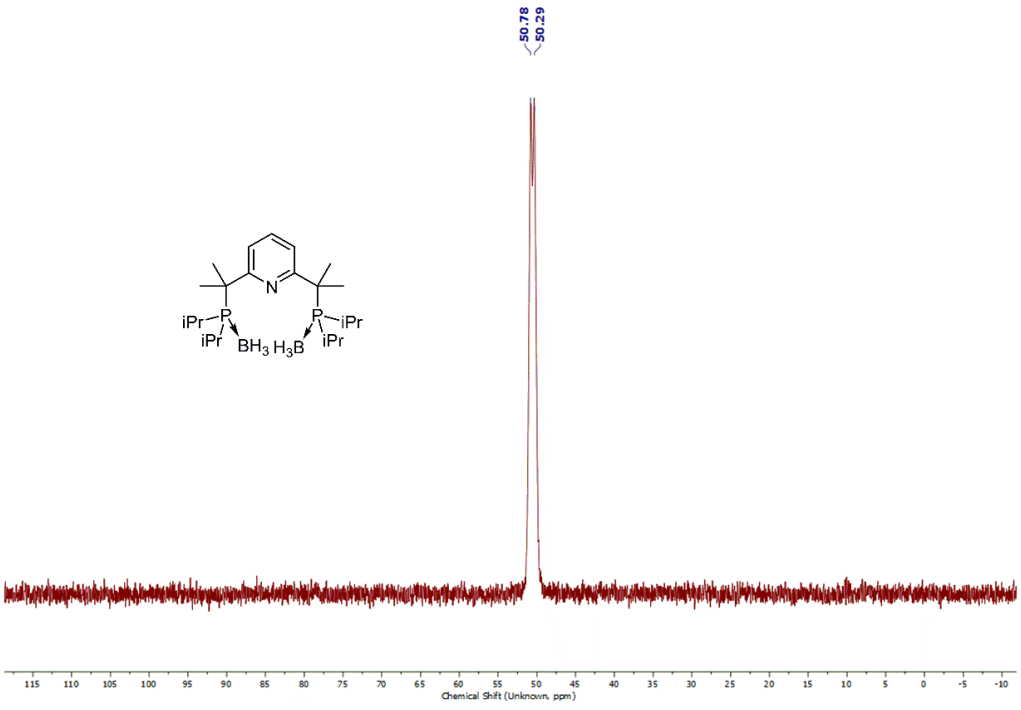

Figure 4.18 $^{31}P\{^{1}H\}$ NMR spectrum of **L2.3** (162 MHz, $CDCl_3$).

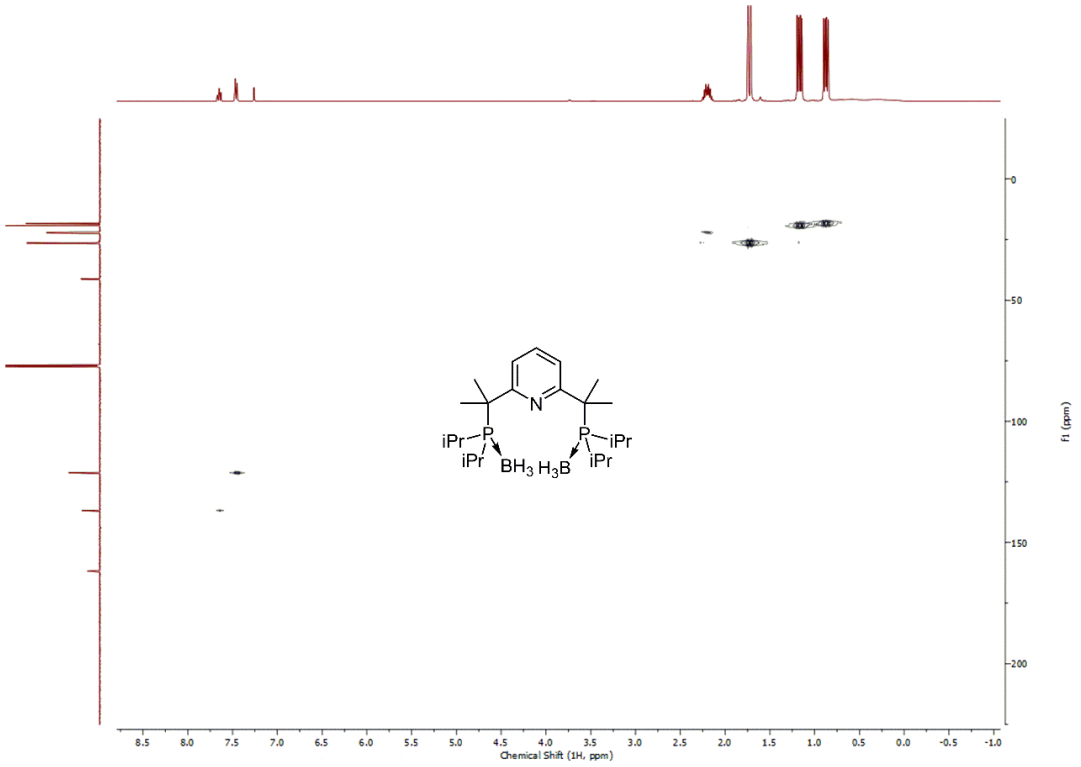

Figure 4.19 ^{1}H-^{13}C HMQC NMR spectrum of **L2.3** ($CDCl_3$).

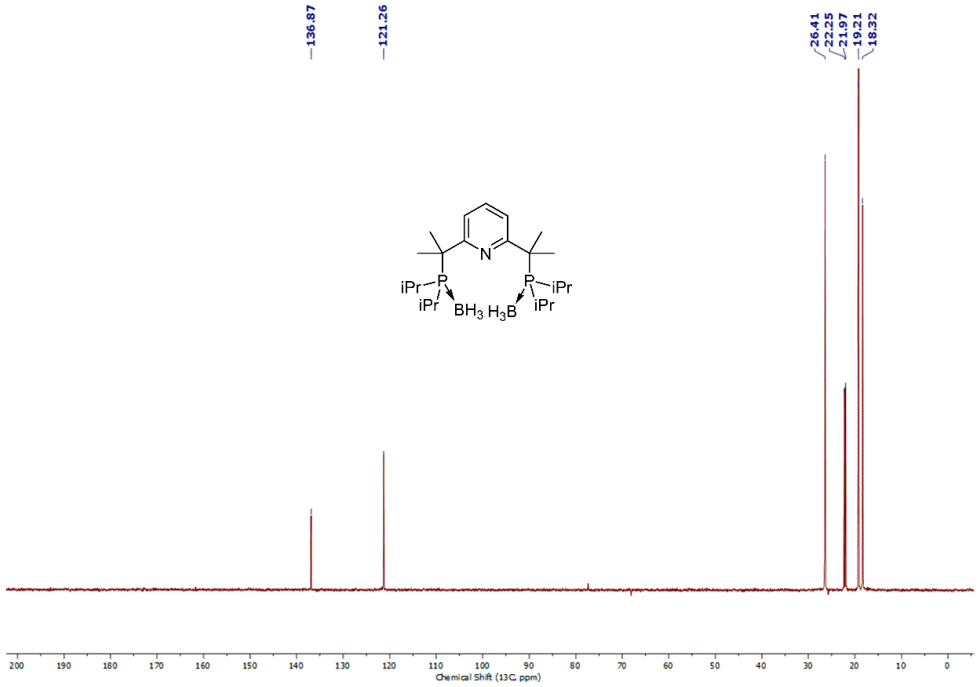

Figure 4.20 DEPT-135 NMR spectrum of **L2.3** (101 MHz, $CDCl_3$).

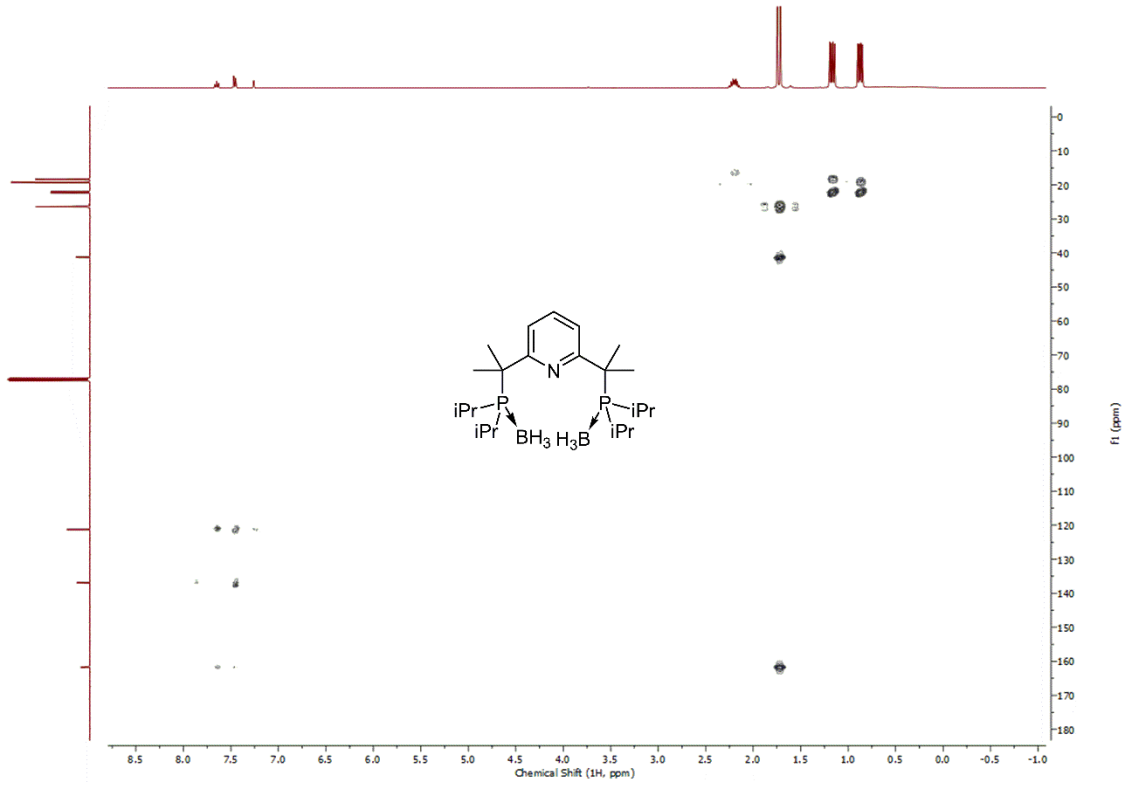

Figure 4.21 ^{1}H-^{13}C HMBC NMR spectrum of L2.3 ($CDCl_3$).

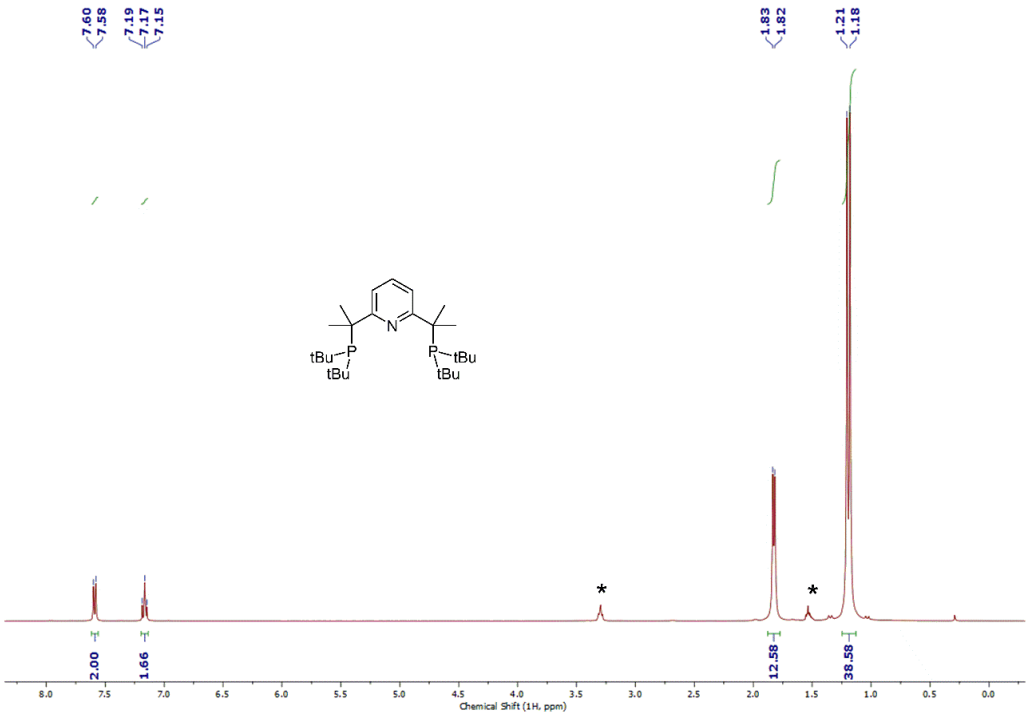

Figure 4.22 ^{1}H NMR spectrum of **L2.6** (400 MHz, C_6D_6). C_6D_6 peak overlaps with a peak at 7.17 ppm. Peaks marked with an asterisk is from residue of pyrrolidine-BH_3 adduct.

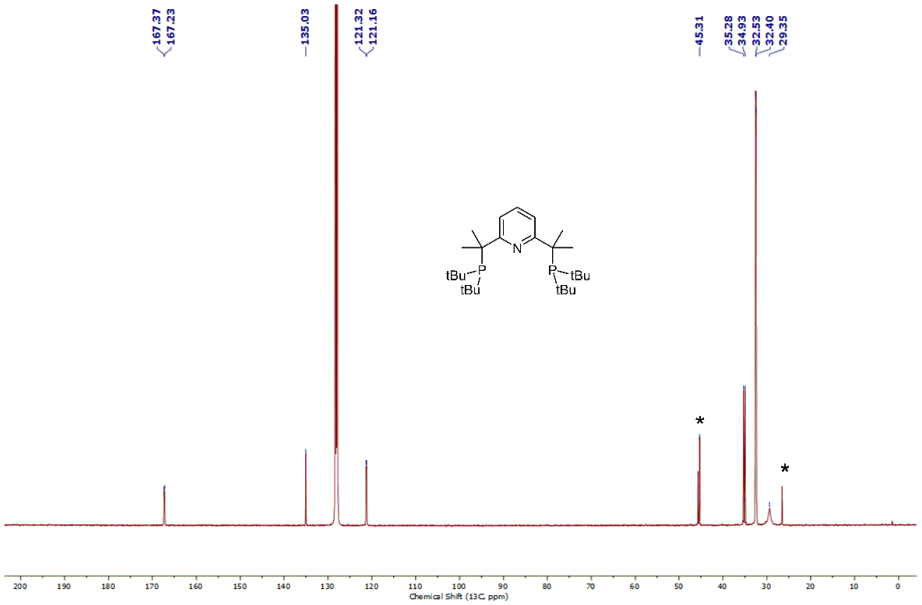

Figure 4.23 $^{13}C\{^{1}H\}$ NMR spectrum of **L2.6** (101 MHz, C_6D_6).

Peaks marked with an asterisk are from residue of pyrrolidine-BH_3 adduct

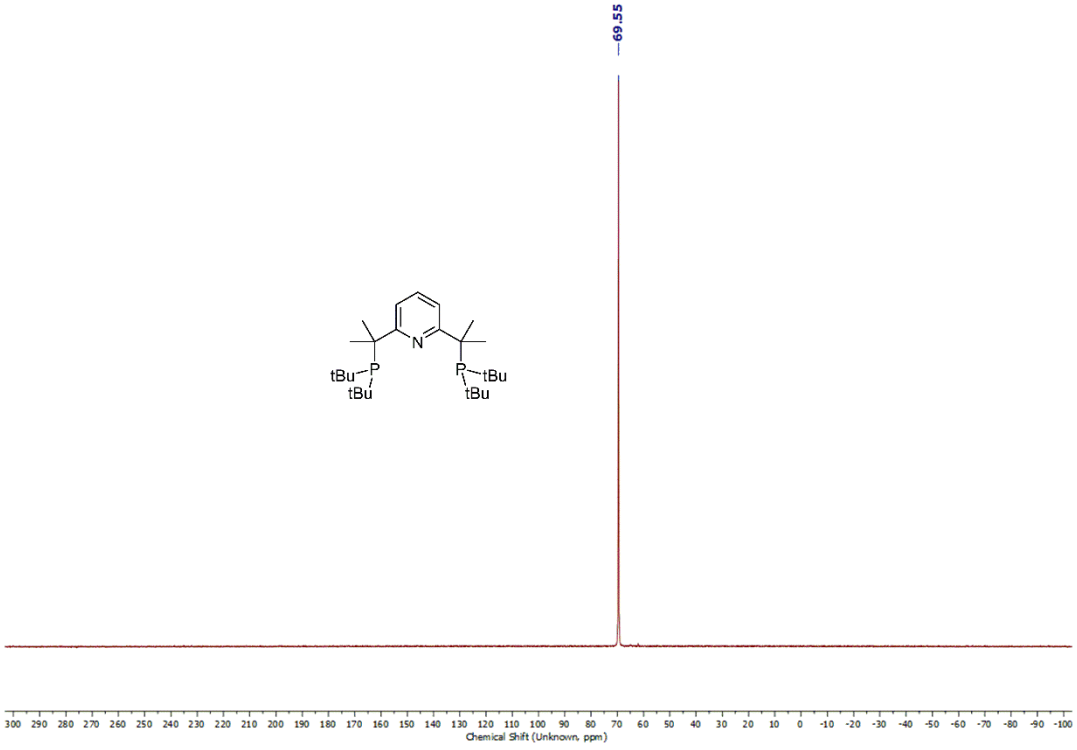

Figure 4.24 $^{31}P\{^{1}H\}$ NMR spectrum of **L2.6** (162 MHz, C_6D_6).

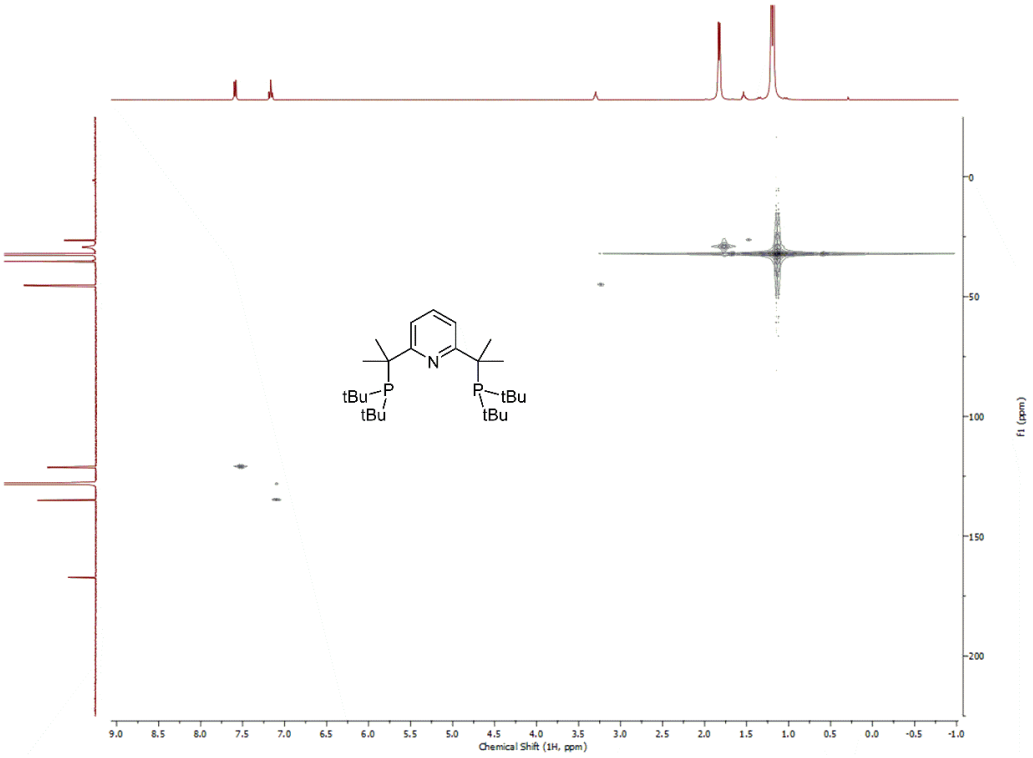

Figure 4.25 ^{1}H-^{13}C HMQC NMR spectrum of L2.6 (C_6D_6).

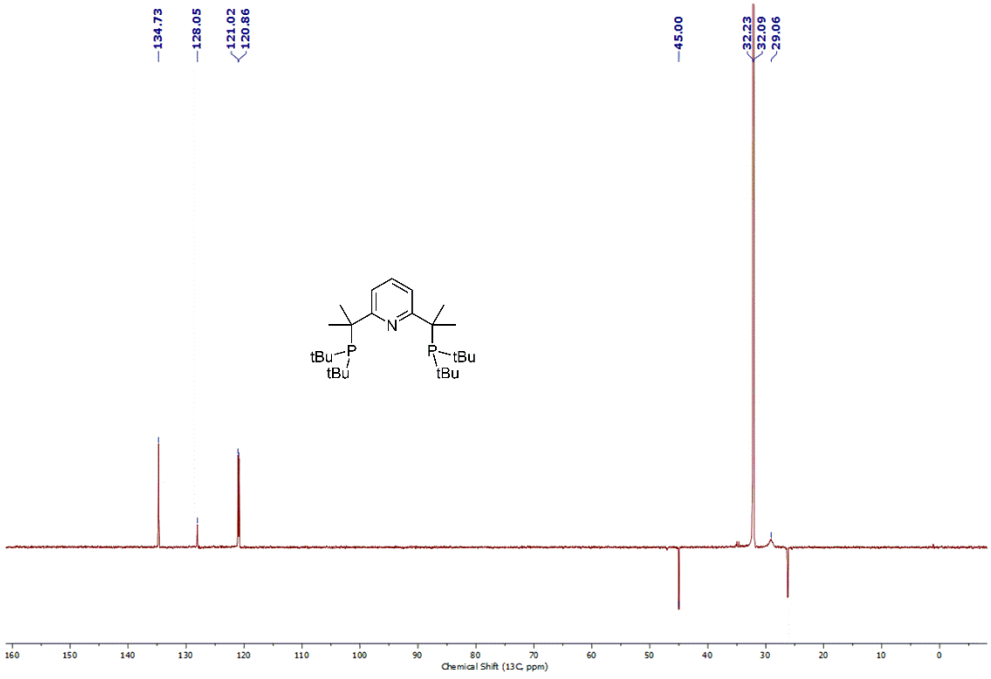

Figure 4.26 DEPT-135 NMR spectrum of **L2.6** (101 MHz, C_6D_6). Peaks marked with an asterisk are from residue of pyrrolidine-BH_3 adduct.

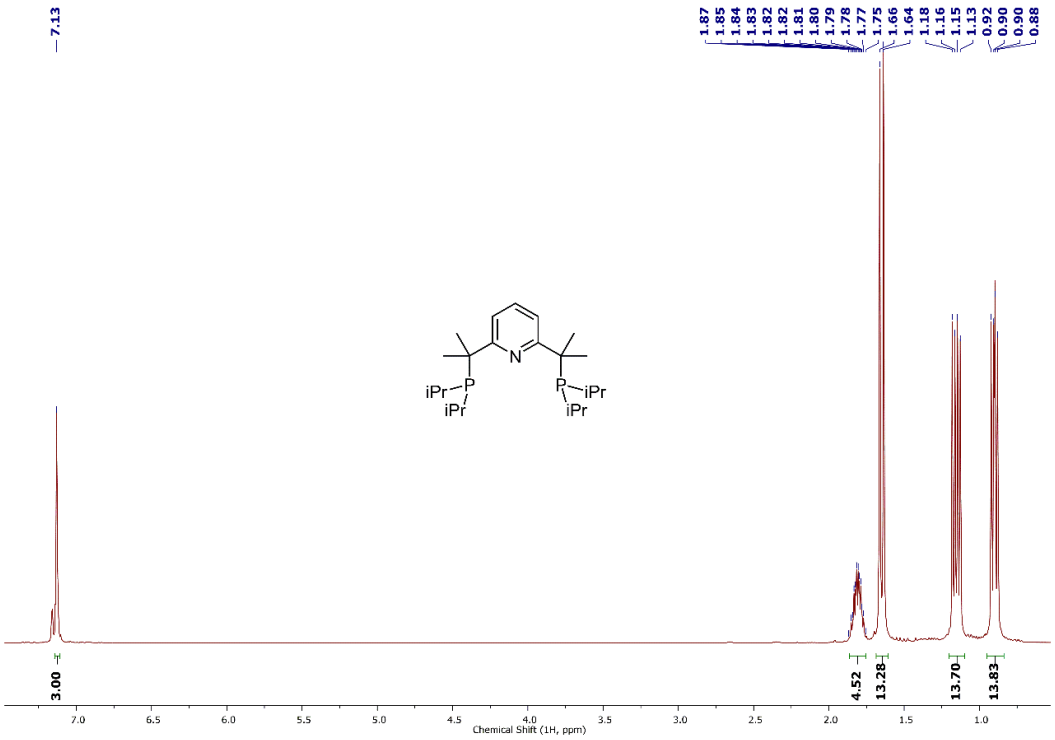

Figure 4.27 ^{1}H NMR spectrum of **L2.5** (400 MHz, C_6D_6).

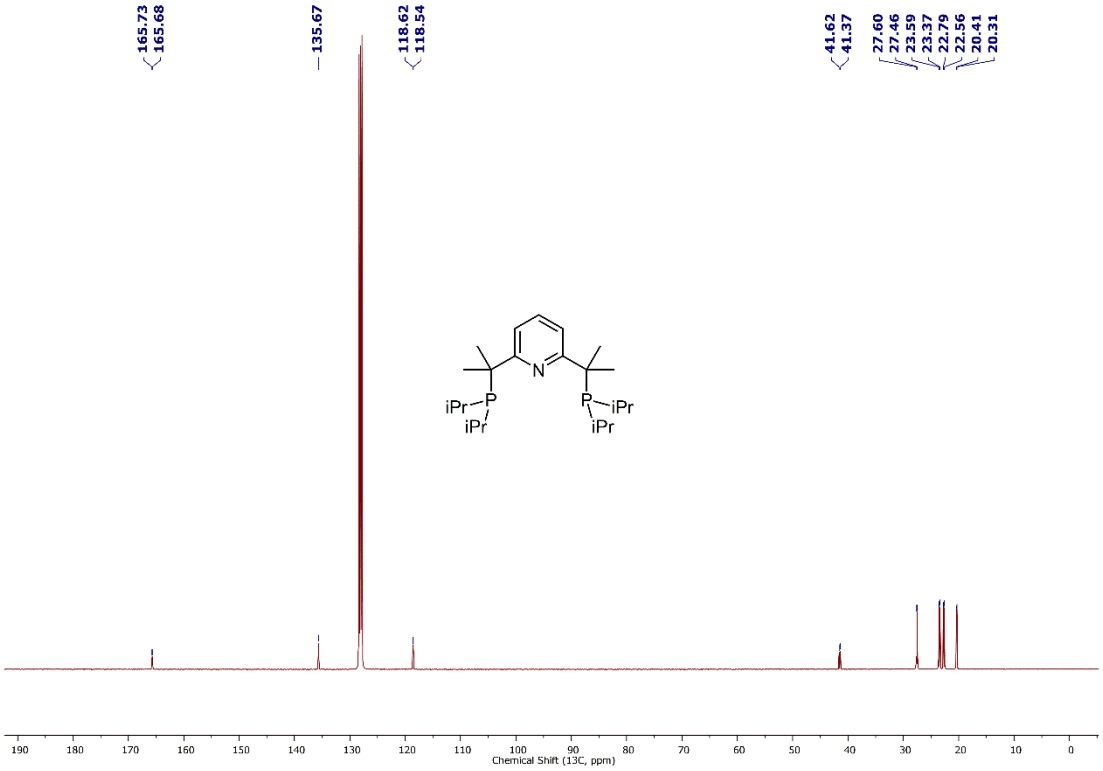

Figure 4.28 $^{13}C\{^{1}H\}$ NMR spectrum of **L2.5** (101 MHz, C_6D_6).

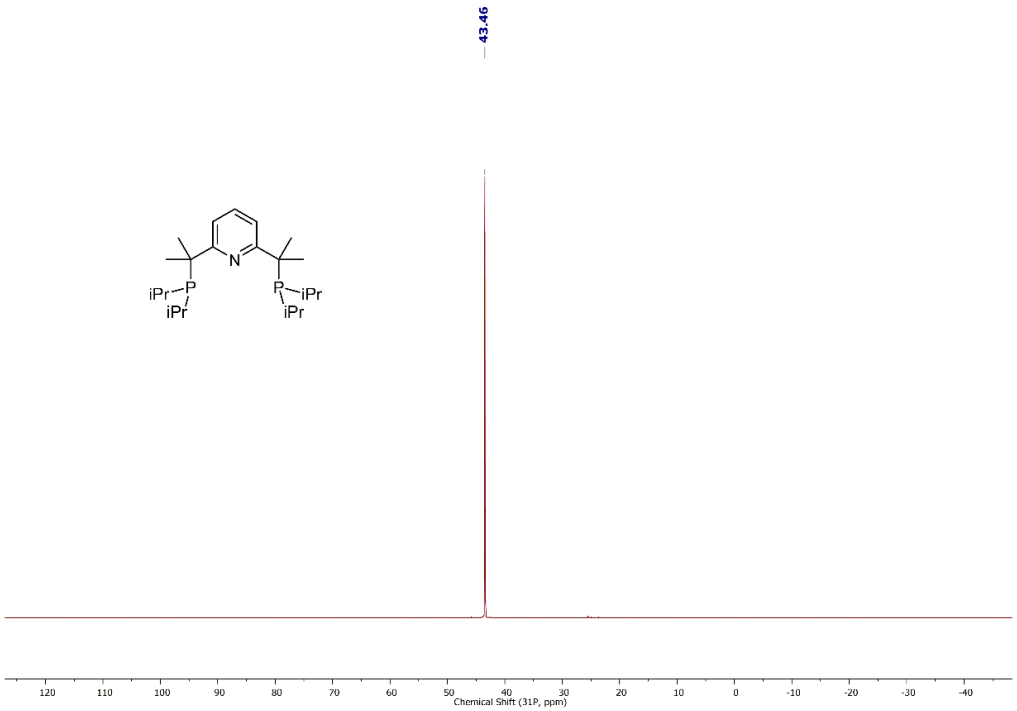

Figure 4.29 $^{31}P\{^{1}H\}$ NMR spectrum of **L2.5** (162 MHz, C_6D_6).

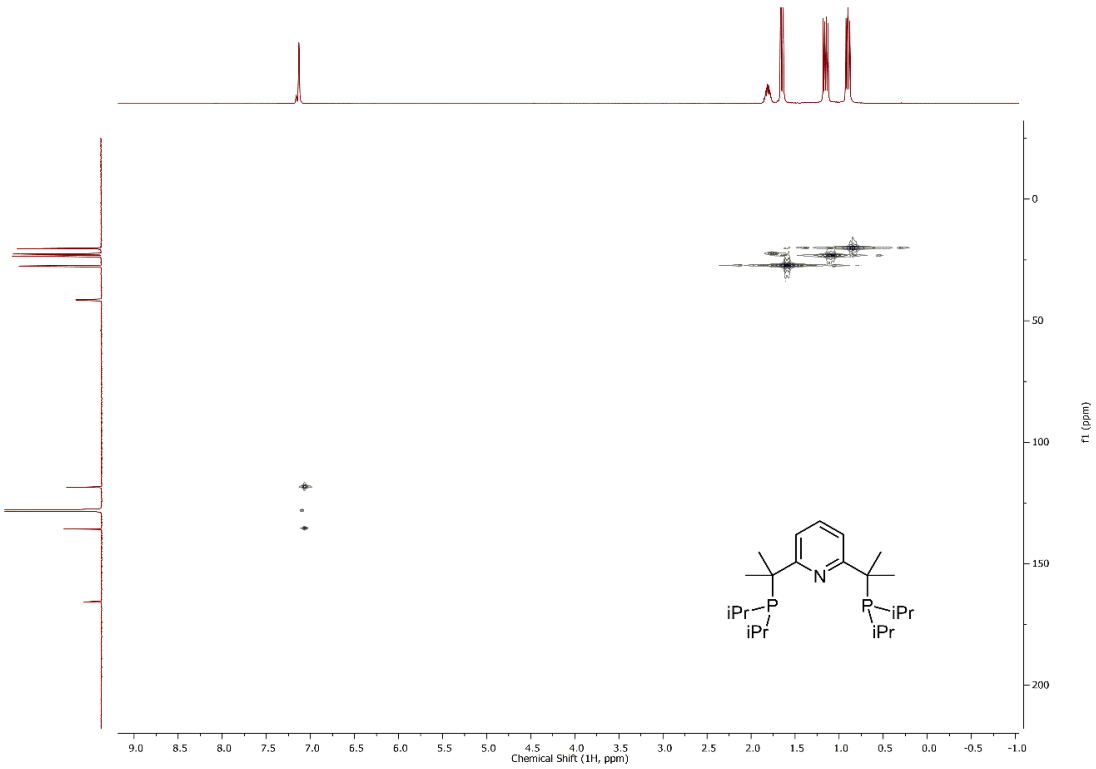

Figure 4.30 ^{1}H-^{13}C HMQC NMR spectrum of **L2.5** (C_6D_6).

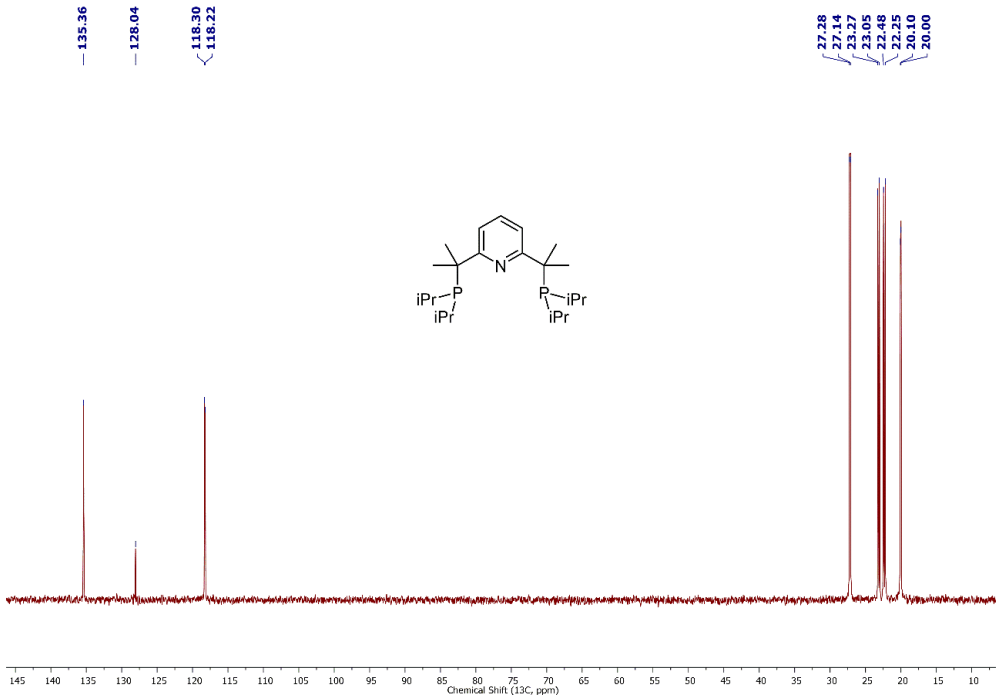

Figure 4.31 DEPT-135 NMR spectrum of **L2.5** (101 MHz, C_6D_6).

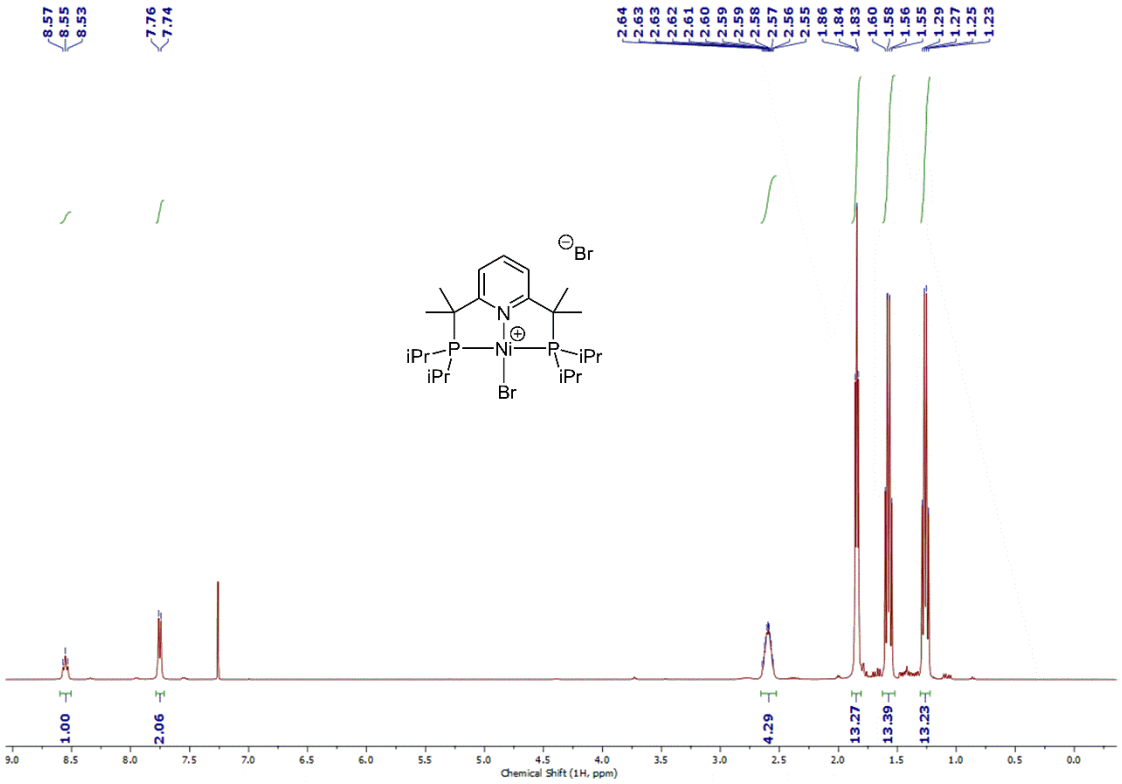

Figure 4.32 ^{1}H NMR spectrum of complex **2.32** (400 MHz, $CDCl_3$).

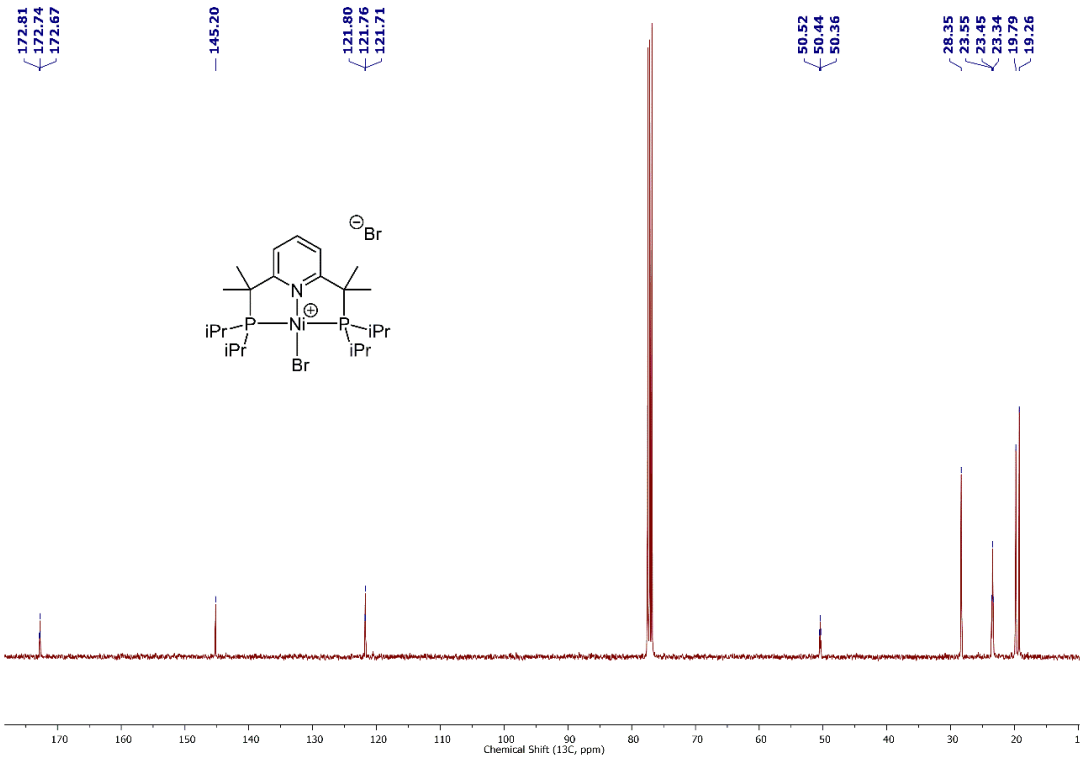

Figure 4.33 $^{13}C\{^{1}H\}$ NMR spectrum of complex **2.32** (101 MHz, $CDCl_3$).

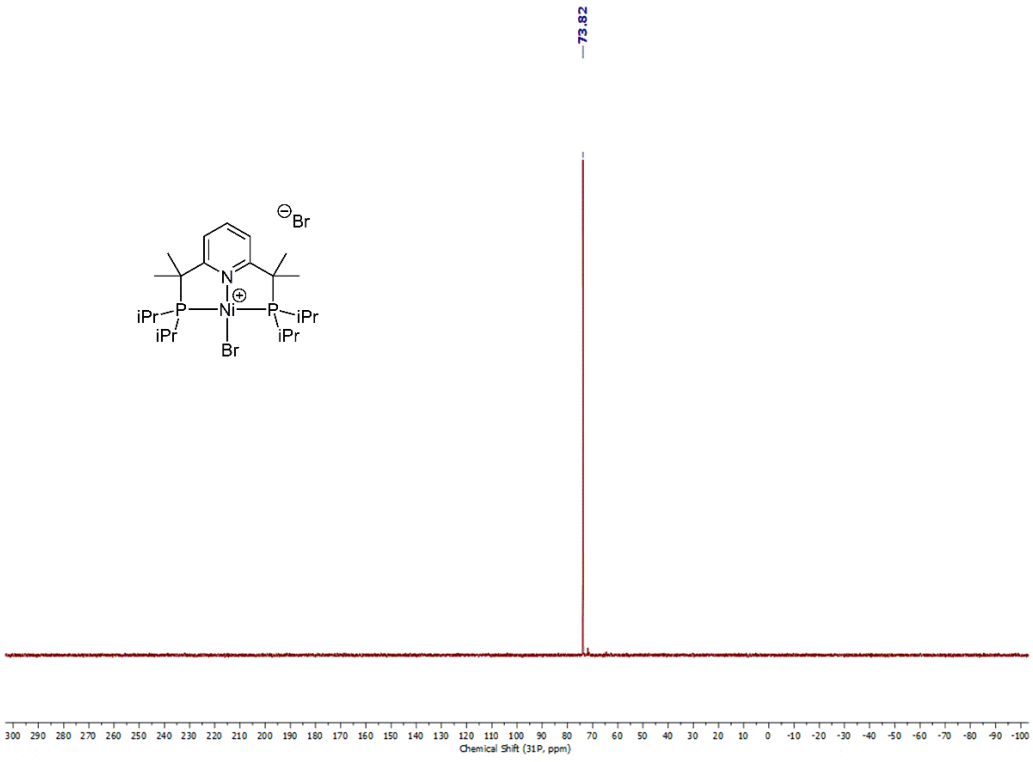

Figure 4.34 $^{31}P\{^{1}H\}$ NMR spectrum of complex **2.32** (162 MHz, $CDCl_3$).

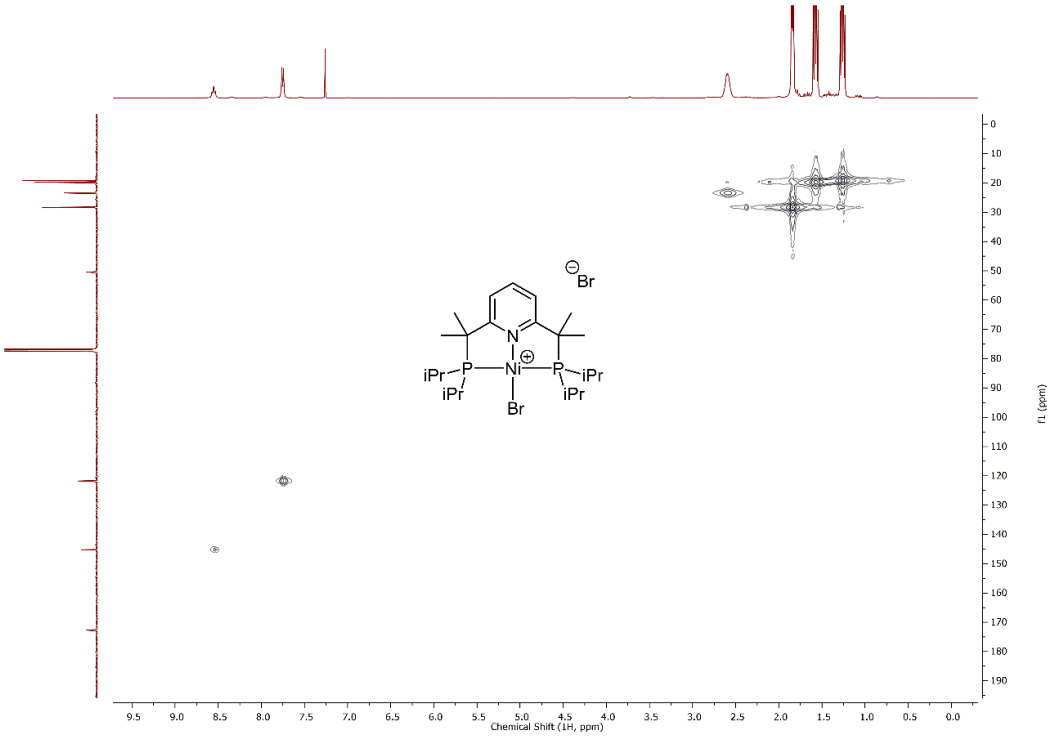

Figure 4.35 ^{1}H-^{13}C HMQC NMR spectrum of complex **2.32** ($CDCl_3$).

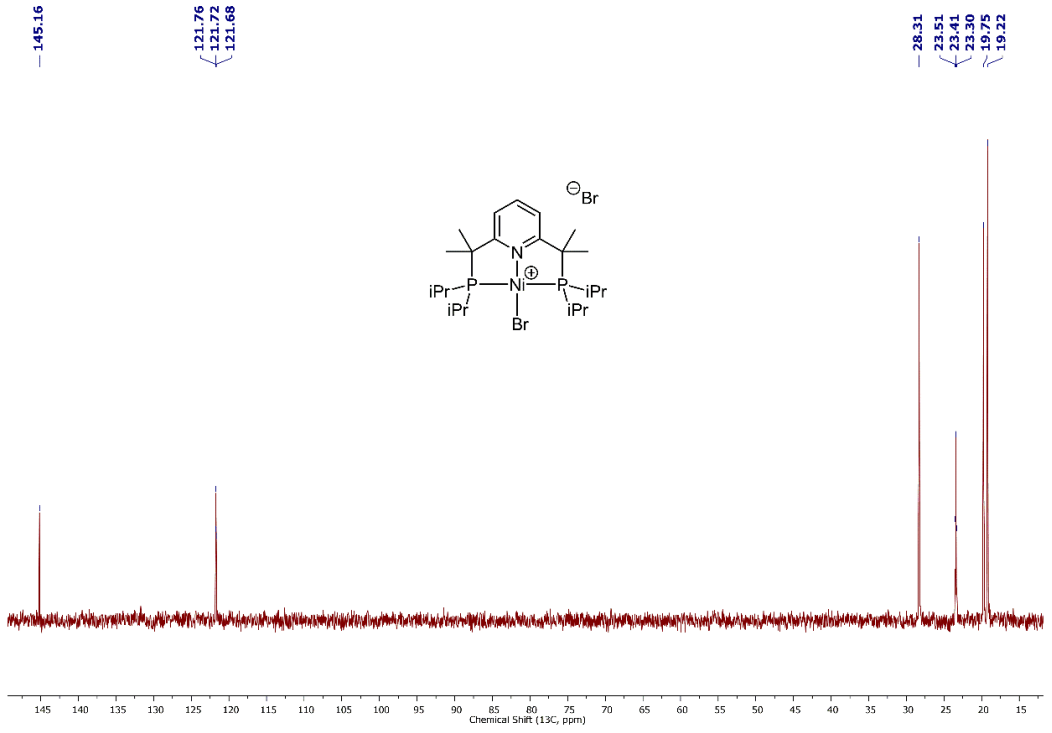

Figure 4.36 DEPT-135 NMR spectrum of complex **2.32** (101 MHz, $CDCl_3$).

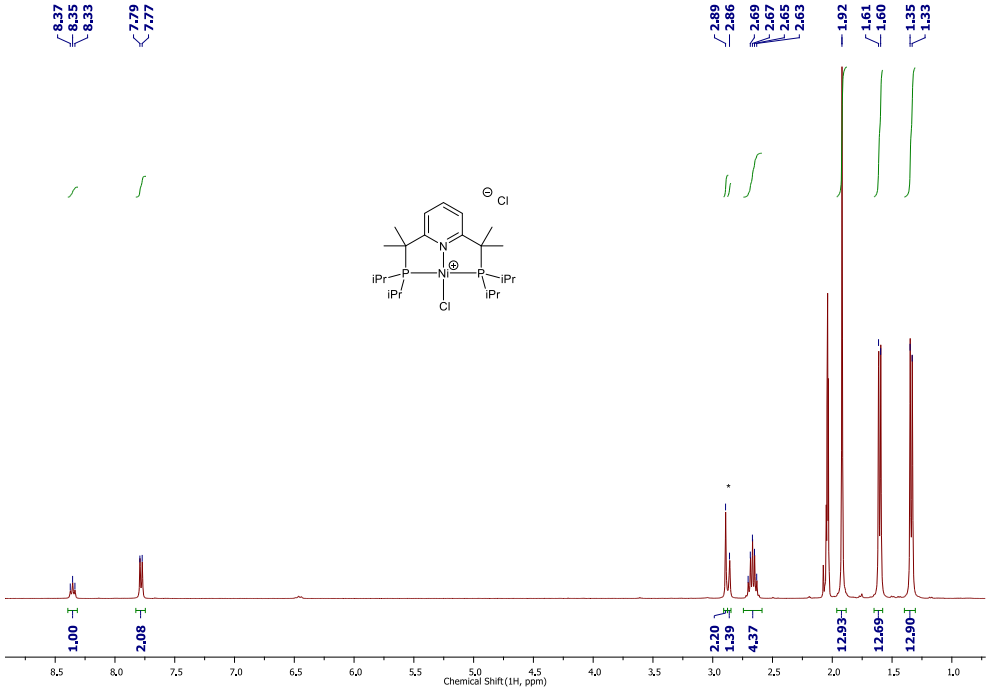

Figure 4.37 ^{1}H NMR spectrum of complex **2.33** (400 MHz, acetone-d_6). Sample stored under air. Peak of H_2O and HDO is represented by an asterisk (*)

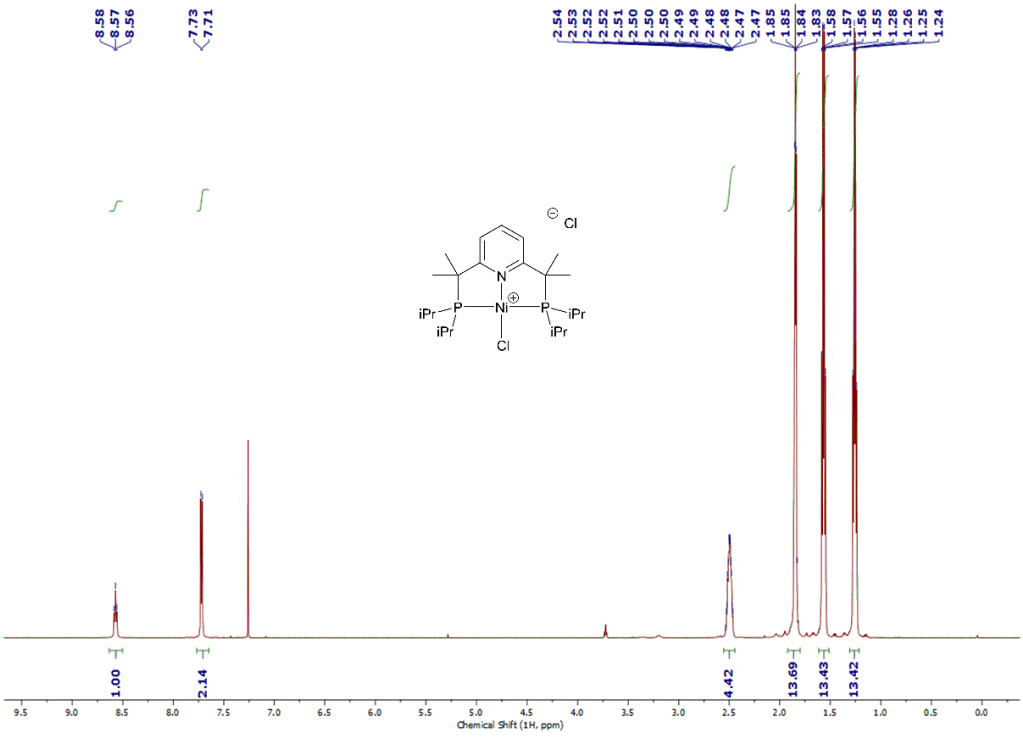

Figure 4.38 ^{1}H NMR spectrum of complex **2.33** (600 MHz, $CDCl_3$).

Sample stored under N_2.

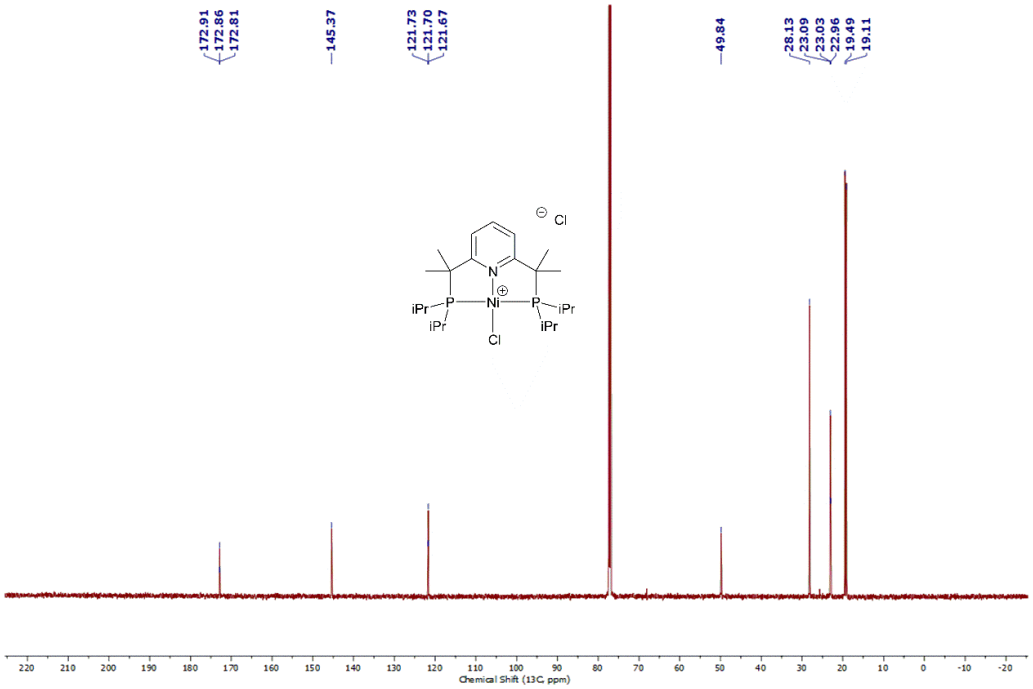

Figure 4.39 $^{13}C\{^{1}H\}$ NMR spectrum of complex **2.33** (151 MHz, $CDCl_3$).

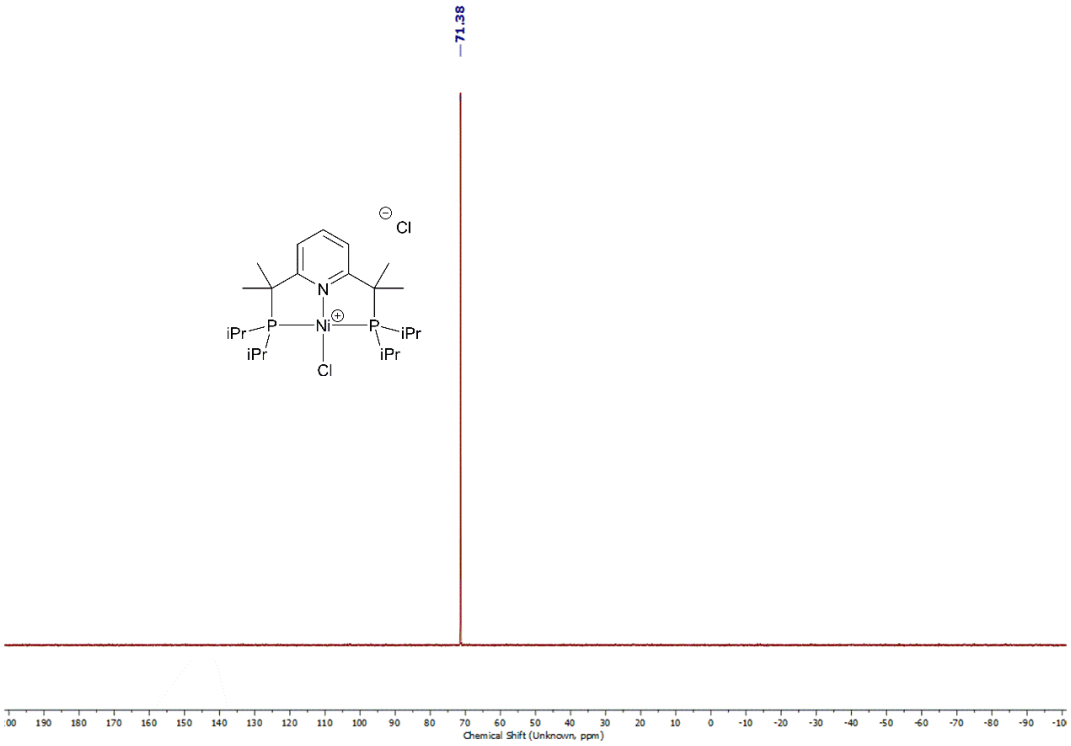

Figure 4.40 $^{31}P\{^{1}H\}$ NMR spectrum of complex **2.33** (242.96 MHz, $CDCl_3$).

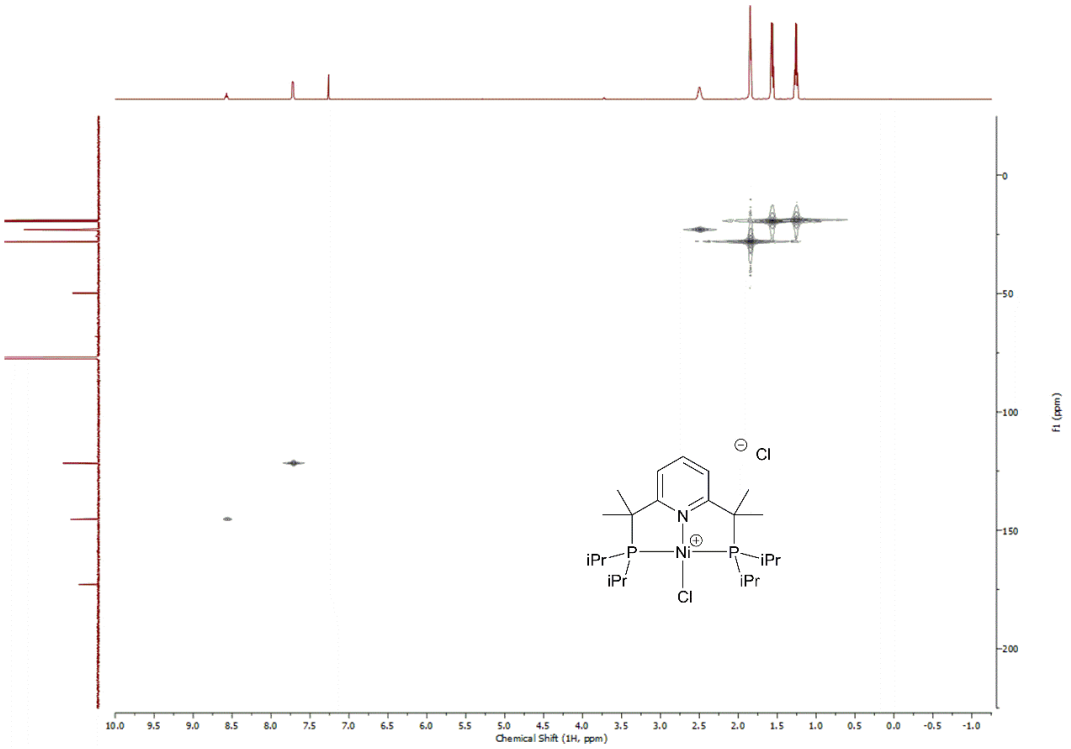

Figure 4.41 ^{1}H-^{13}C HMQC NMR spectrum of complex **2.33** ($CDCl_3$).

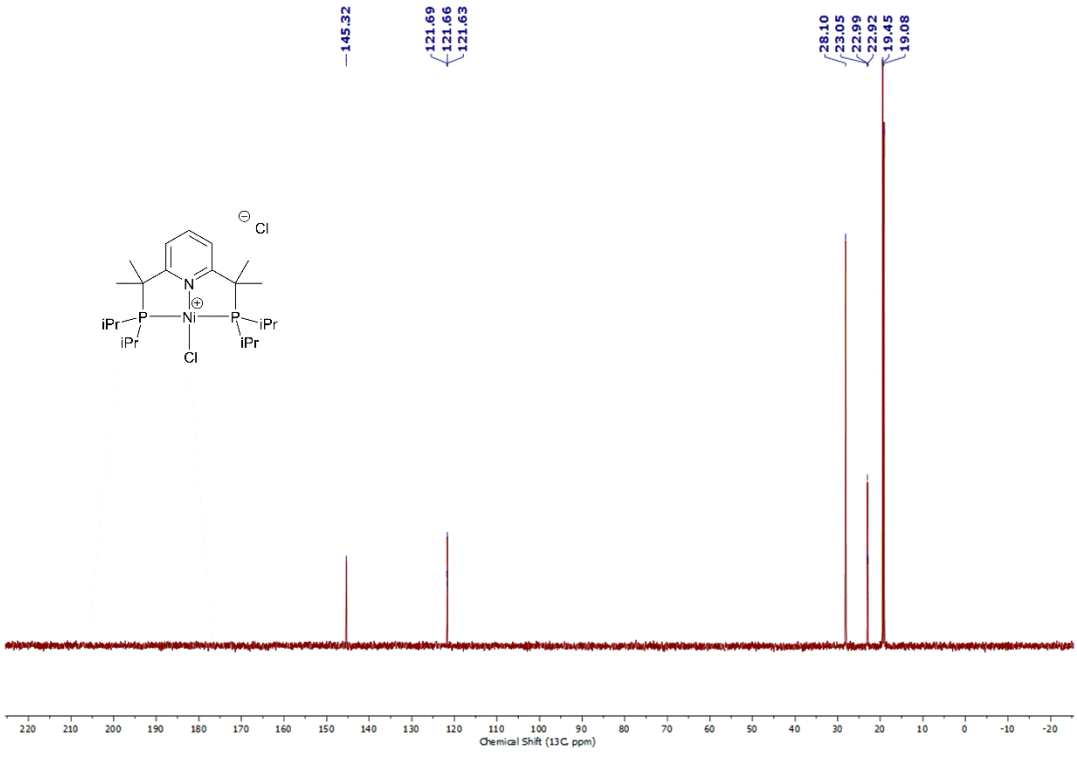

Figure 4.42 DEPT-135 NMR spectrum of complex **2.33** (151 MHz, $CDCl_3$).

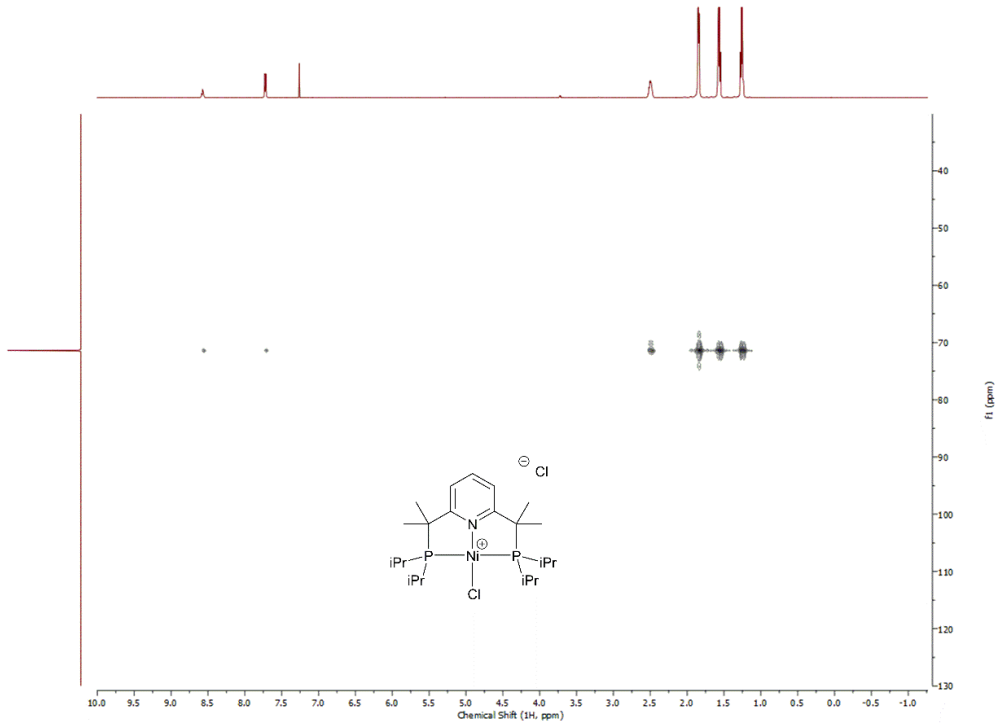

Figure 4.43 ^{1}H-$^{31}P\{^{1}H\}$ HMQC NMR spectrum of complex **2.33** ($CDCl_3$).

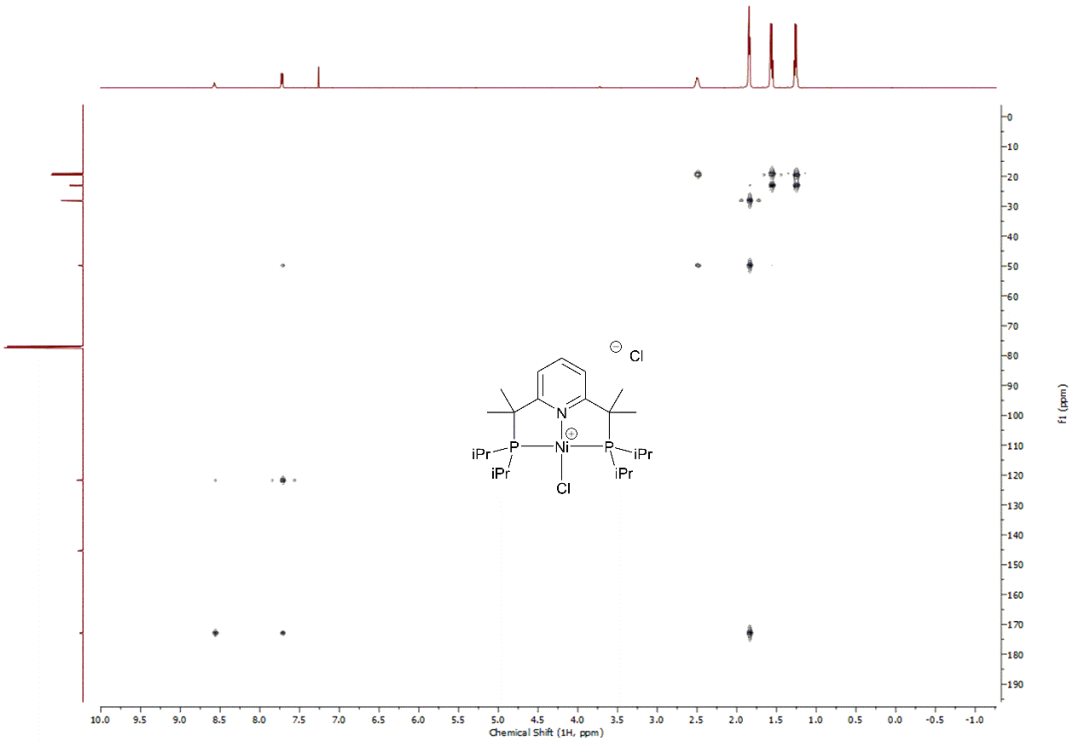

Figure 4.44 ^{1}H-$^{13}C\{^{1}H\}$ HMBC NMR spectrum of complex **2.33** ($CDCl_3$).

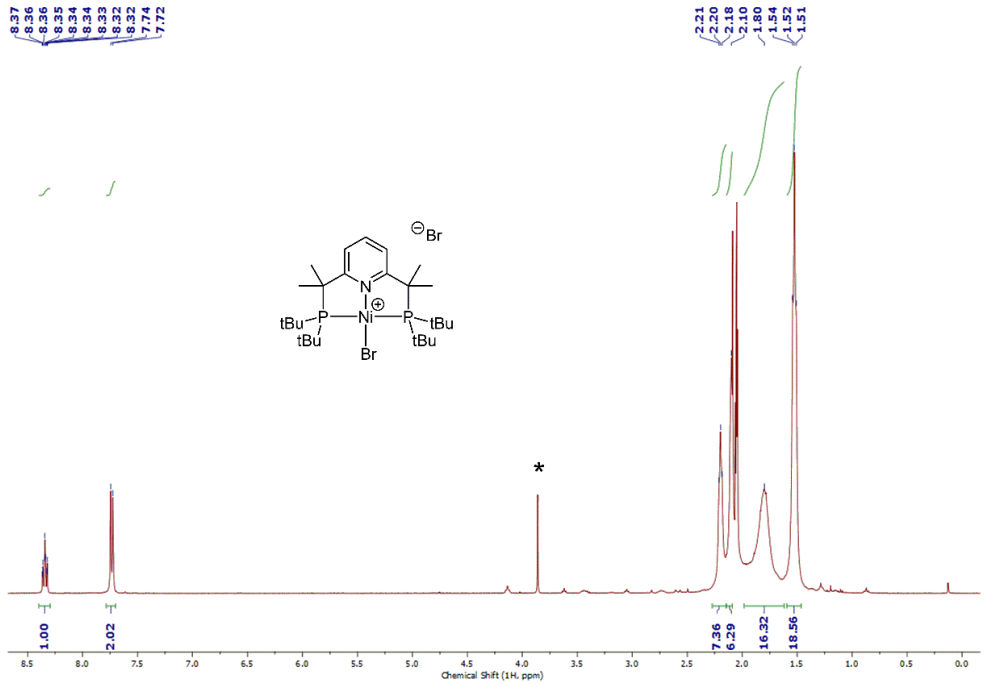

Figure 4.45 ^{1}H NMR spectrum of complex **2.34** (400 MHz, acetone-d_6). Peak of trace solvent is present and marked by an asterisk (*)

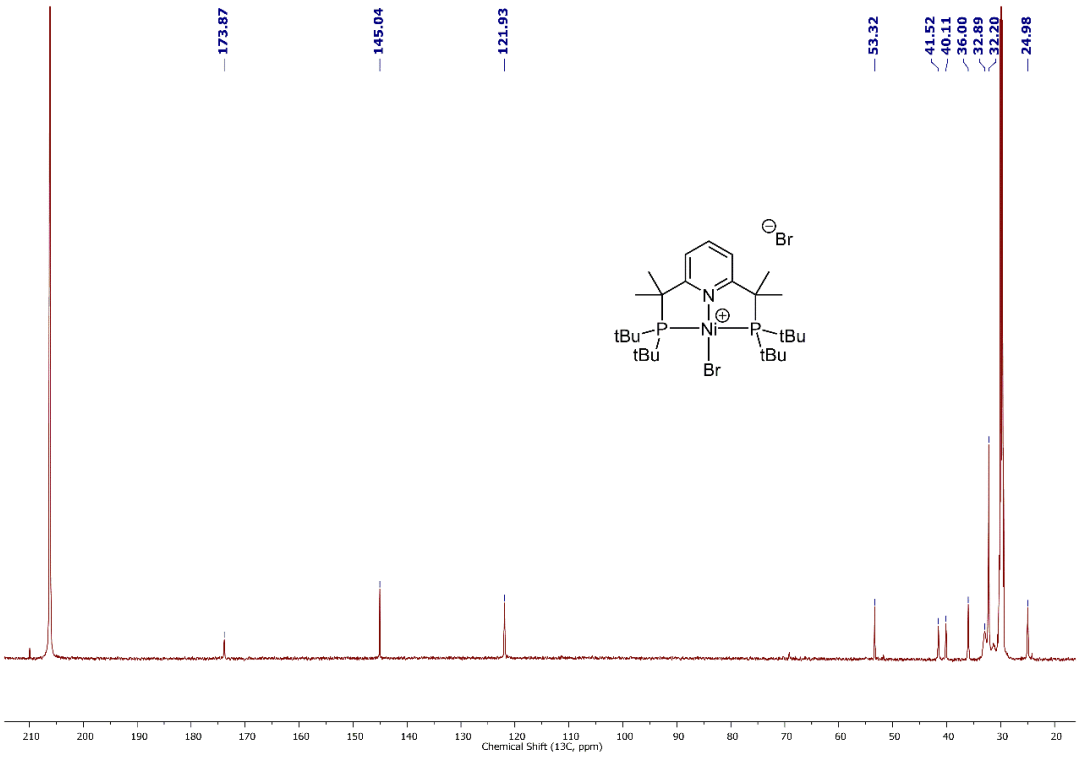

Figure 4.46 ^{13}C{^{1}H} NMR spectrum of complex **2.34** (101 MHz, acetone-d_6).

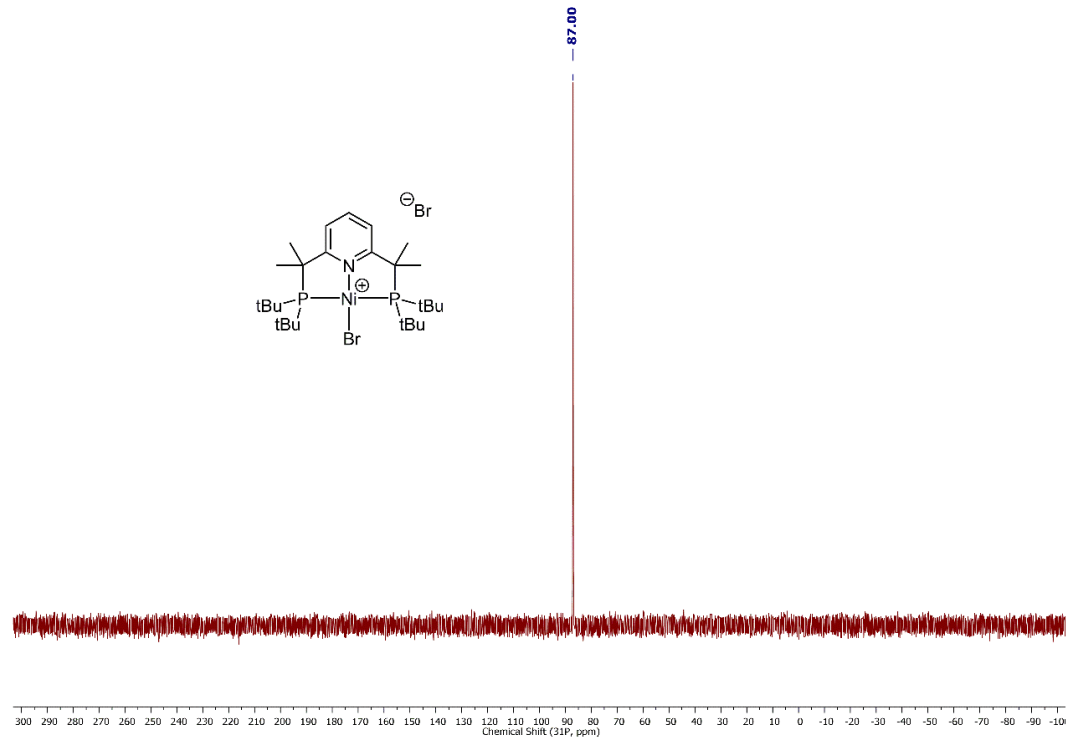

Figure 4.47 $^{31}P\{^{1}H\}$ NMR spectrum of complex **2.34** (162 MHz, acetone-d_6).

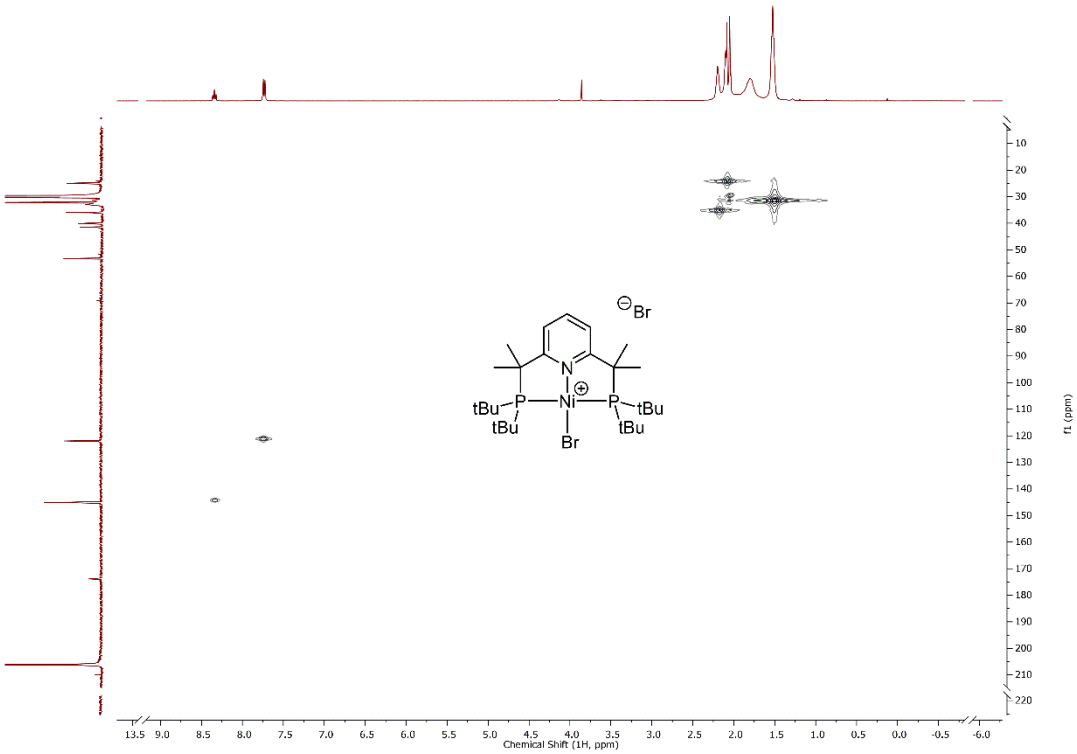

Figure 4.48 ^{13}C-^{1}H HMQC NMR spectrum of complex **2.34** (acetone-d_6).

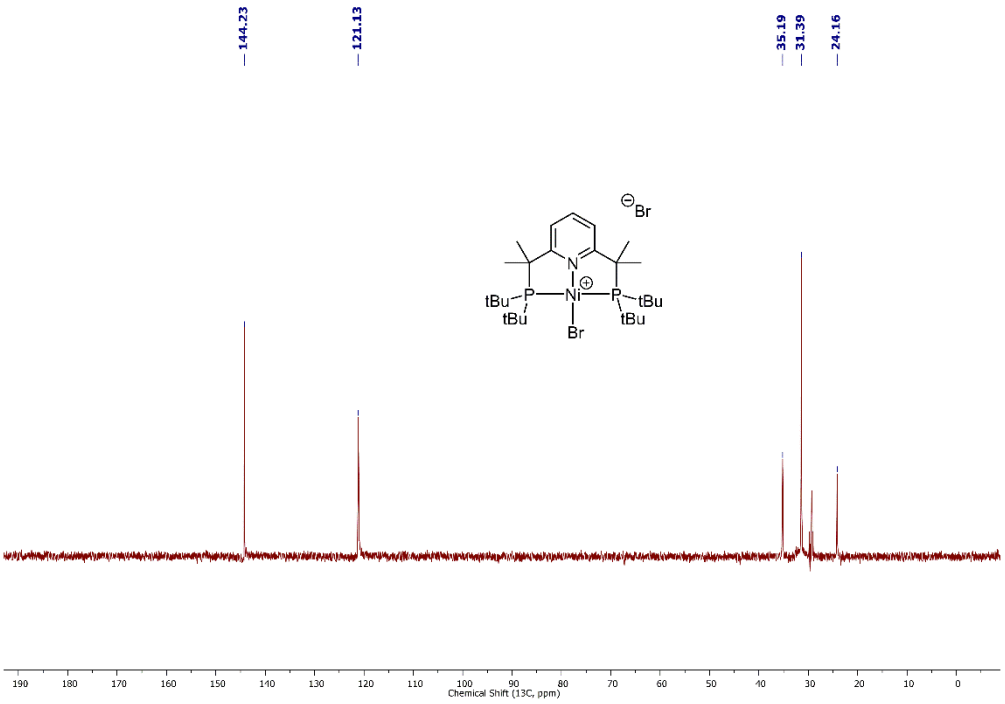

Figure 4.49 DEPT-135 NMR spectrum of complex 2.34 (101 MHz, acetone-d_6).

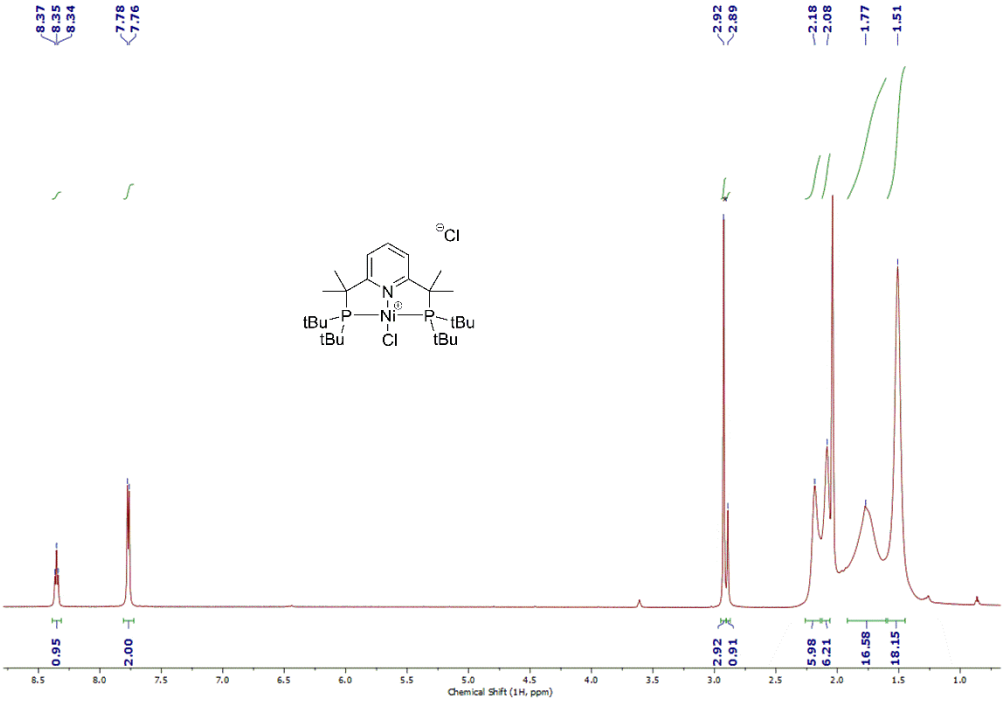

Figure 4.50 ^{1}H NMR spectrum of complex **2.35** (600 MHz, acetone-d_6). Peaks of H_2O and HDO are present and marked by an asterisk (*)

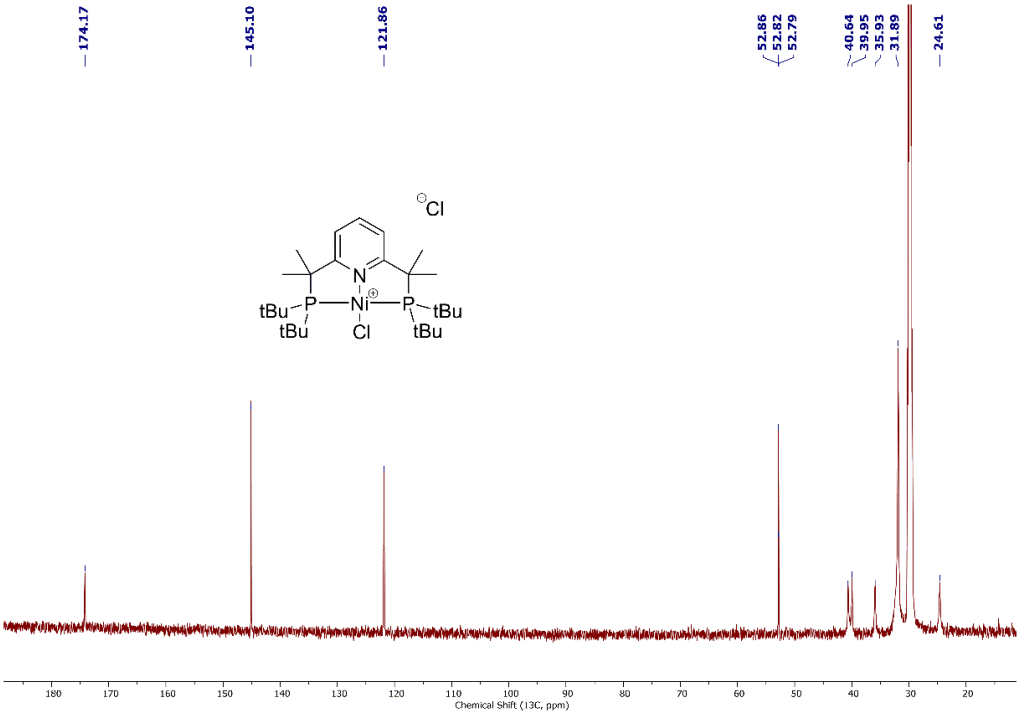

Figure 4.51 $^{13}C\{^{1}H\}$ NMR spectrum of complex **2.35** (151 MHz, acetone-d_6).

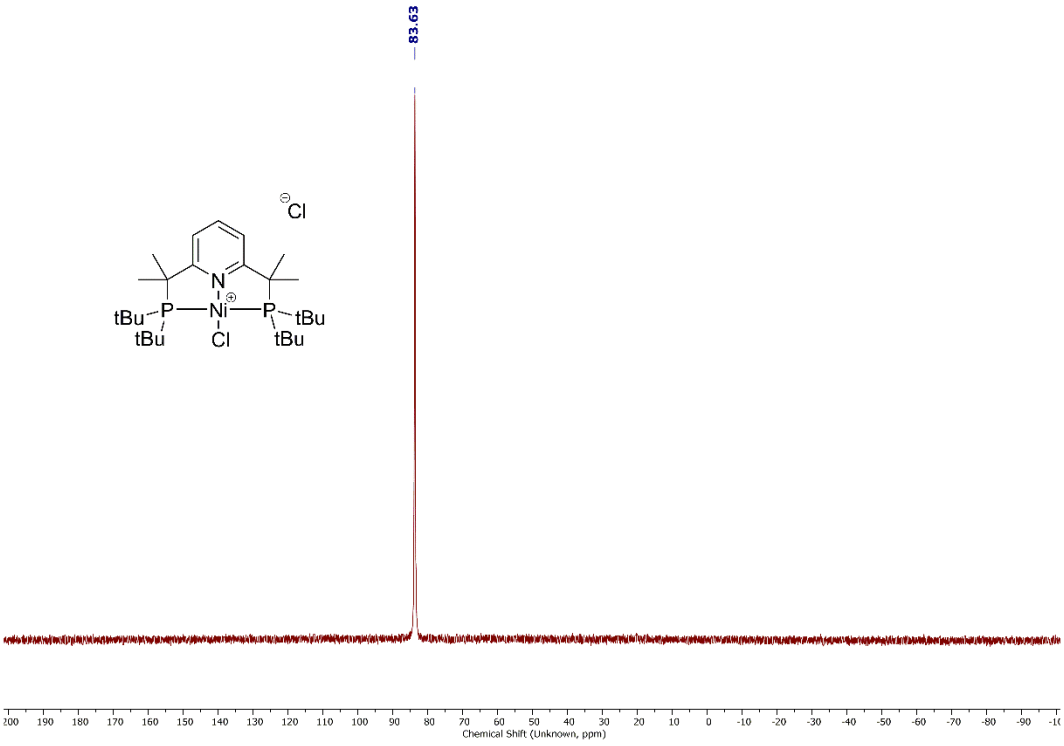

Figure 4.52 $^{31}P\{^{1}H\}$ NMR spectrum of complex **2.35** (262 MHz, acetone-d_6).

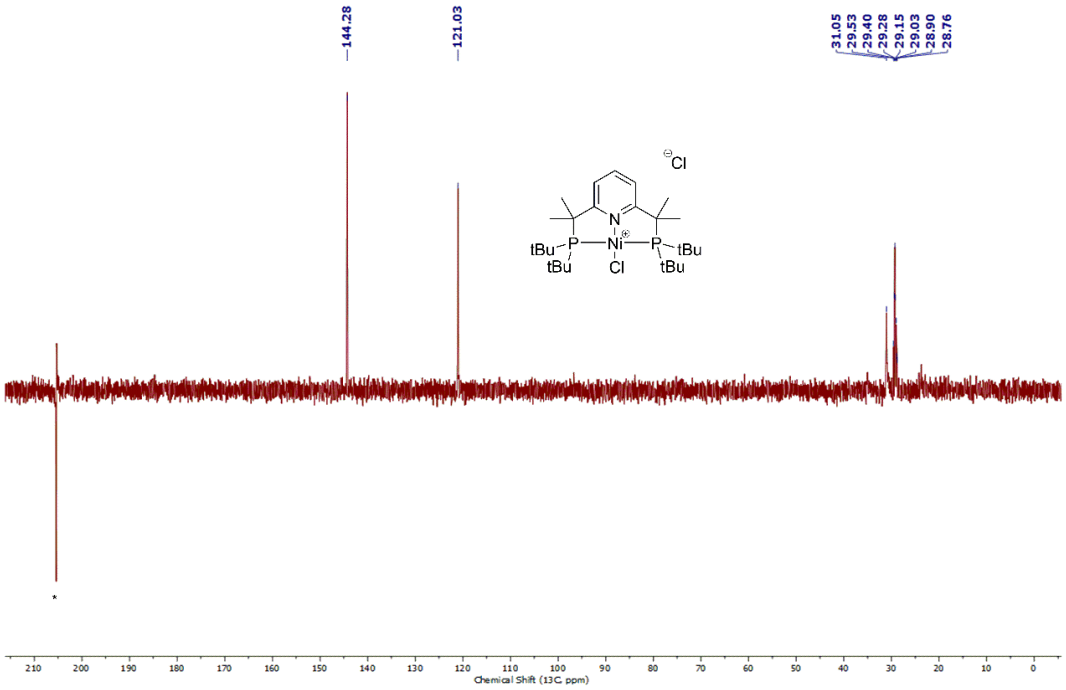

Figure 4.53 DEPT-135 NMR spectrum of complex **2.35** (151 MHz, acetone-d_6). Signal of acetone solvent are marked by an asterisk.

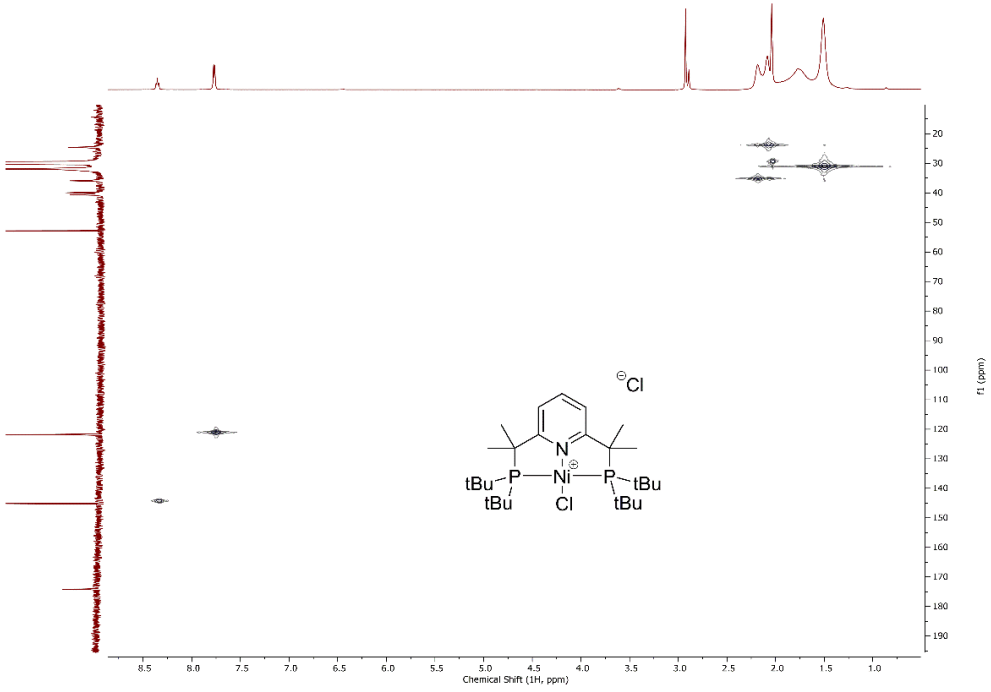

Figure 4.54 ^{1}H-^{13}C HMQC NMR spectrum of complex **2.35** (acetone-d_6).

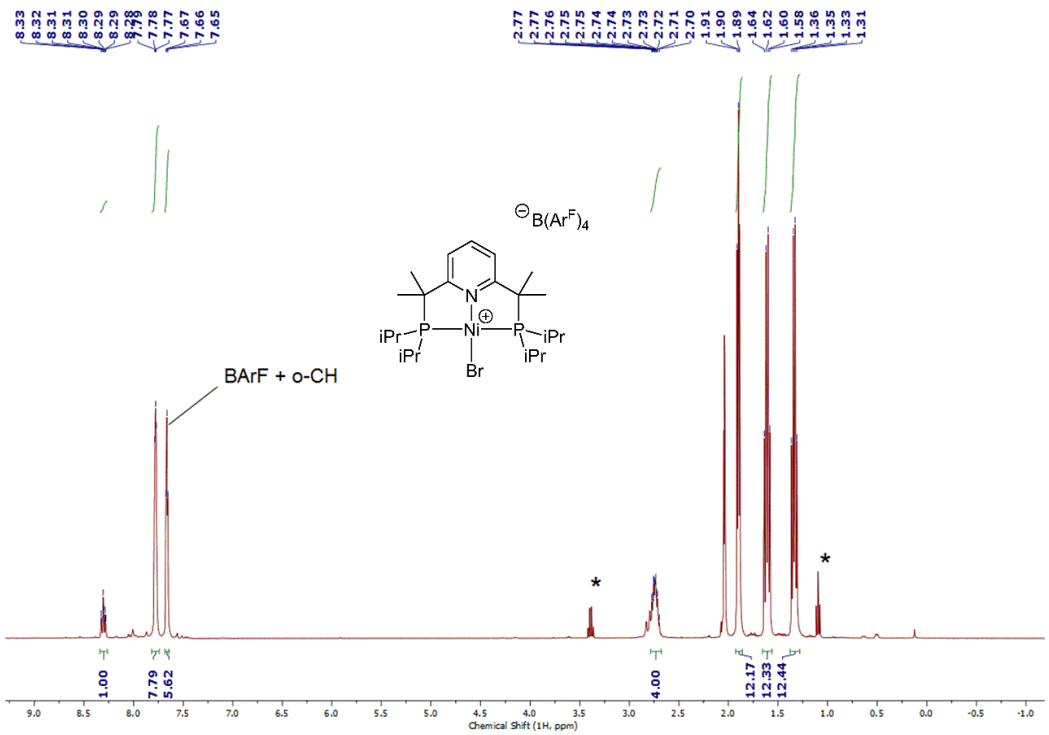

Figure 4.55 ^{1}H NMR spectrum of complex **2.36** (400 MHz, acetone-d_6). Peaks of trace diethyl ether solvent is present and marked by an asterisk (*)

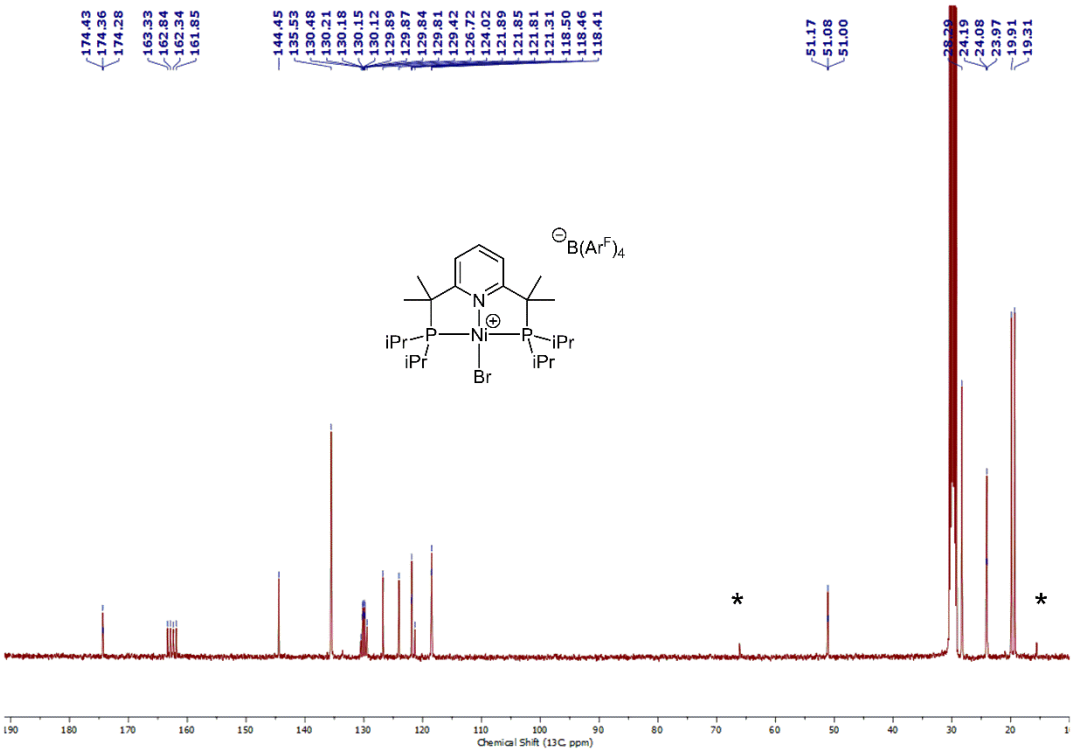

Figure 4.56 ^{13}C{^{1}H} NMR spectrum of complex **2.36** (101 MHz, acetone-d_6). Peaks marked by an asterisk are from traces of diethyl ether.

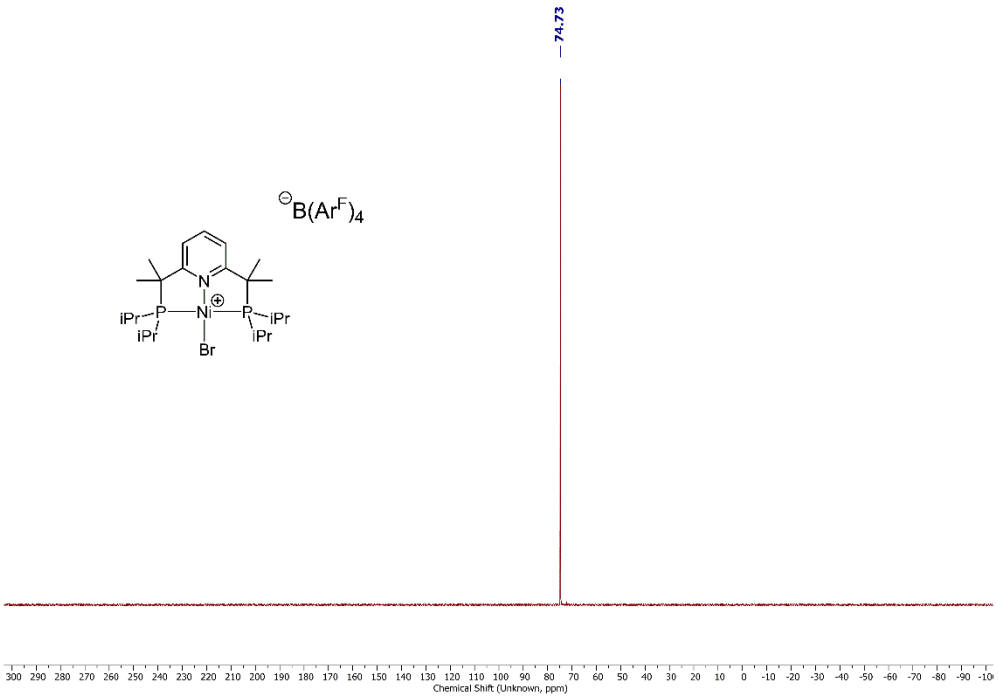

Figure 4.57 $^{31}P\{^{1}H\}$ NMR spectrum of complex **2.36** (162 MHz, acetone-d_6).

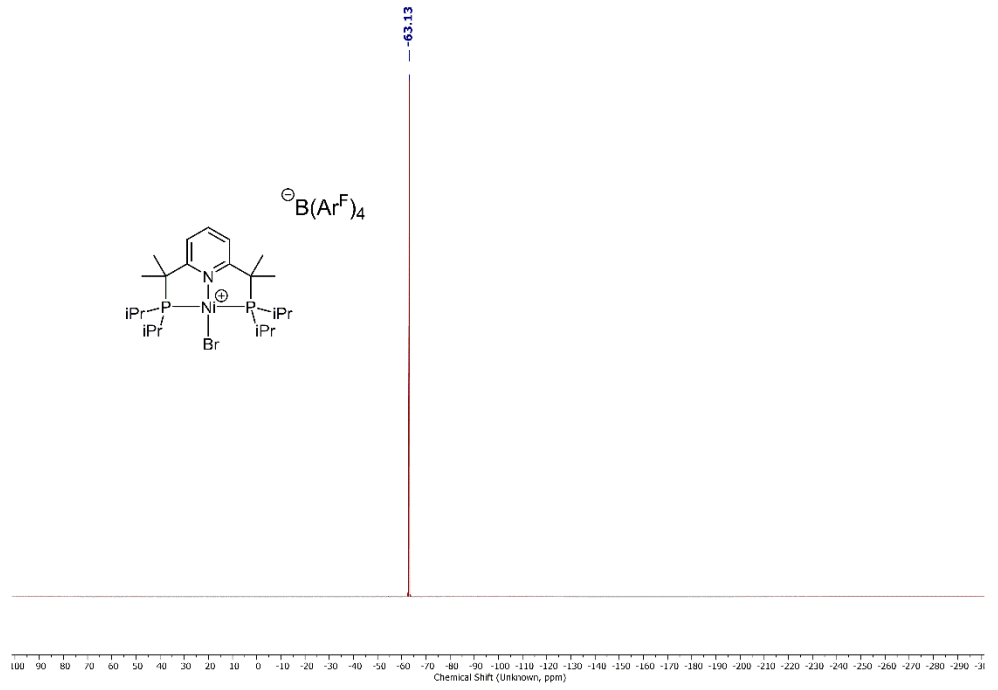

Figure 4.58 ^{19}F NMR spectrum of complex **2.36** (376.2 MHz, acetone-d_6).

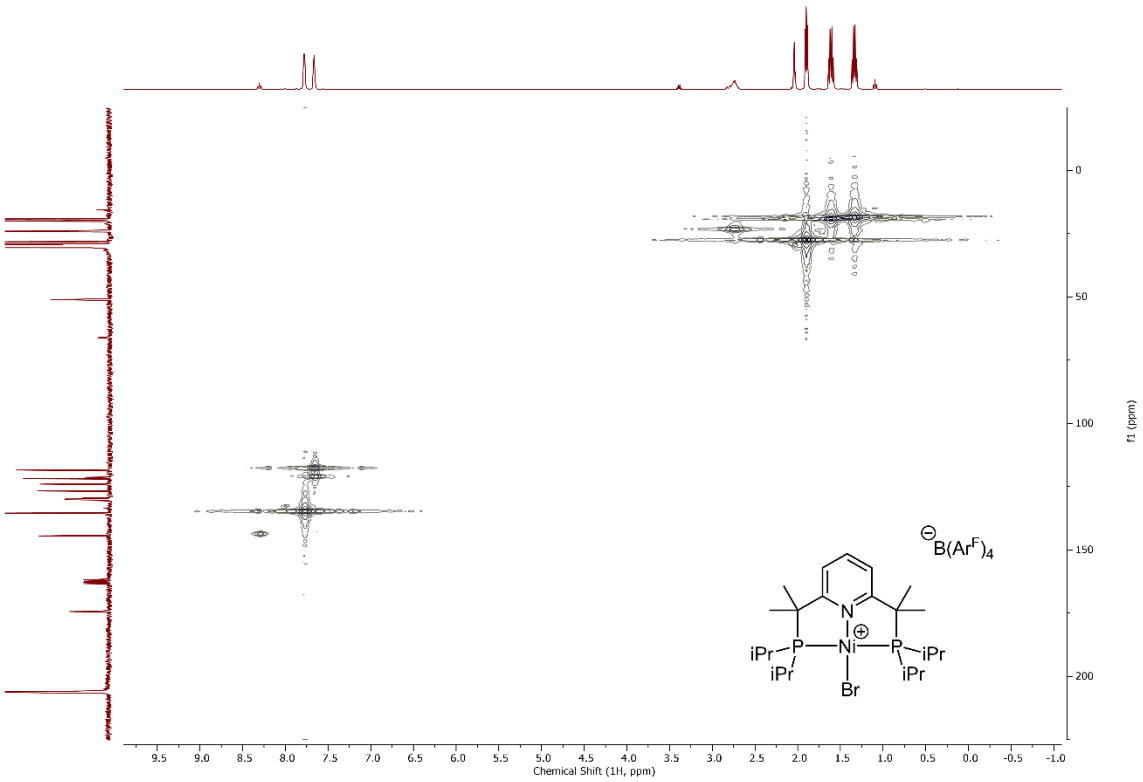

Figure 4.59 ^{1}H-^{13}C HMQC NMR spectrum of complex **2.36** (acetone-d_6).

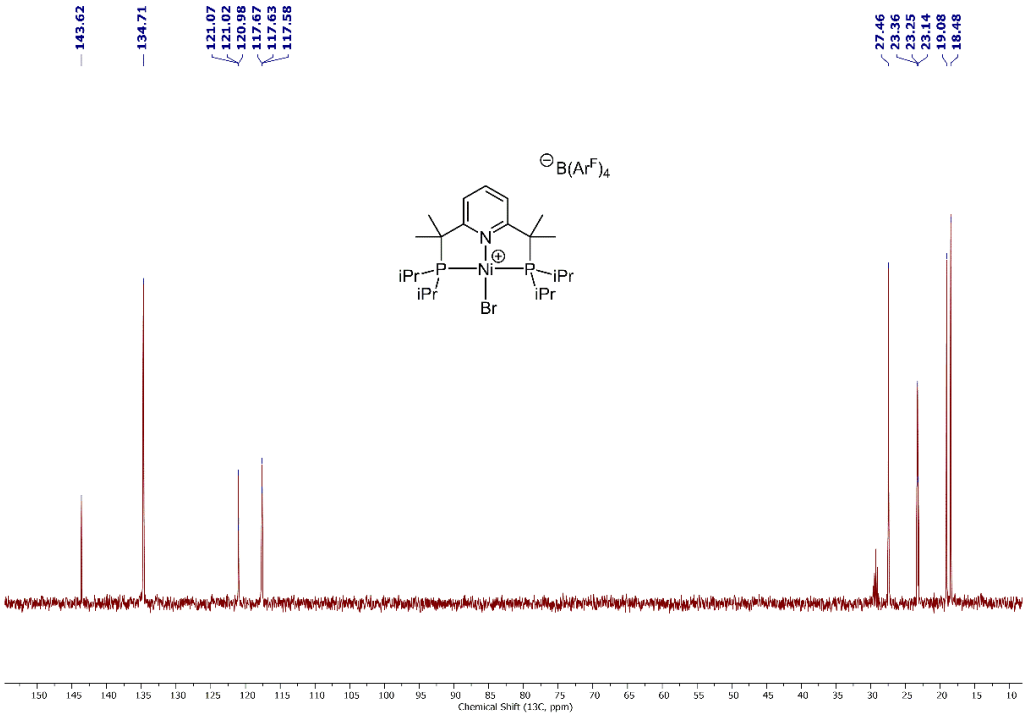

Figure 4.60 DEPT-135 NMR spectrum of **2.36** (101 MHz, acetone-d_6).

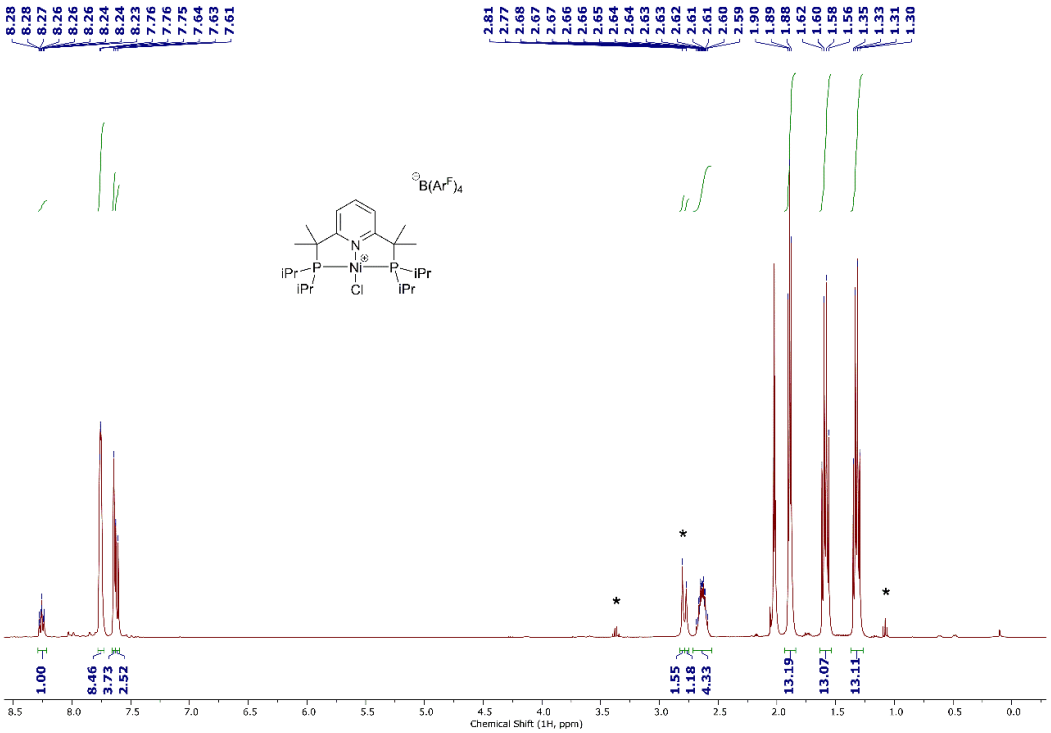

Figure 4.61 ^{1}H NMR spectra of complex **2.37** (400 MHz, acetone-d_6). Peaks of trace diethyl ether solvent and water are present and marked by asterisks (*)

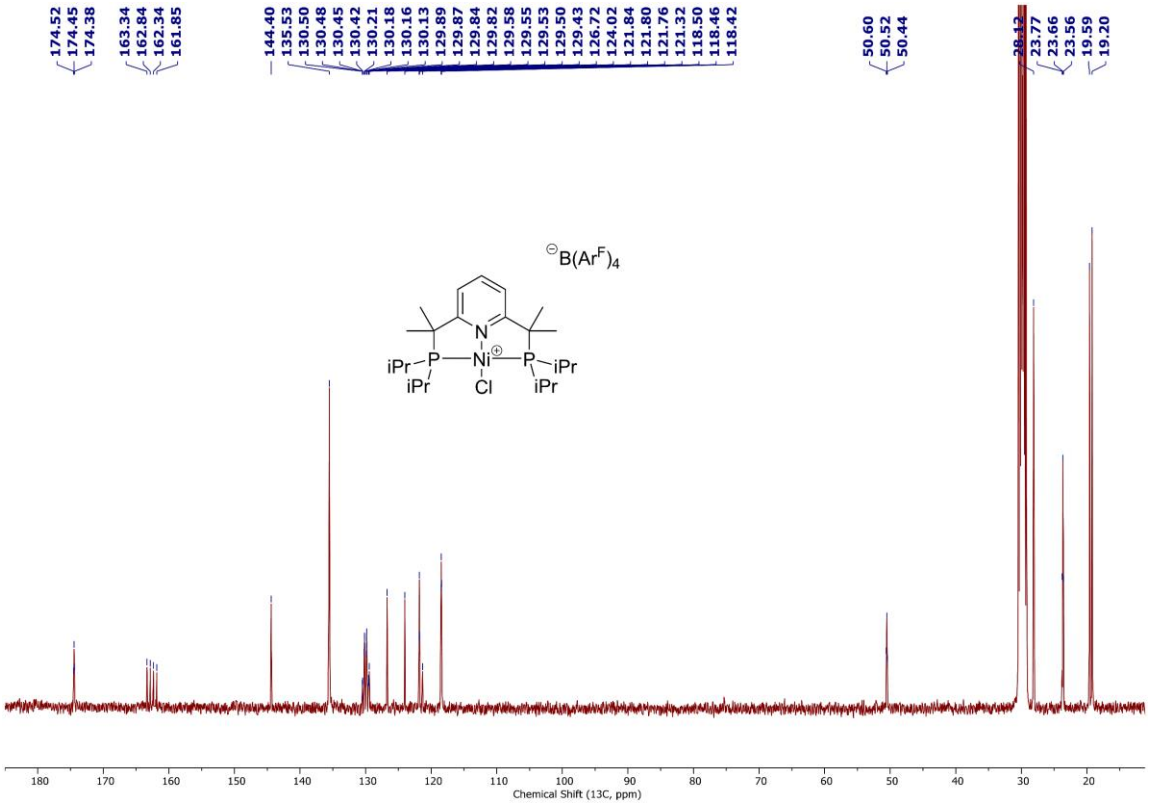

Figure 4.62 ^{13}C{^{1}H} NMR spectrum of 2.37 (101 MHz, acetone-d_6).

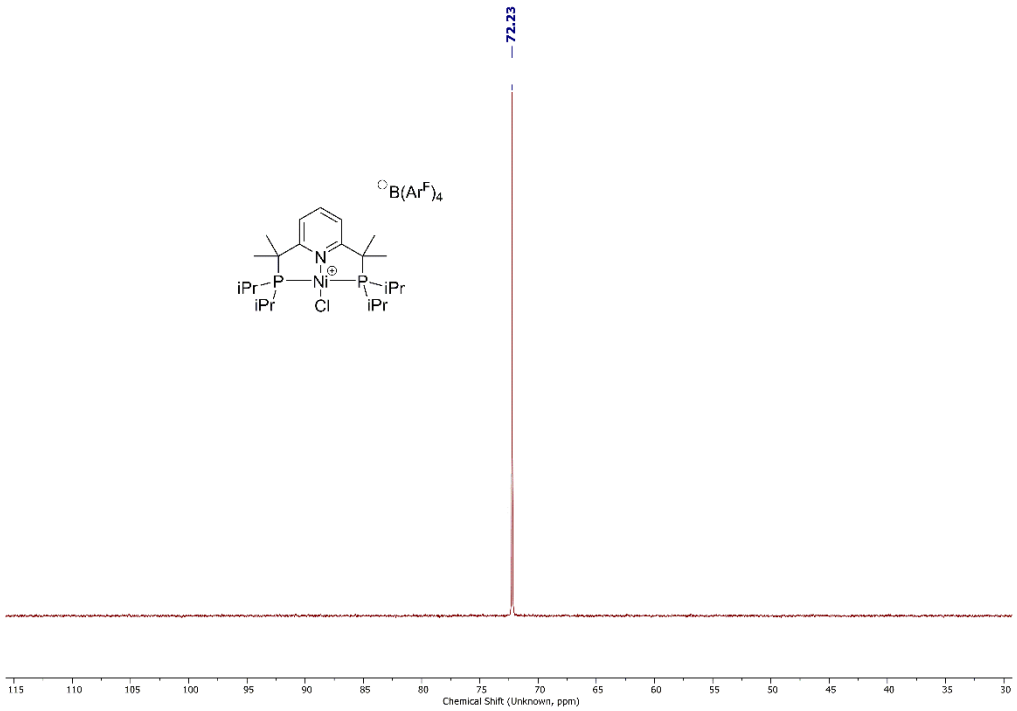

Figure 4.63 $^{31}P\{^{1}H\}$ NMR spectrum of **2.37** (162 MHz, acetone-d_6).

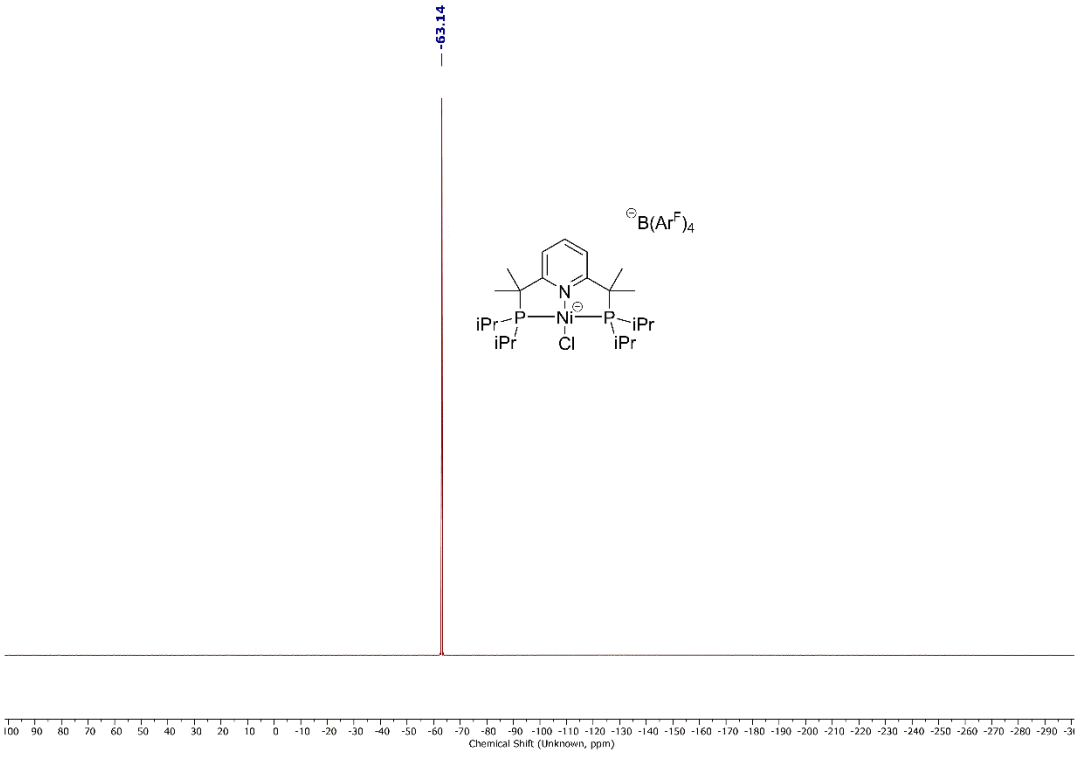

Figure 4.64 ^{19}F NMR spectrum of **2.37** (376.2 MHz, acetone-d_6).

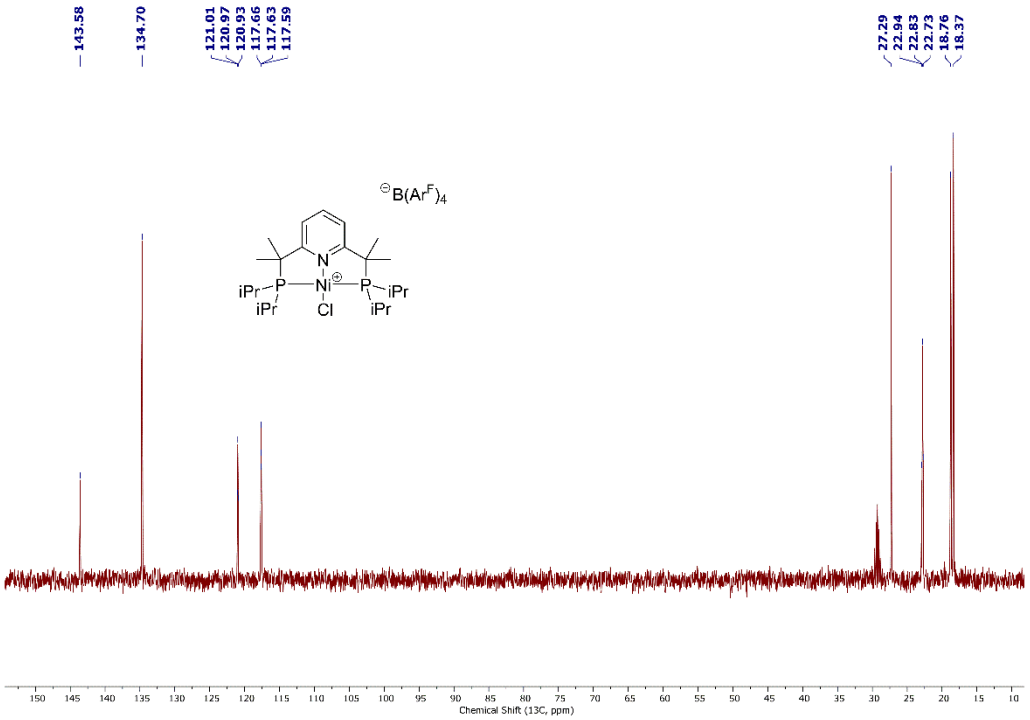

Figure 4.65 DEPT-135 NMR spectrum of **2.37** (101 MHz, acetone-d_6).

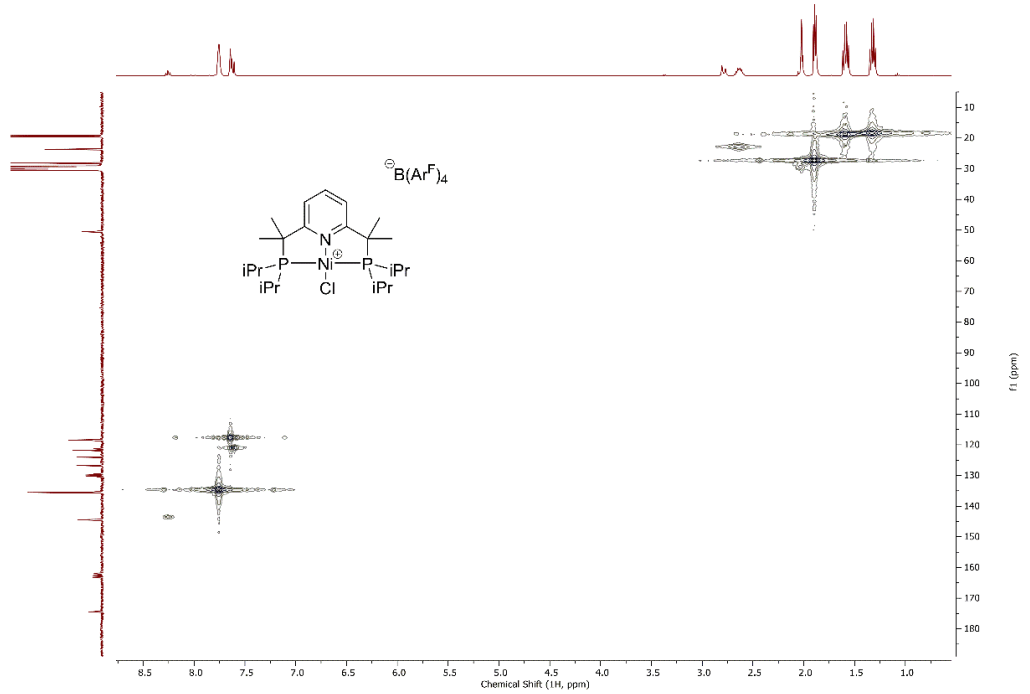

Figure 4.66 ^{1}H-^{13}C HMQC NMR spectrum of **2.37** (acetone-d_6)

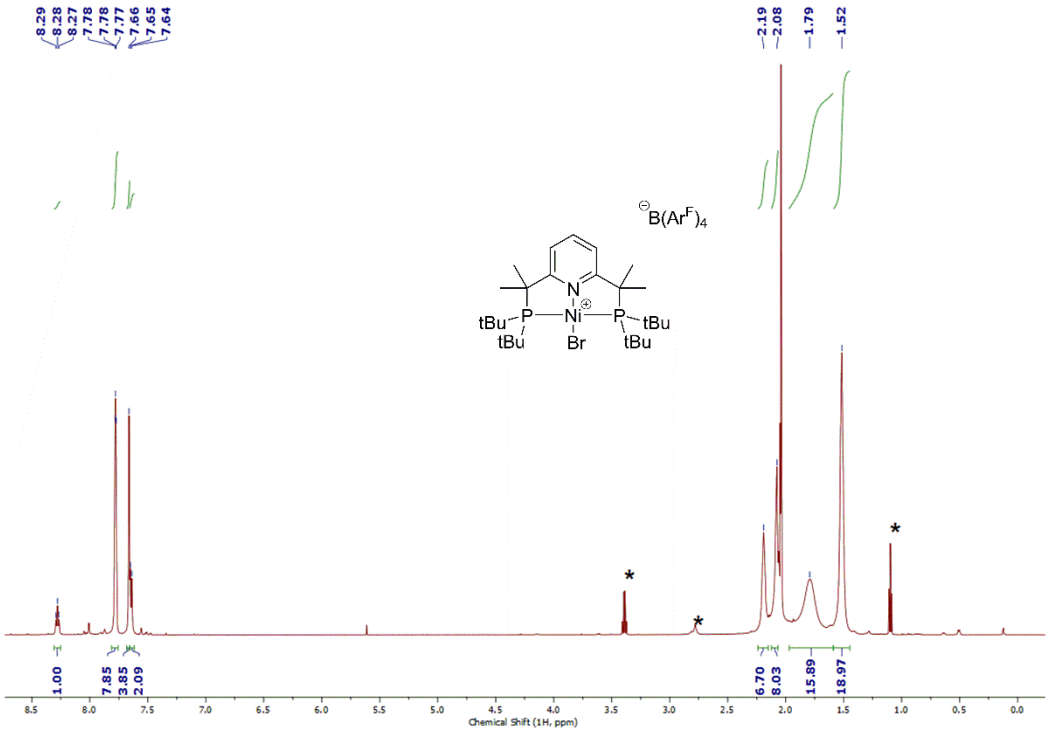

Figure 4.67 ^{1}H NMR spectrum of complex **2.38** at room temperature (600 MHz, acetone-d_6). Peaks of trace diethyl ether and water are present and marked with asterisks (*)

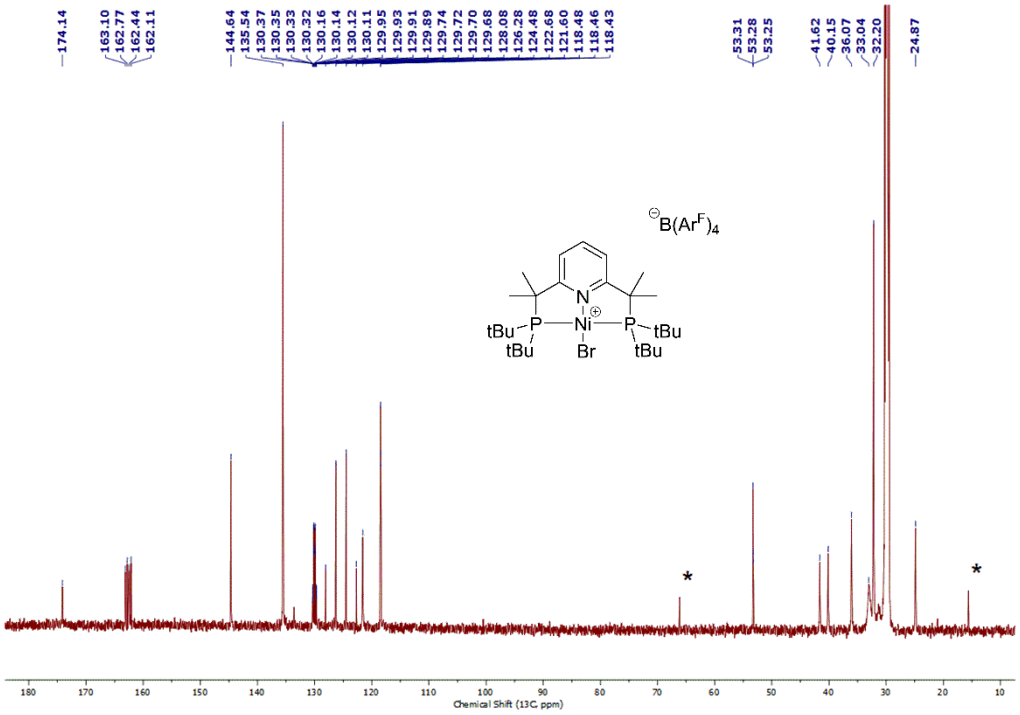

Figure 4.68 ^{13}C{^{1}H} NMR spectrum of complex **2.38** (151 MHz, acetone-d_6). Peaks of trace diethylether solvent are present and marked with asterisks (*)

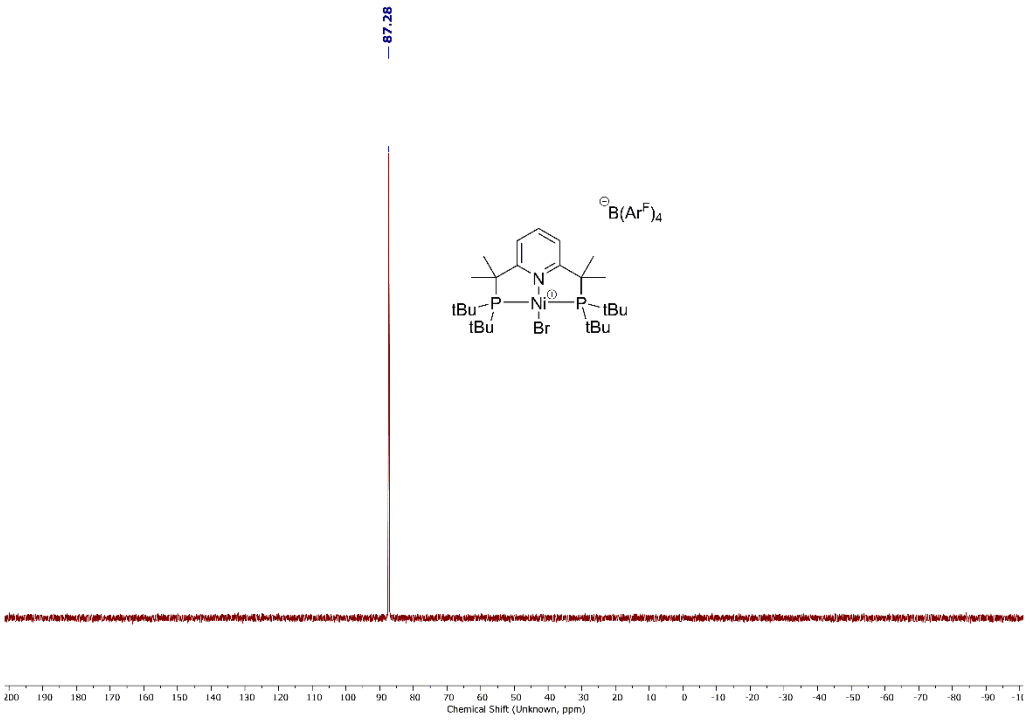

Figure 4.69 $^{31}P\{^{1}H\}$ NMR spectrum of complex **2.38** (243 MHz, acetone-d_6).

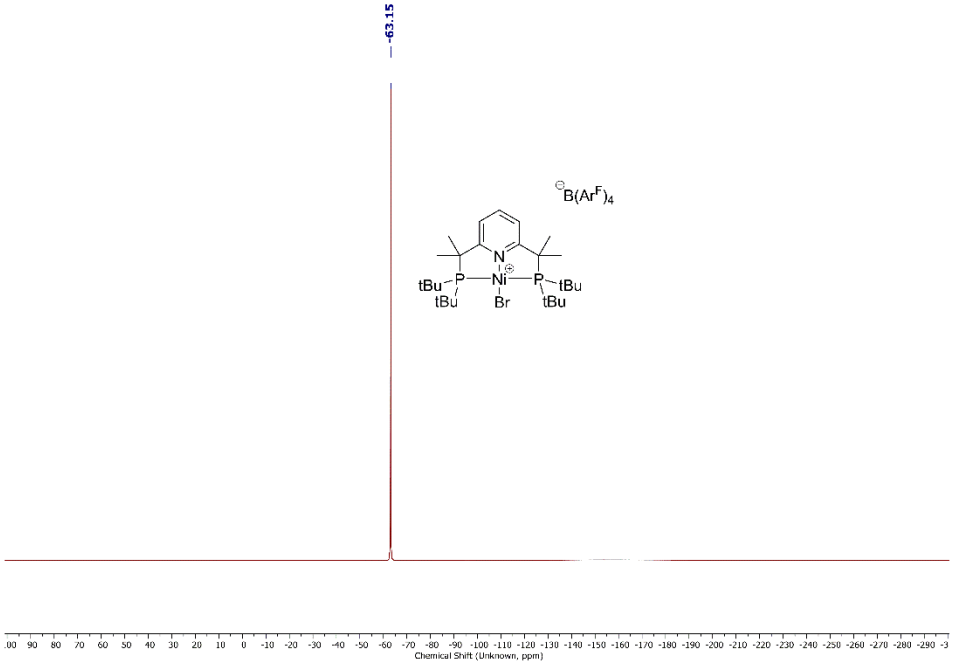

Figure 4.70 ^{19}F NMR spectrum of complex **2.38** (565 MHz, acetone-d_6)

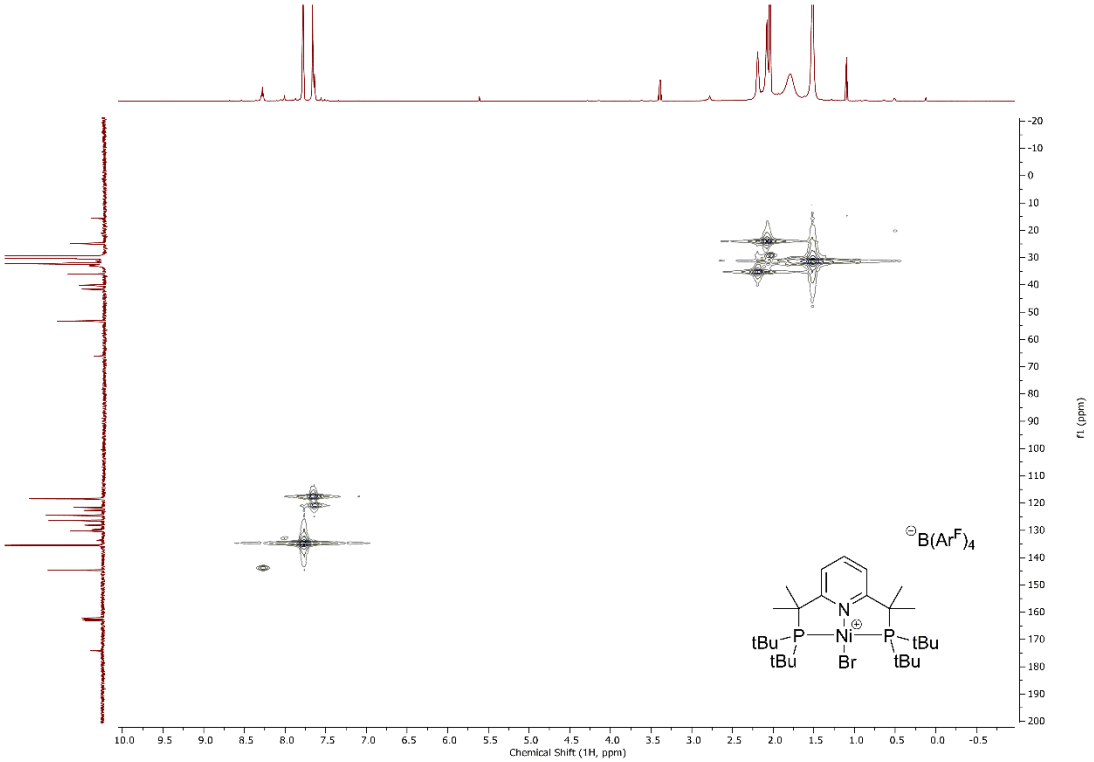

Figure 4.71 ^{1}H-^{13}C HMQC NMR spectrum of complex **2.38** (acetone-d_6).

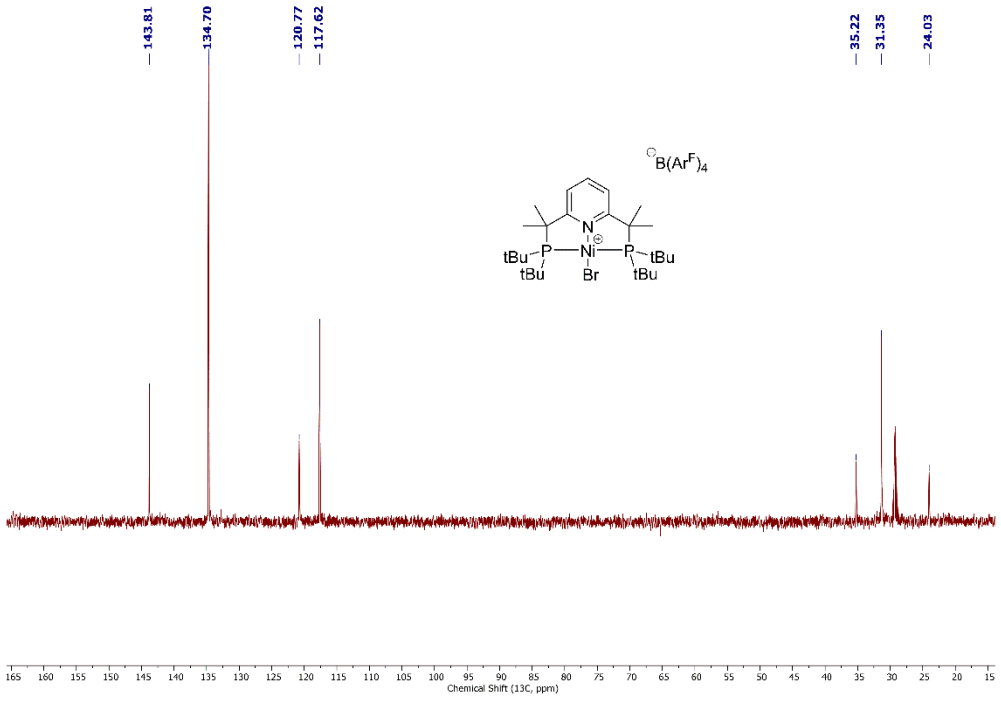

Figure 4.72 DEPT-135 NMR spectrum of complex **2.38** (151 MHz, acetone-d_6).

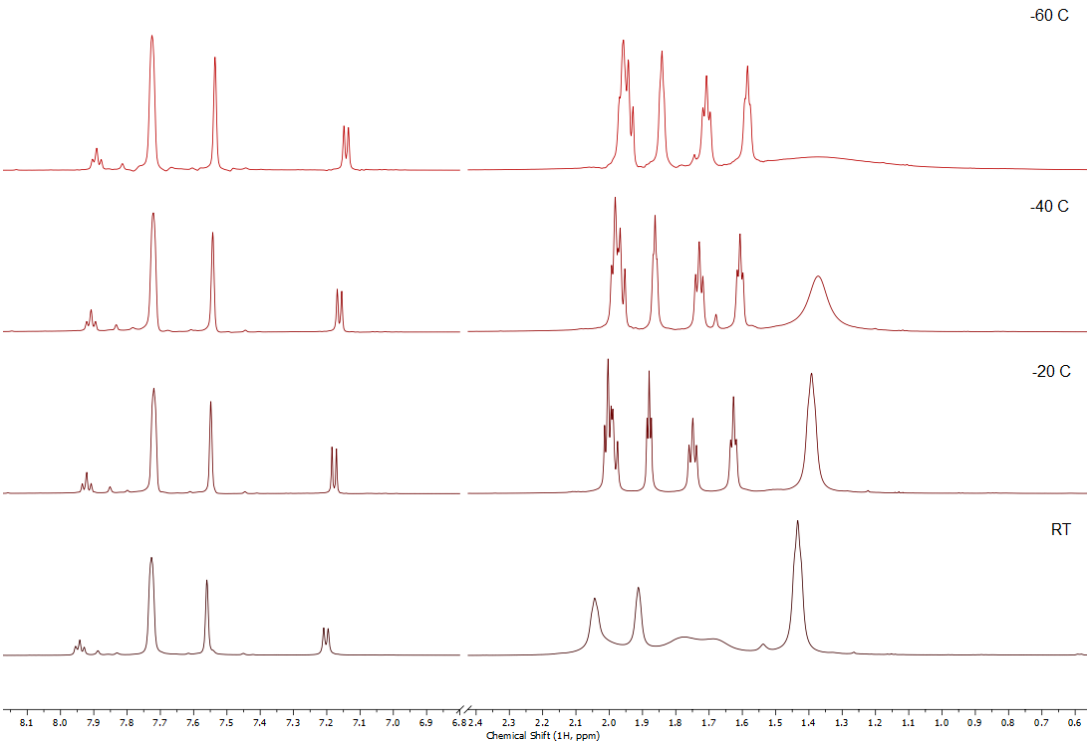

Figure 4.73 Variable temperature ^{1}H NMR spectra of complex **2.38** (600 MHz, CD_2Cl_2). Aromatic and aliphatic regions were selected to show the changes.

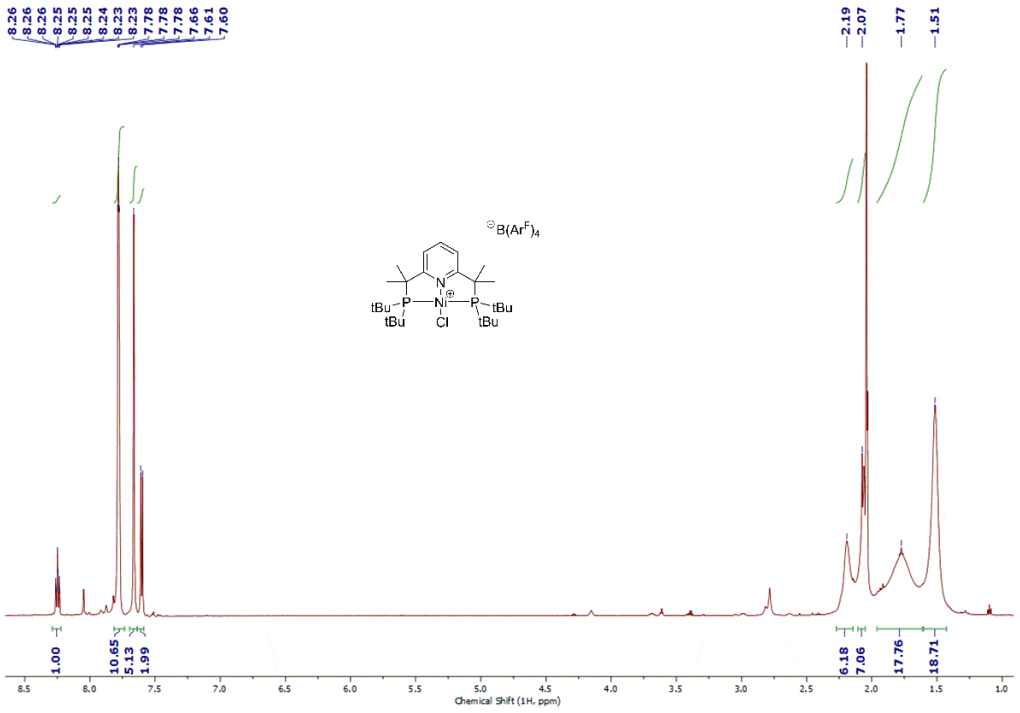

Figure 4.74 ^{1}H NMR spectrum of complex **2.39** (400 MHz, acetone-d_6).

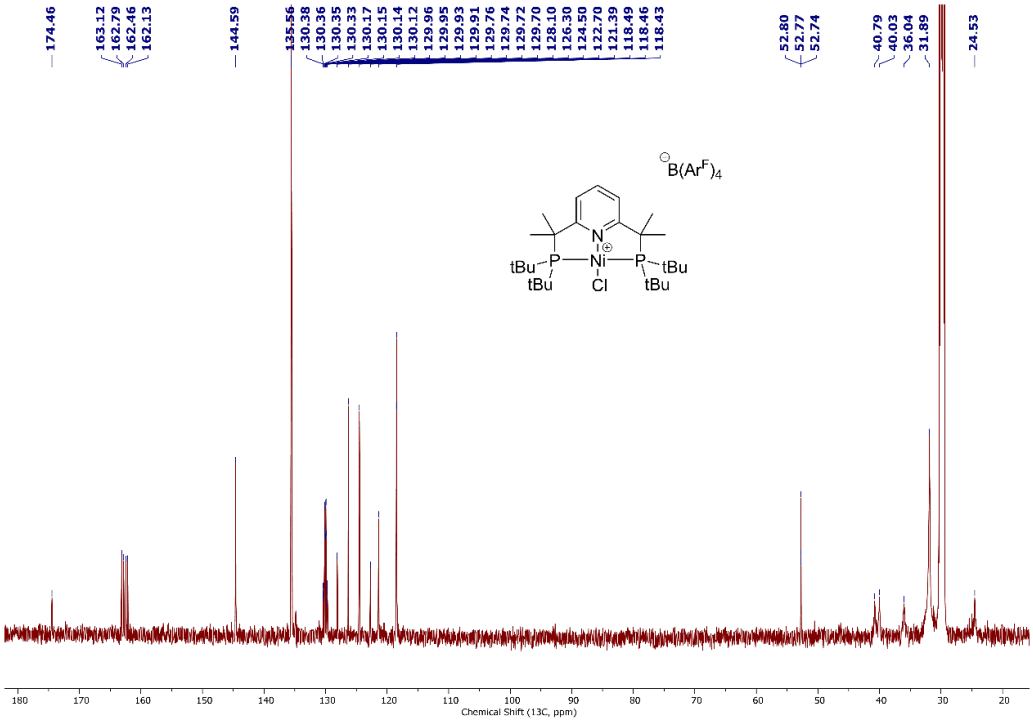

Figure 4.75 $^{13}C\{^{1}H\}$ NMR spectrum of complex **2.39** (101 MHz, acetone-d_6)

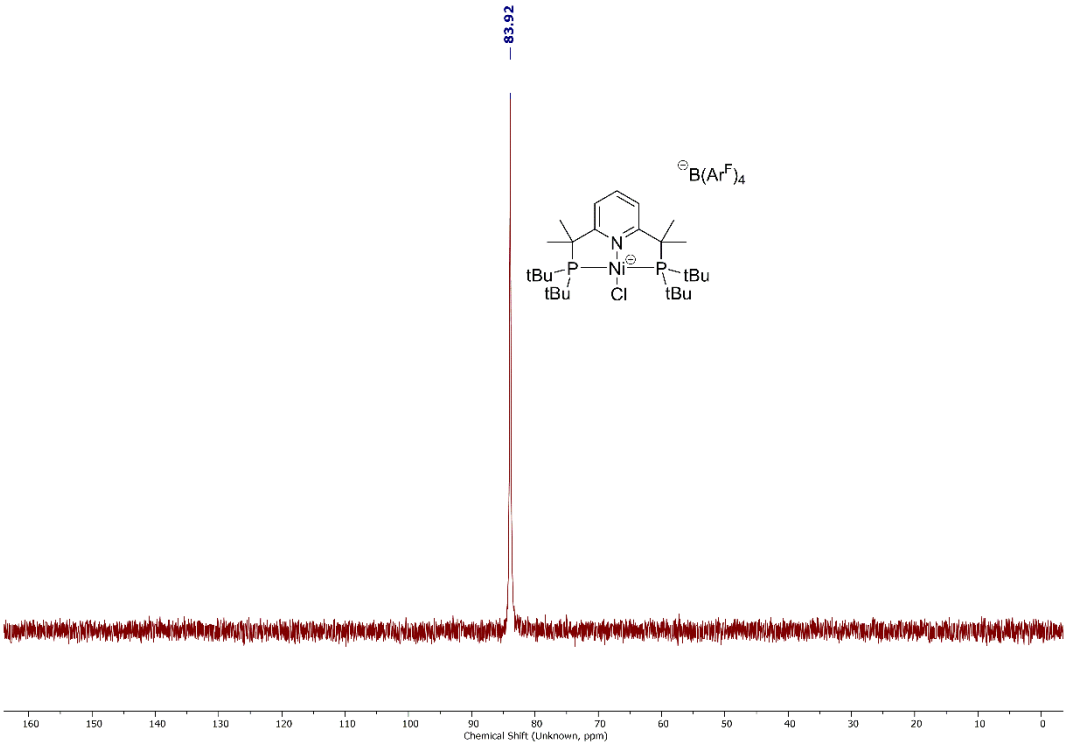

Figure 4.76 $^{31}P\{^{1}H\}$ NMR spectrum of 2.39 (162 MHz, acetone-d_6).

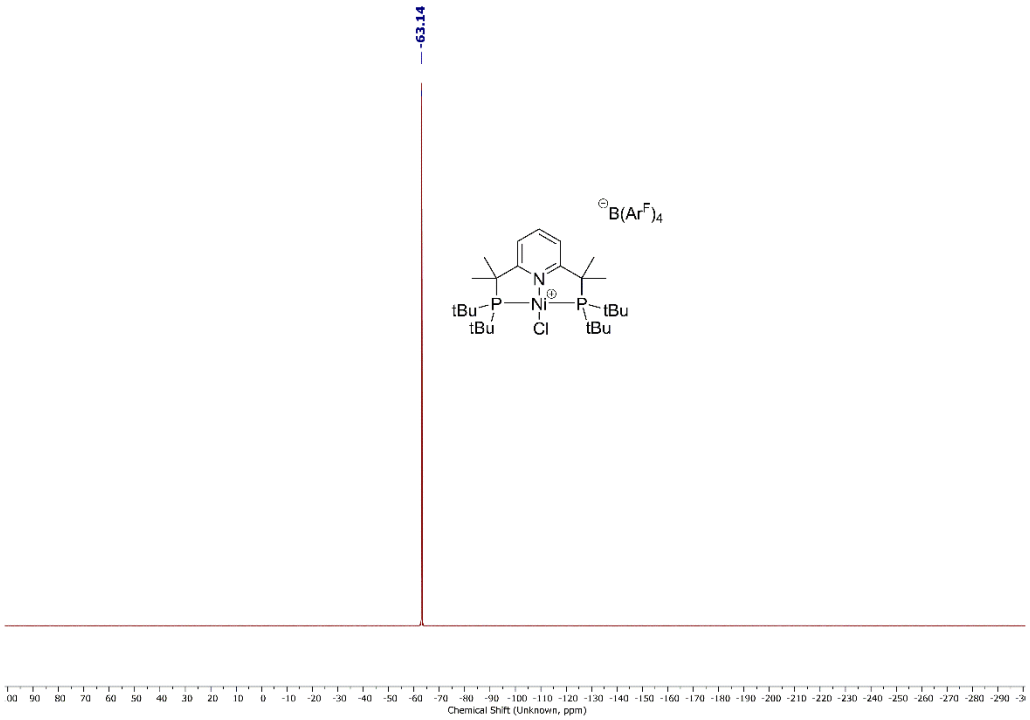

Figure 4.77 $^{19}F\{^{1}H\}$ NMR spectrum of complex **2.39** (376.2 MHz, acetone-d_6).

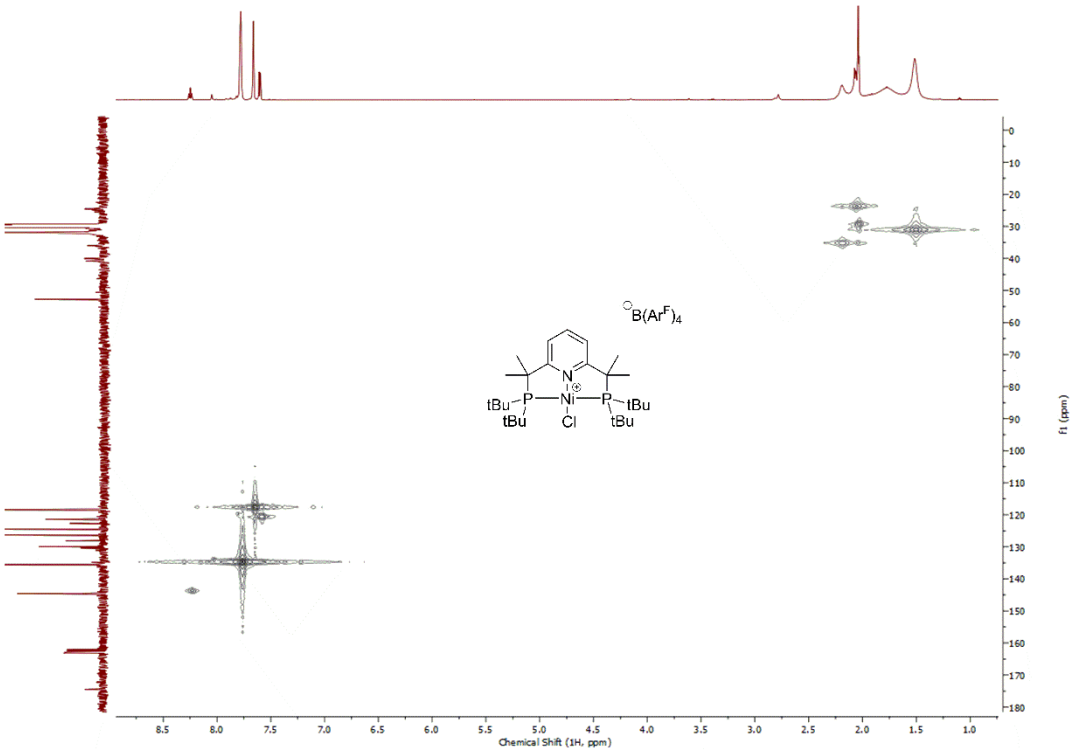

Figure 4.78 ^{1}H-^{13}C HMQC NMR spectrum of complex **2.39** (acetone-d_6)

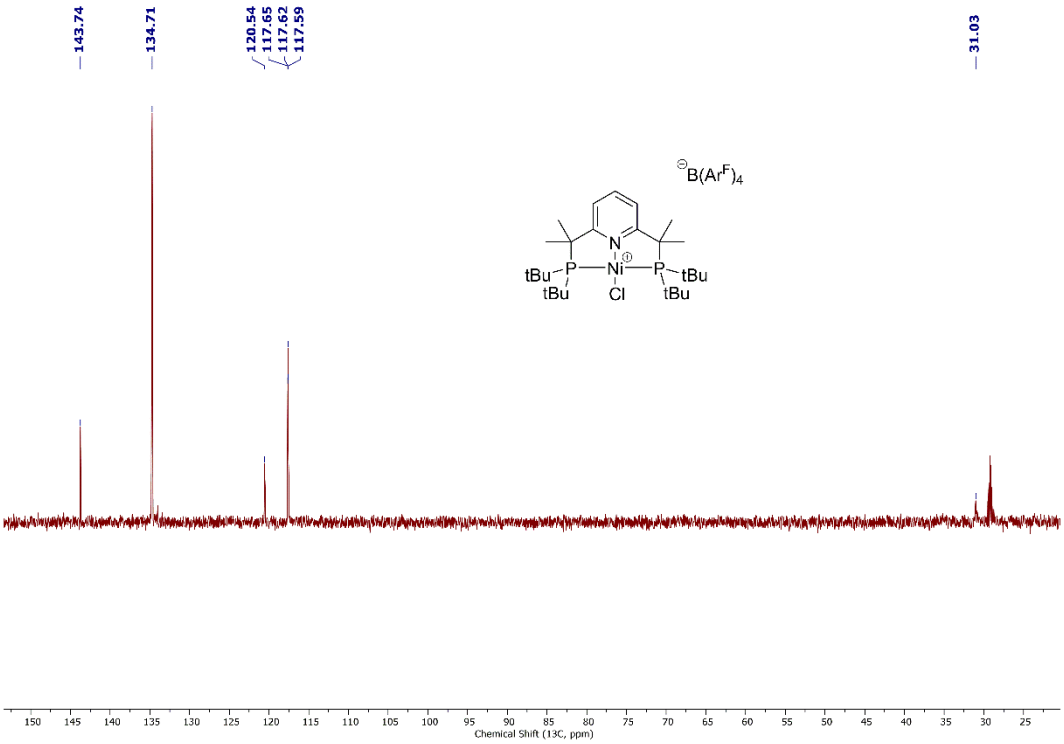

Figure 4.79 DEPT-135 NMR spectrum of complex **2.39** (101 MHz, acetone-d_6).

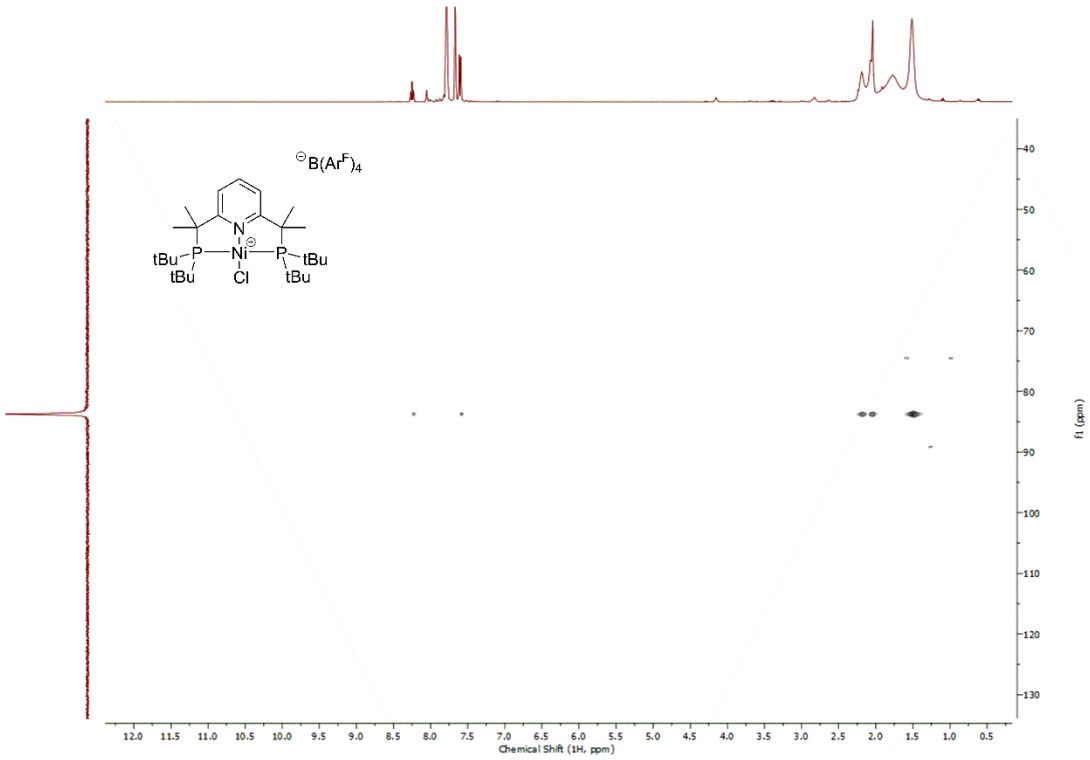

Figure 4.80 ^{1}H-^{31}P HMBC NMR spectra of **2.39** (acetone-d_6). ^{1}H-^{31}P HMBC spectrum shows long-range coupling between *para*-proton of pyridine and P-atom consistent with observed coupling in ^{1}H NMR spectrum.

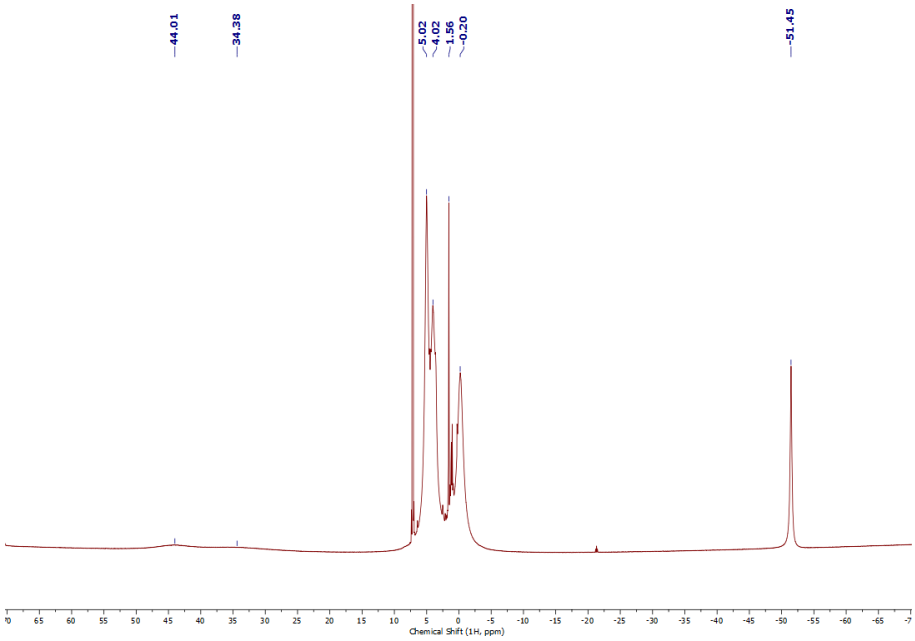

Figure 4.81 ^{1}H NMR spectrum of complex **2.40** (400 MHz, C_6D_6).

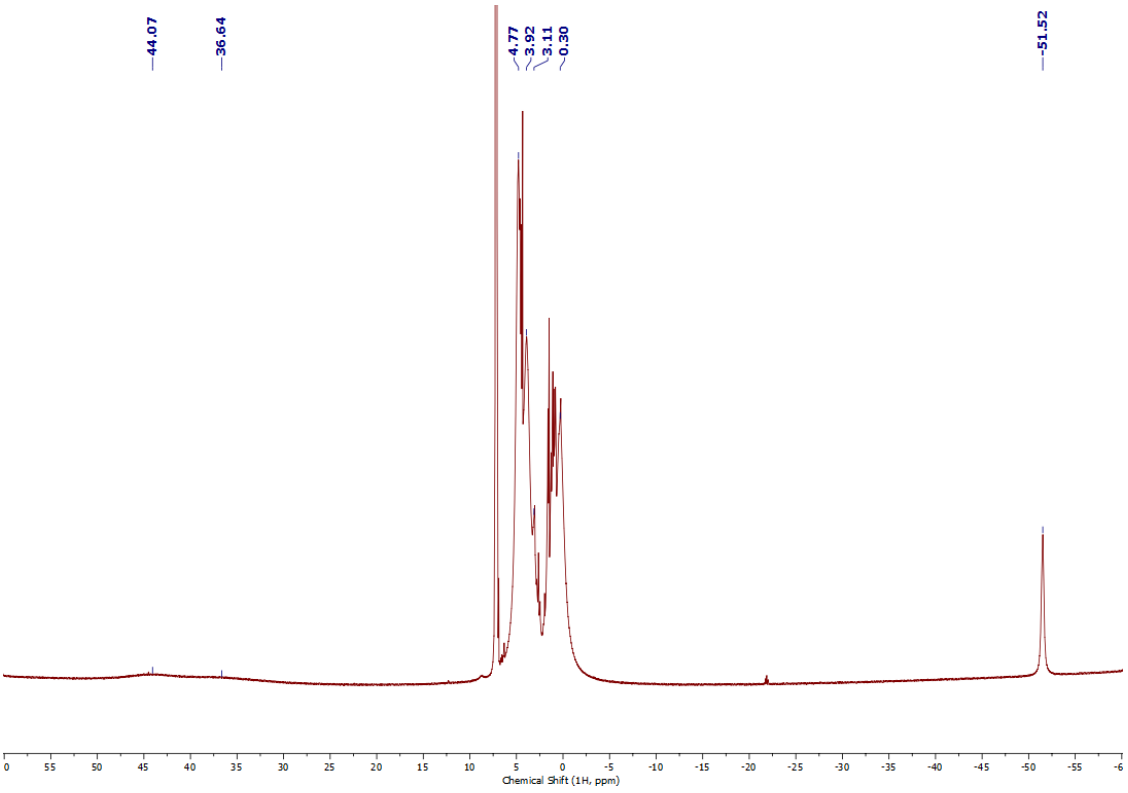

Figure 4.82 ^{1}H NMR spectrum of complex **2.41** (400 MHz, C_6D_6).

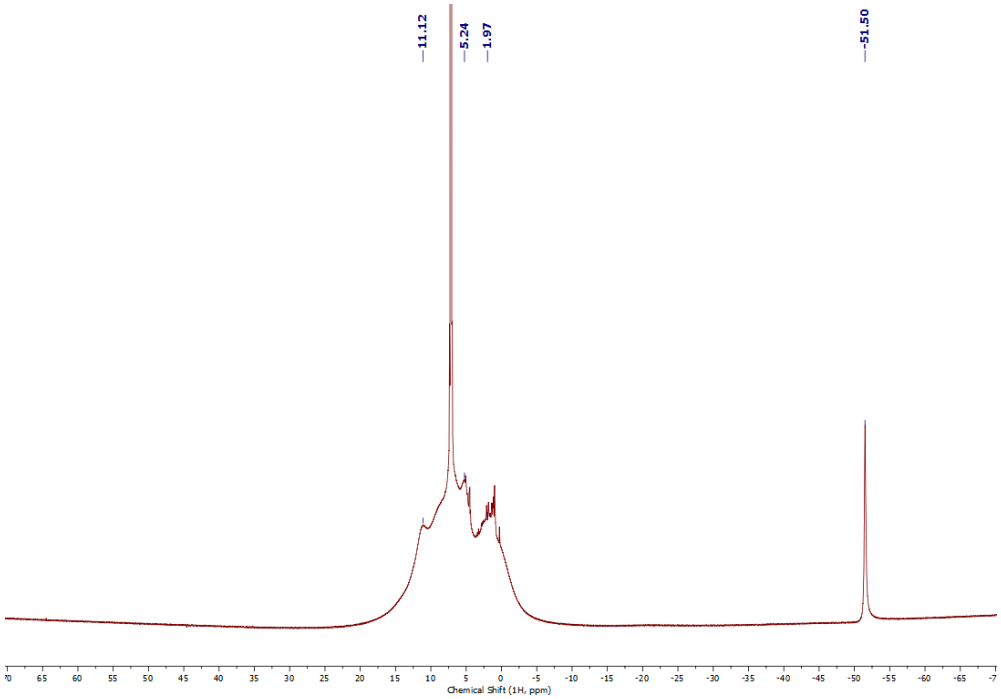

Figure 4.83 ^{1}H NMR spectrum of complex **2.42** (400 MHz, C_6D_6).

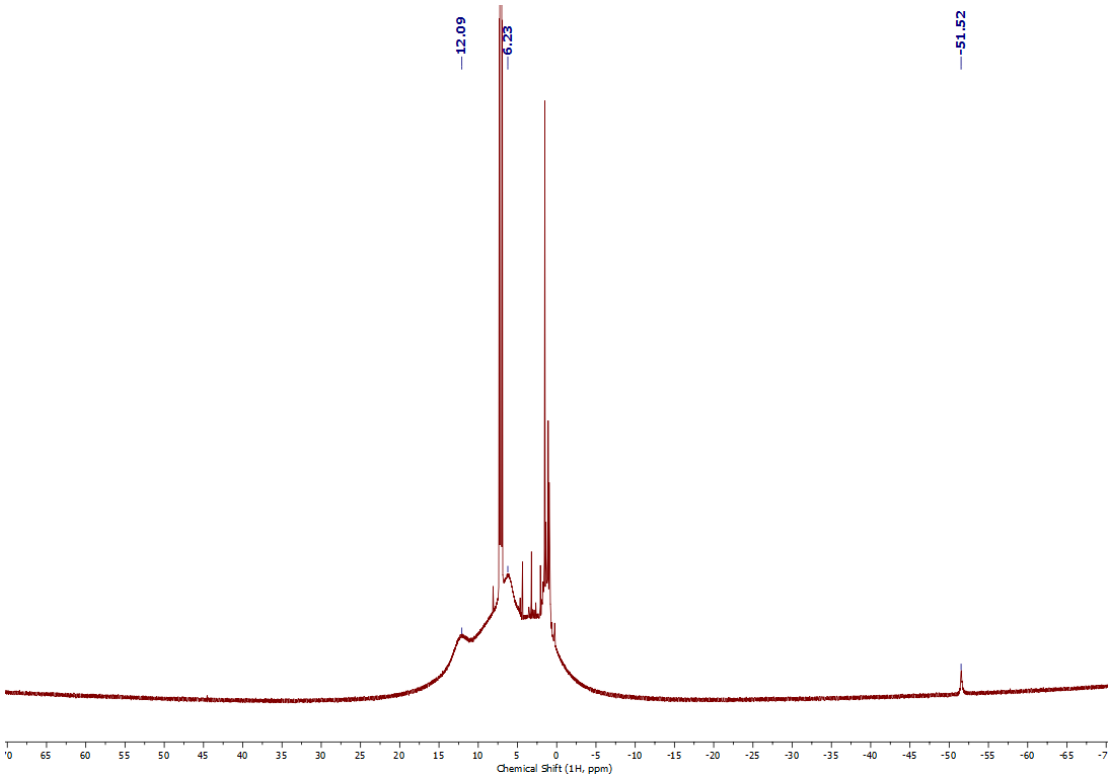

Figure 4.84 ^{1}H NMR spectrum of complex **2.43** (400 MHz, C_6D_6).

4.3 UV-vis spectra

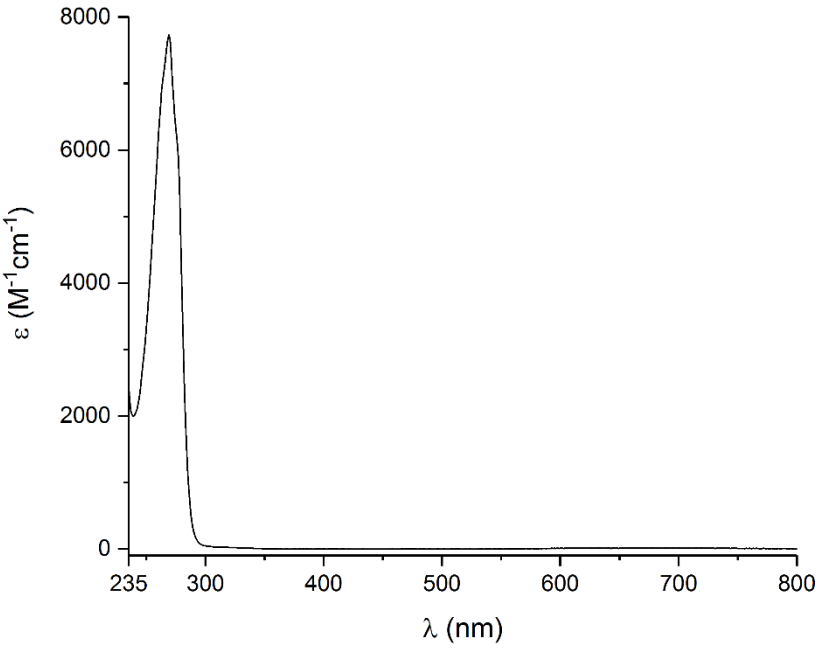

Figure 4.85 UV-vis spectrum of **L2.3**.

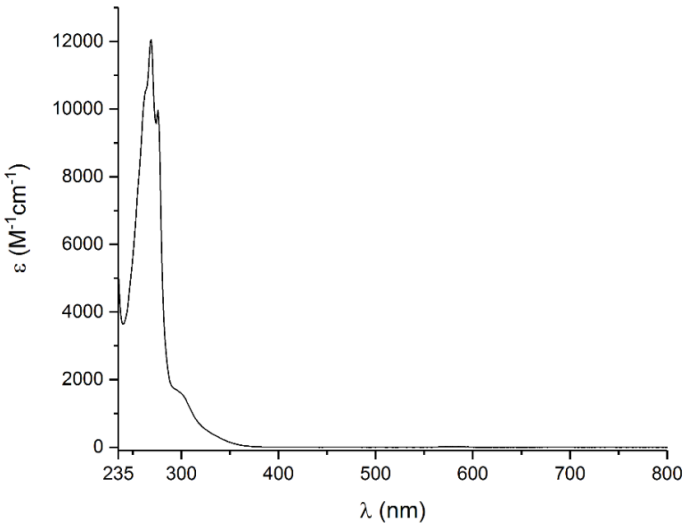

Figure 4.86 UV-vis spectrum of **L2.4**.

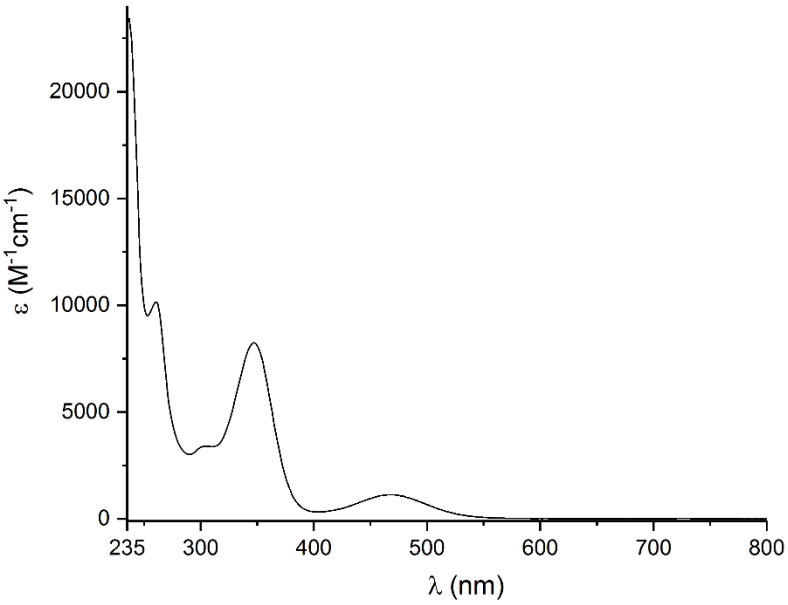

Figure 4.87 UV-vis spectrum of complex **2.32**.

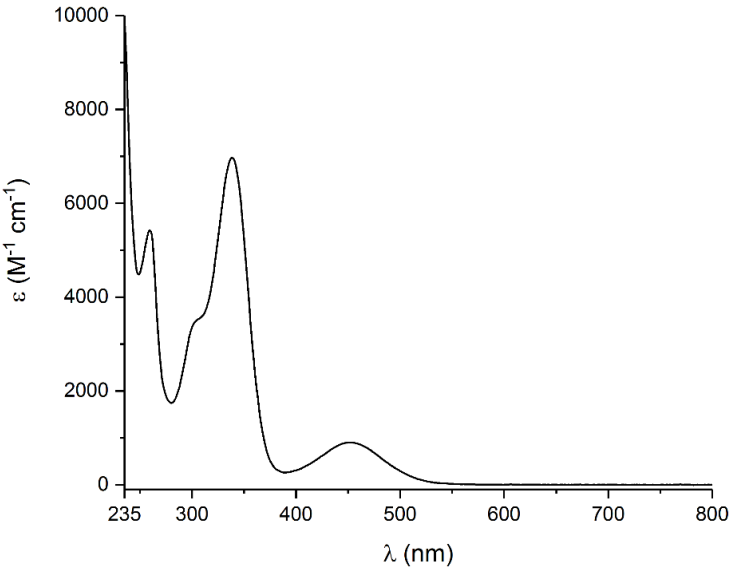

Figure 4.88 UV-vis spectrum of complex **2.33**.

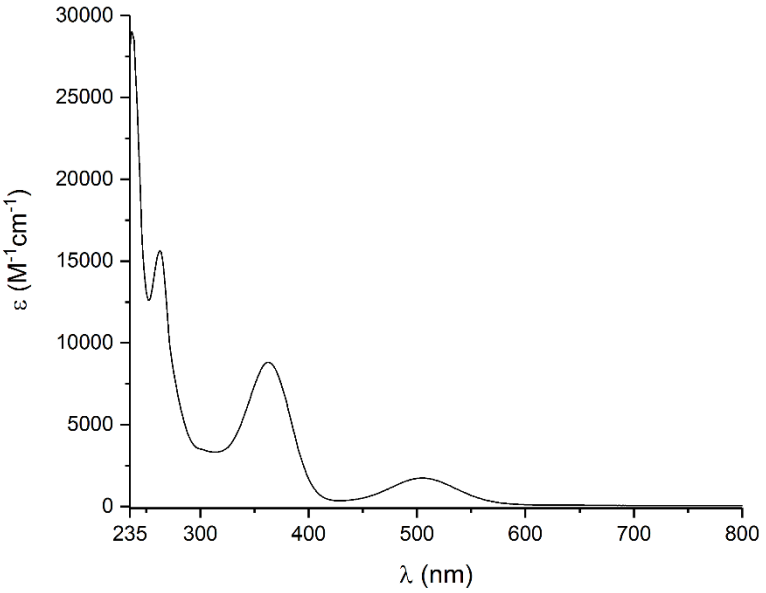

Figure 4.89 . UV-vis spectrum of complex **2.34**.

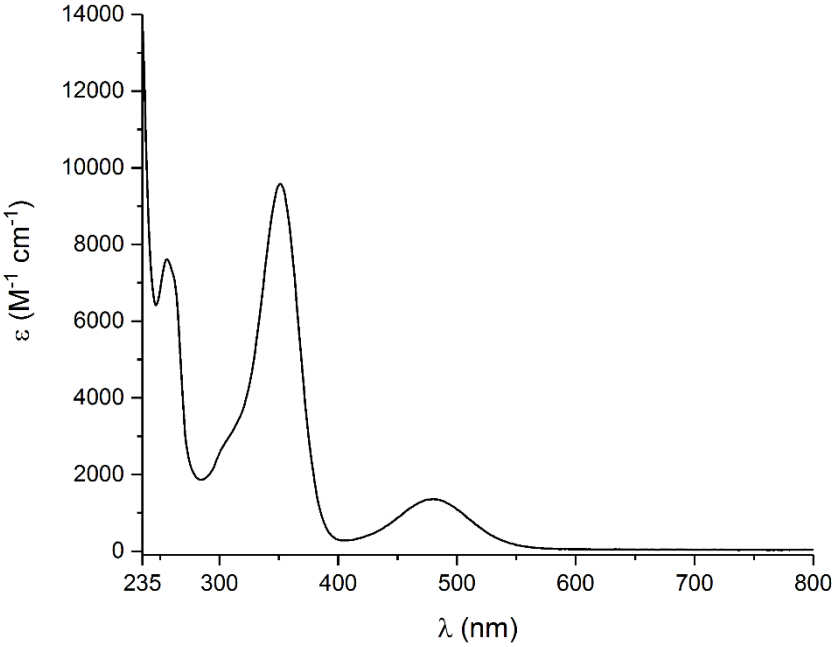

Figure 4.90 UV-vis spectrum of complex **2.35**

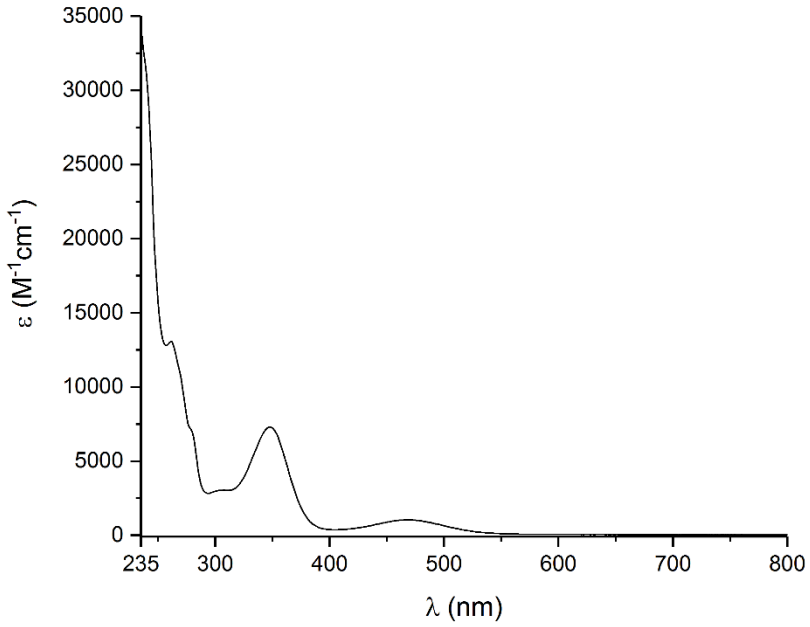

Figure 4.91 UV-vis spectrum of complex **2.36**.

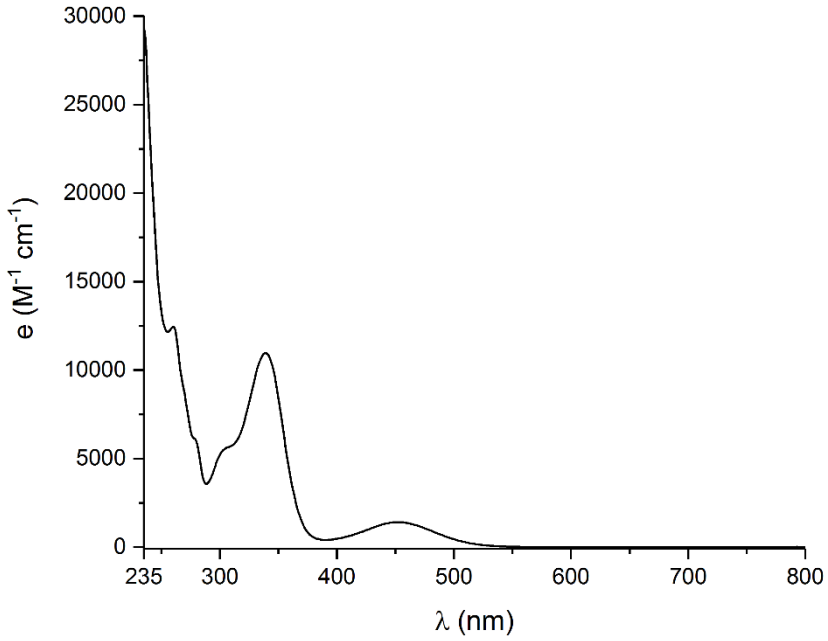

Figure 4.92 UV-vis spectrum of complex **2.37**.

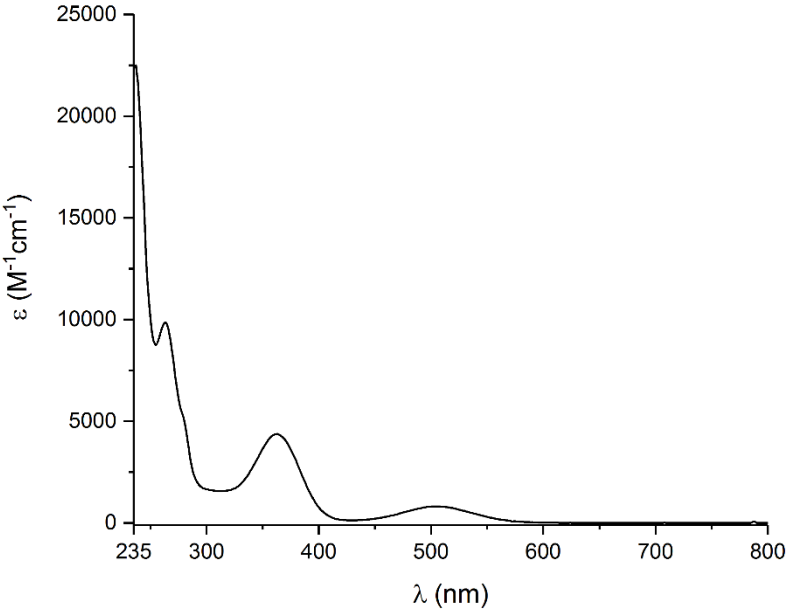

Figure 4.93 UV-vis spectrum of complex **2.38**.

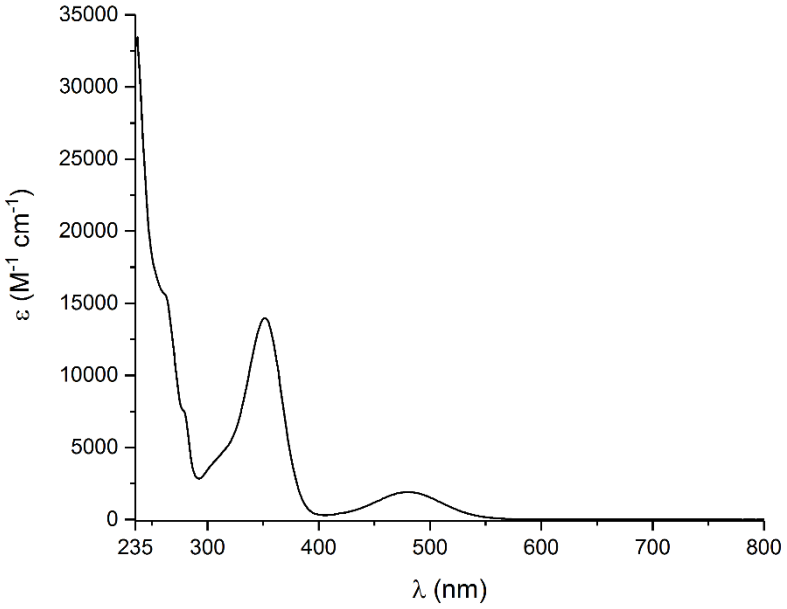

Figure 4.94 UV-vis spectrum of complex **2.39**.

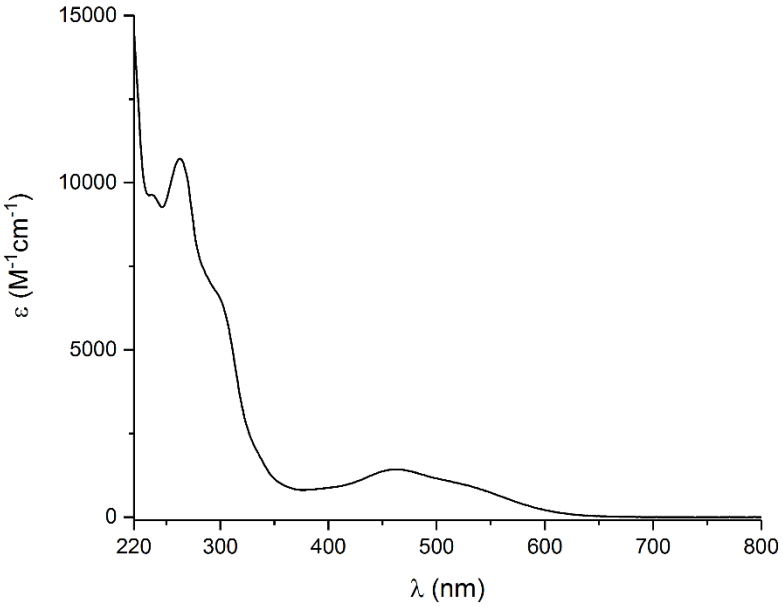

Figure 4.95 UV-vis spectrum of complex **2.40**.

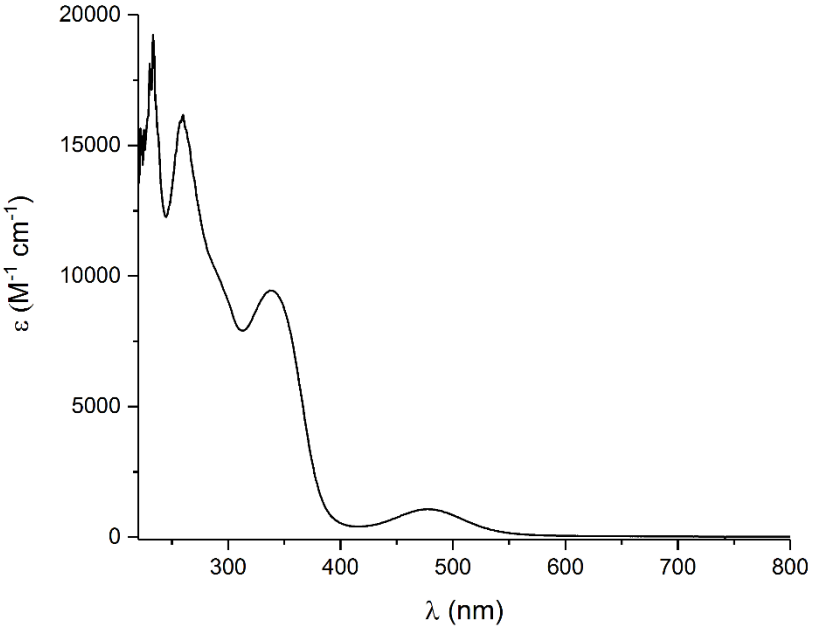

Figure 4.96 UV-vis spectrum of complex **2.41**

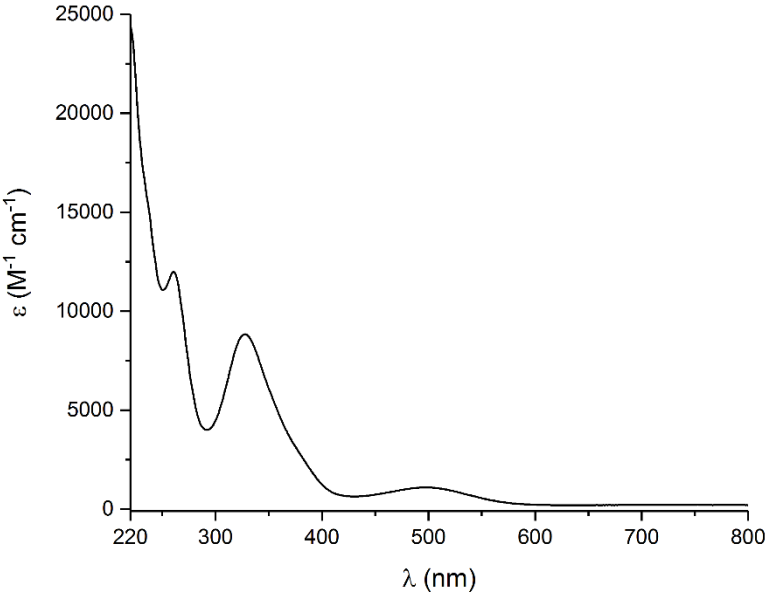

Figure 4.97 UV-vis spectrum of complex **2.42**.

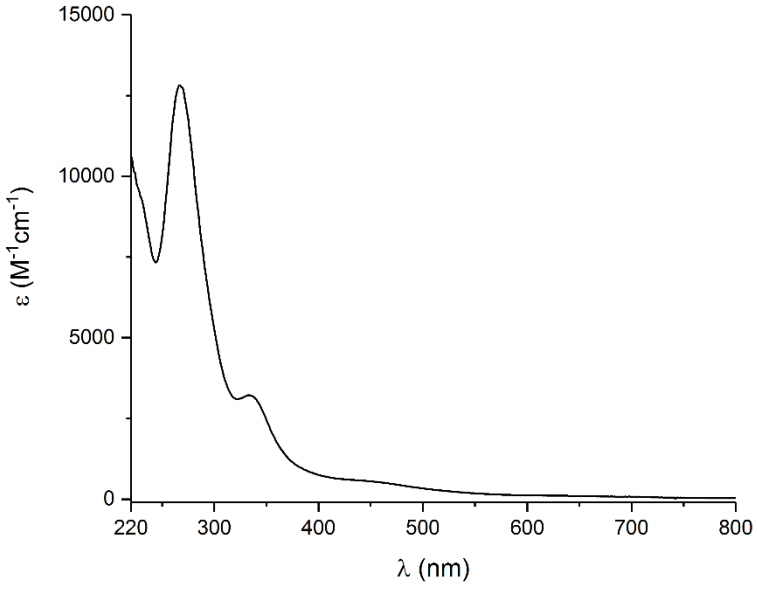

.

Figure 4.98 UV-vis spectrum of complex **2.43**

4.4 Cyclic voltammograms and coulometric studies

Table 4.6 Redox potentials for **L2.3** and **L2.4**.

Ligands	E_{ox} (mV)	E_{red} (mV)
L2.3	1783, 922	N/A
L2.4	1869, 1163	-2852

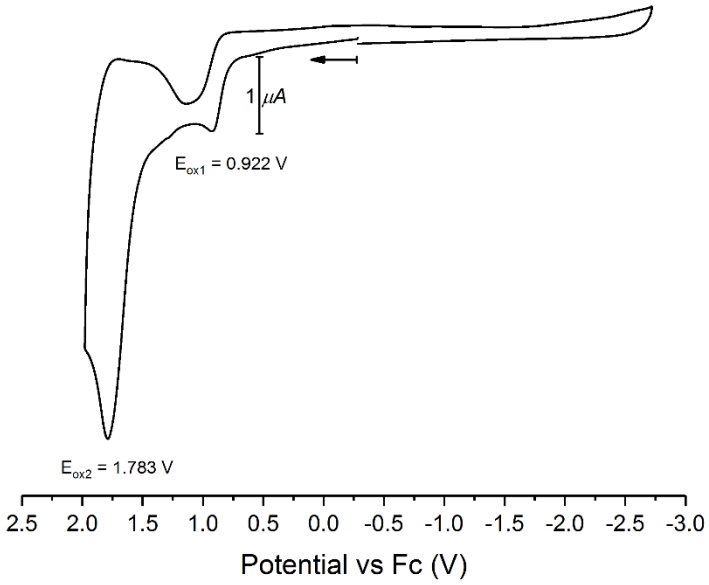

Figure 4.99 Full cyclic voltammogram of ligand **L2.4**.

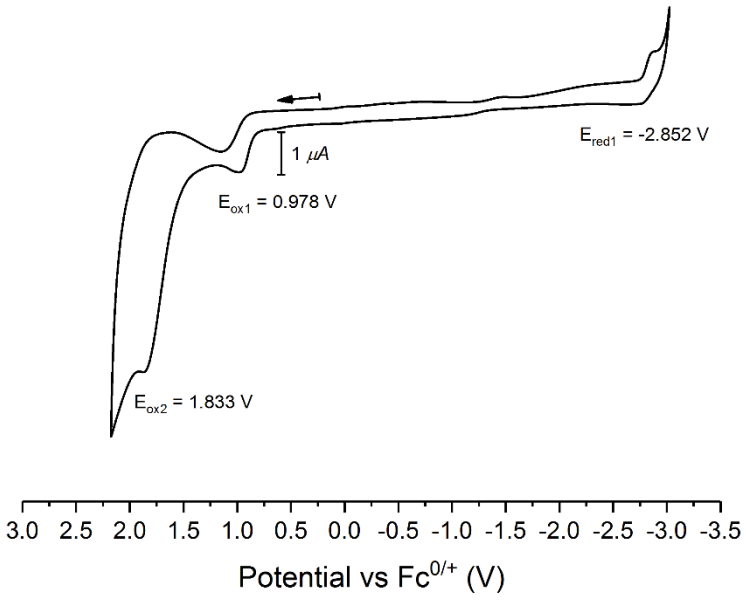

Figure 4.100 Cyclic voltammogram of ligand **L2.5**.

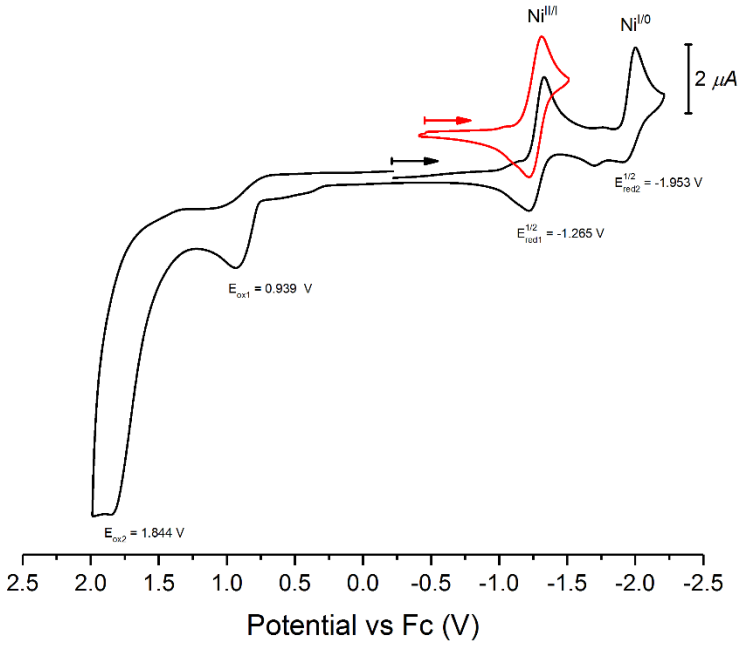

Figure 4.101 Full cyclic voltammogram of complex **2.36.** Red trace is a CV recorded in a shorter range to estimate reversibility of Ni^{II}/Ni^{I} wave; the curve was translated upwards in the vertical direction for clarity.

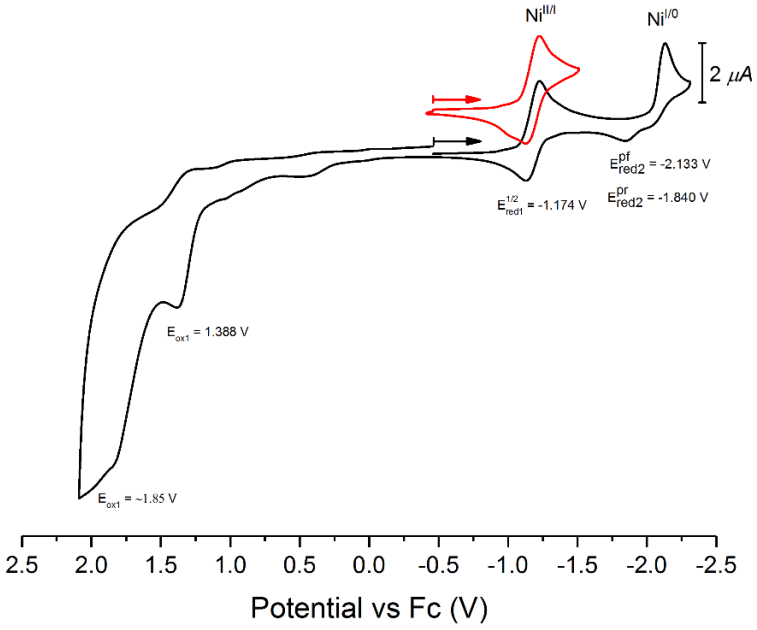

Figure 4.102 Full cyclic voltammogram of complex **2.38**. Red trace is a CV recorded in a shorter range to estimate reversibility of Ni^{II}/Ni^{I} wave; the curve was translated upwards in the vertical direction for clarity.

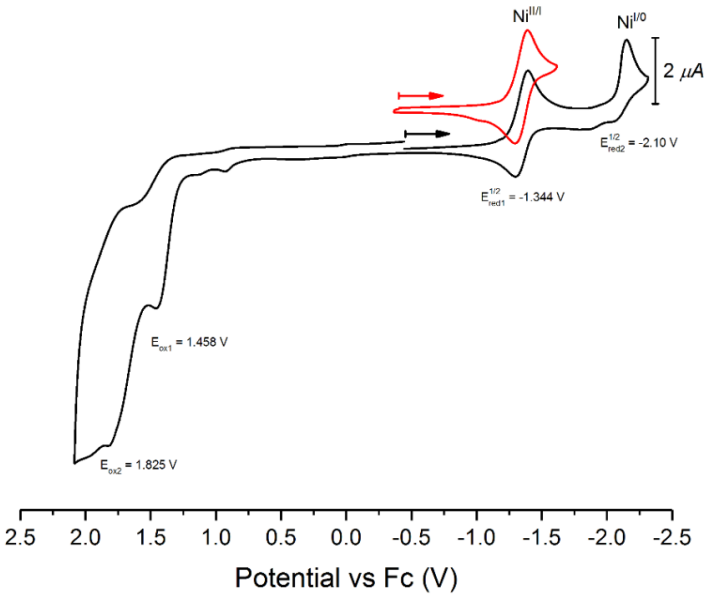

Figure 4.103 Full cyclic voltammogram of complex **2.39.** Red trace is a CV recorded in a shorter range to estimate reversibility of Ni^{II}/Ni^{I} wave; the curve was translated upwards in the vertical direction for clarity.

4.5 FT-IR spectra

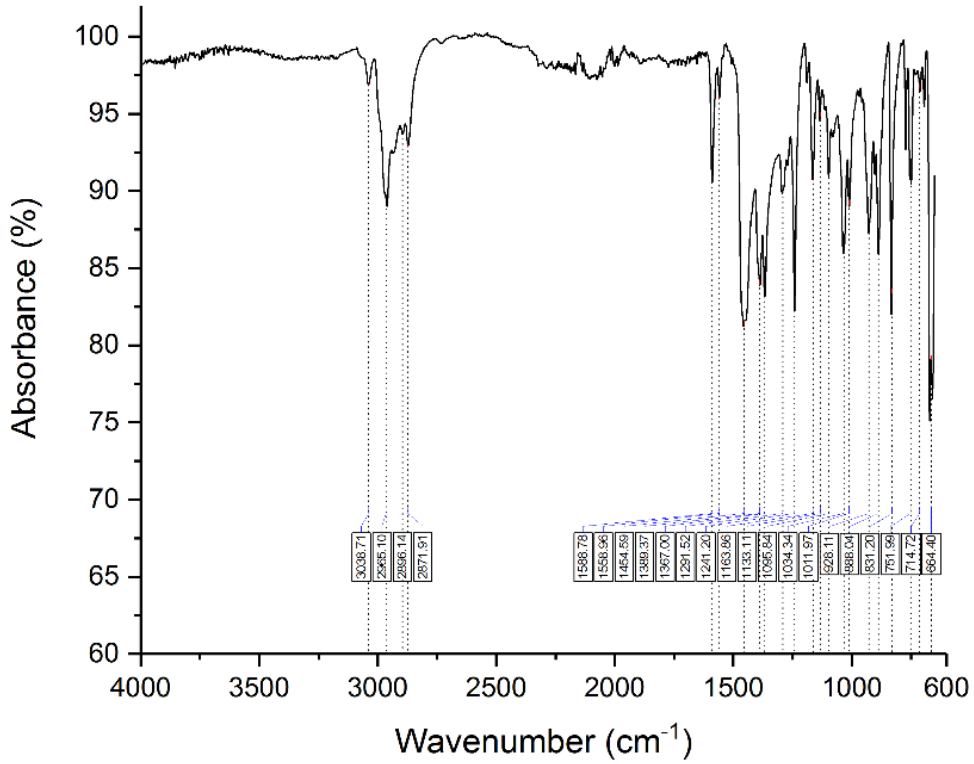

Figure 4.104 FT-IR (ATR) spectrum of **2.32** (solid).

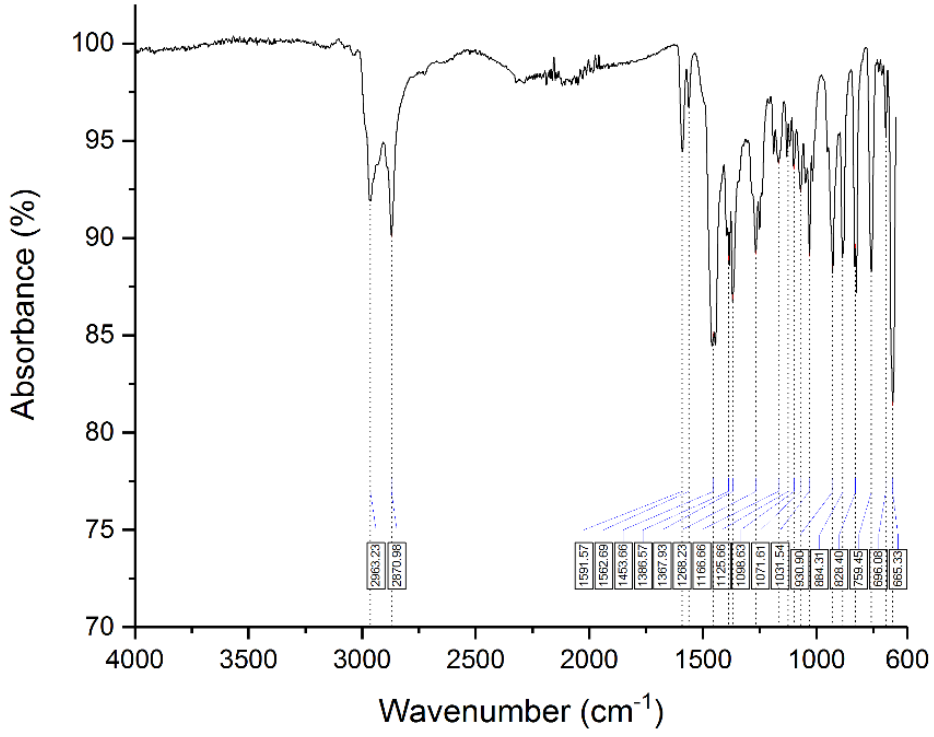

Figure 4.105 FT-IR (ATR) spectrum of **2.33** (solid).

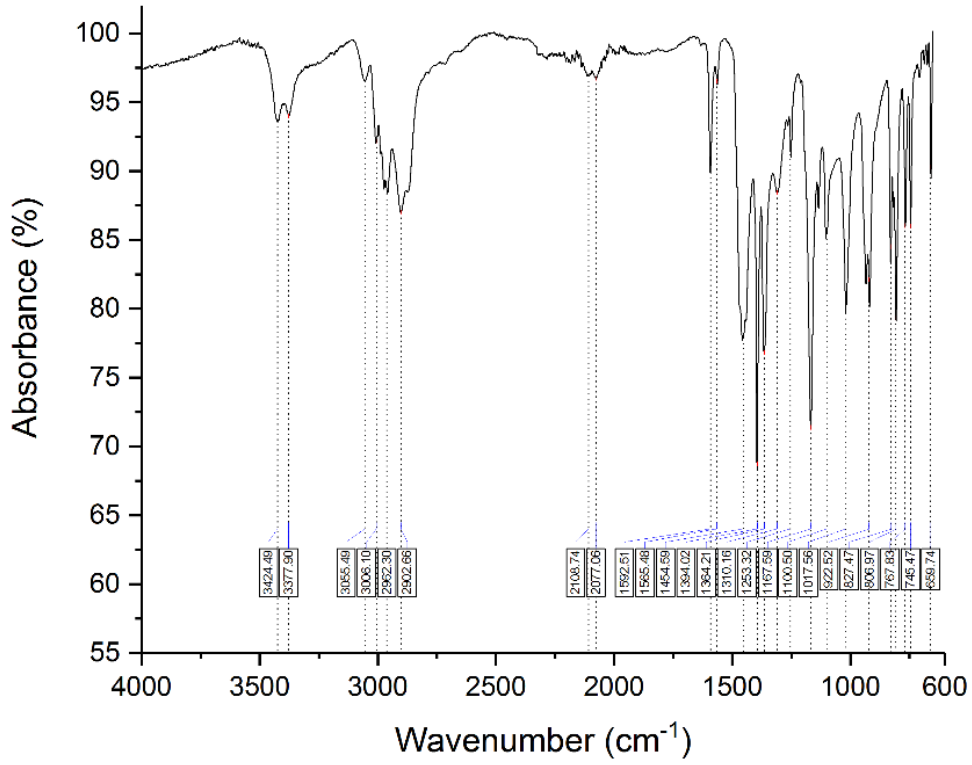

Figure 4.106 FT-IR (ATR) spectrum of **2.34** (solid).

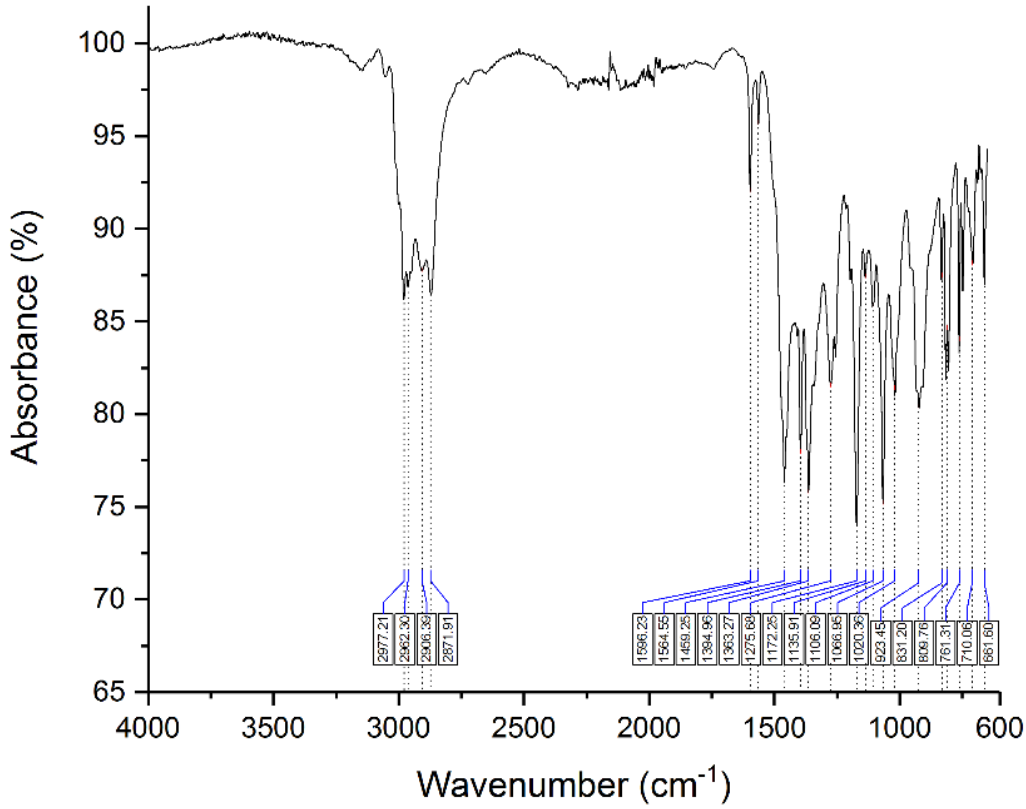

Figure 4.107 FT-IR (ATR) spectrum of **2.35** (solid).

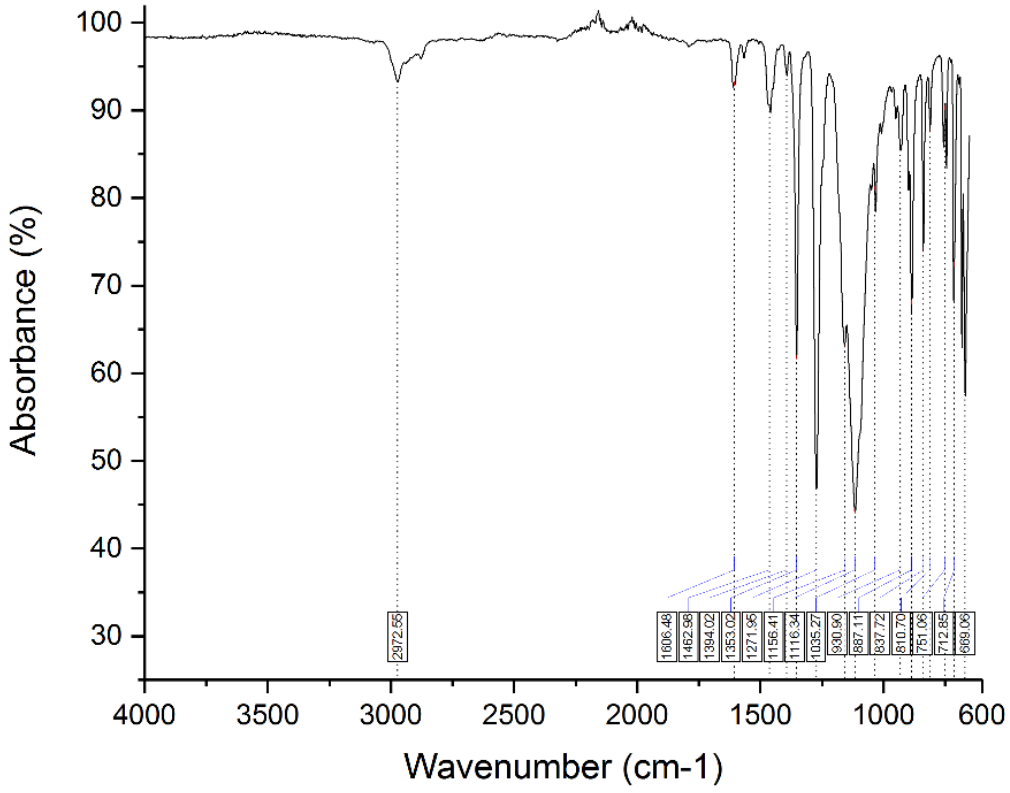

Figure 4.108 FT-IR (ATR) spectrum of **2.36** (solid).

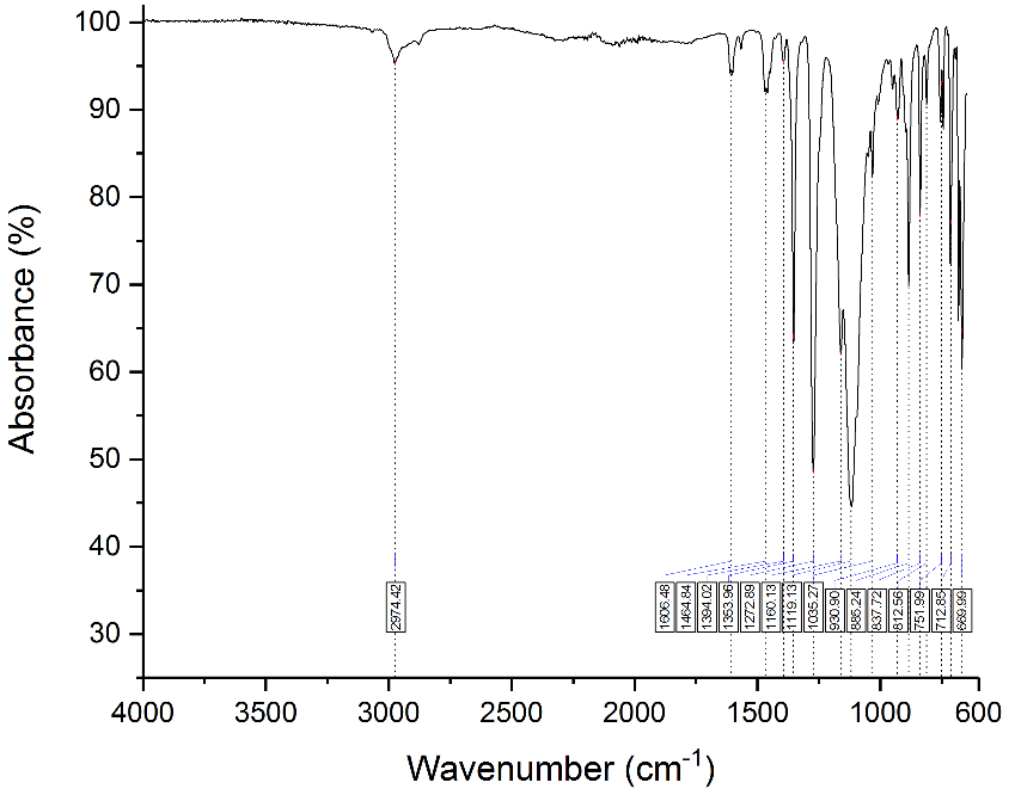

Figure 4.109 FT-IR (ATR) spectrum of **2.37** (solid**).**

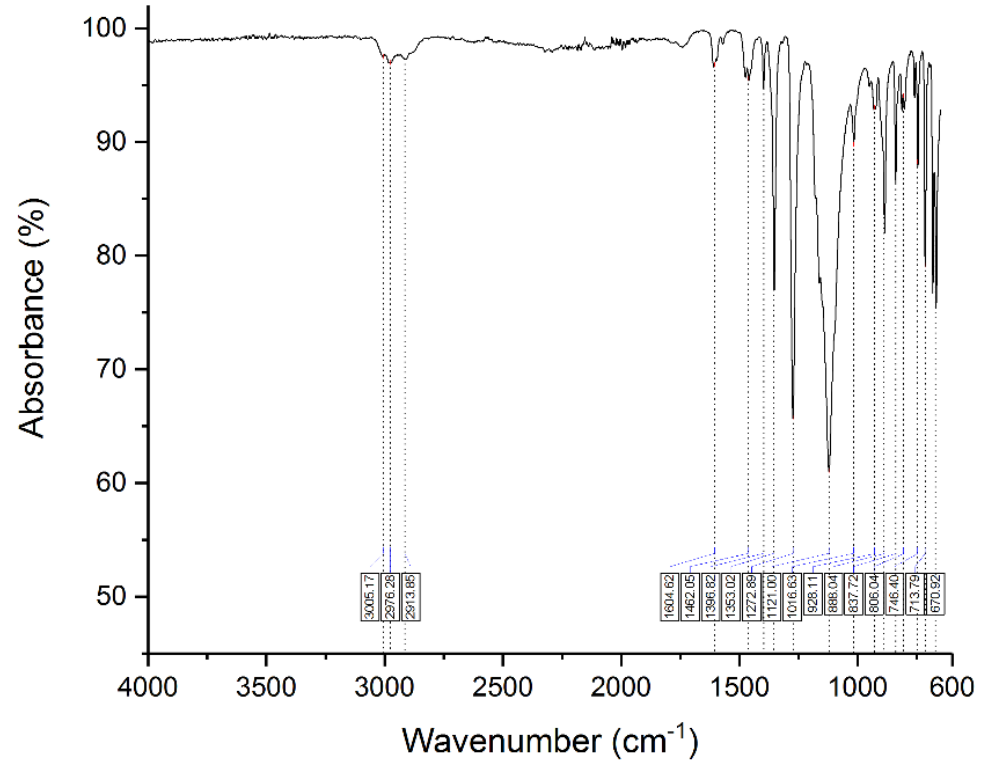

Figure 4.110 FT-IR (ATR) spectrum of **2.38** (solid).

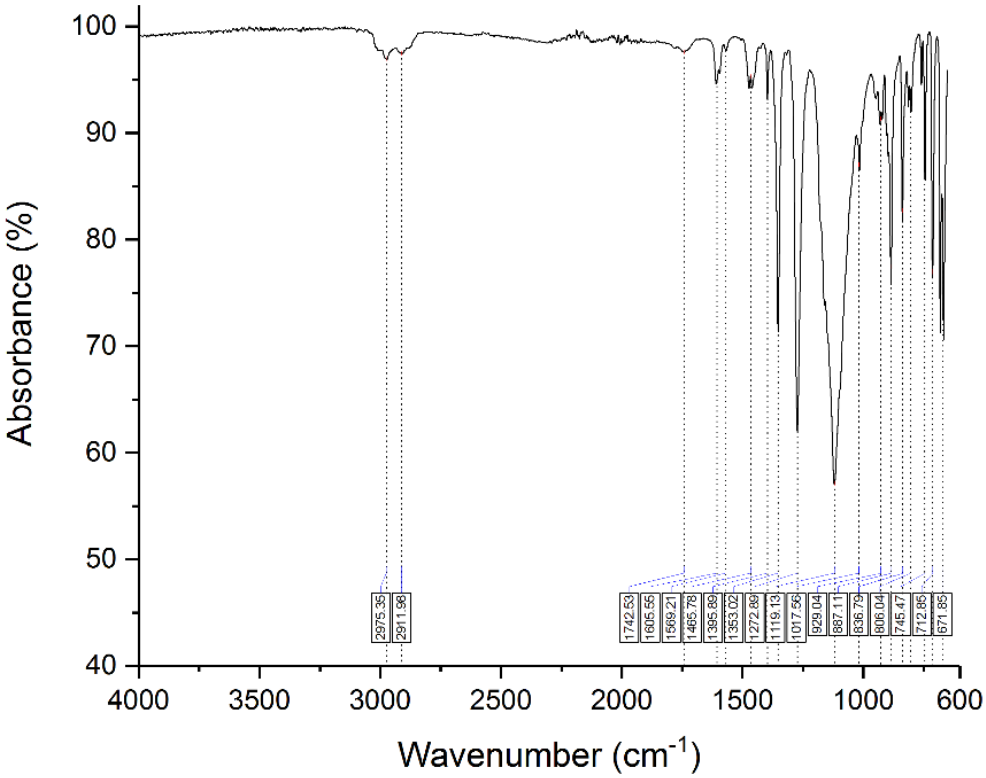

Figure 4.111 FT-IR (ATR) spectrum of **2.39** (solid).

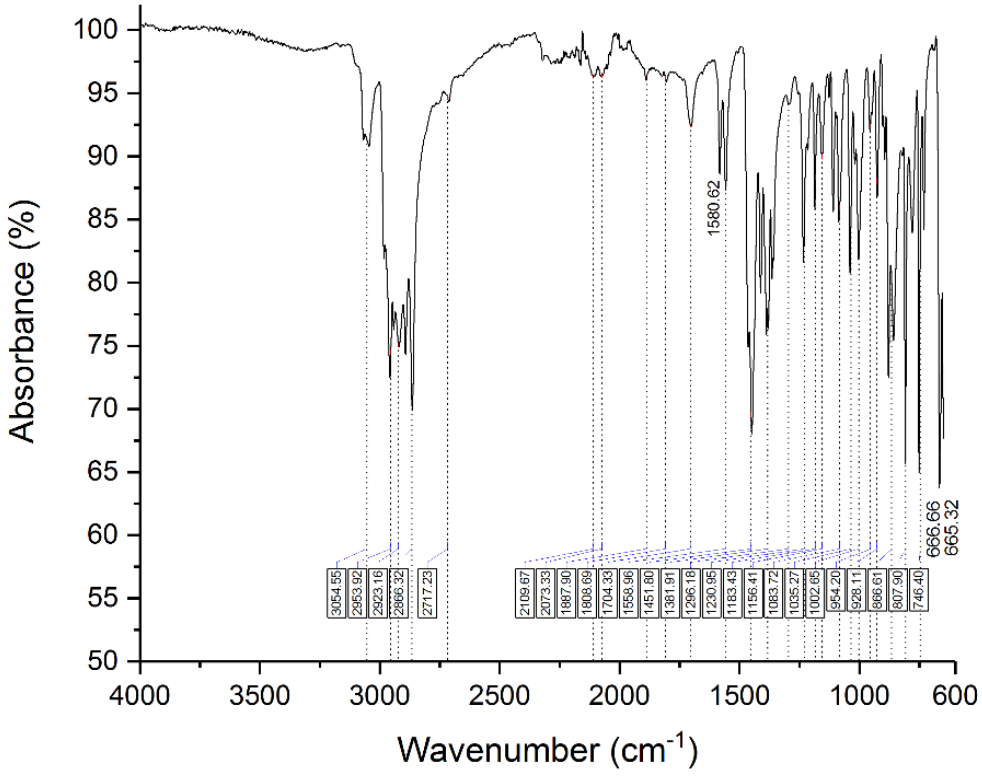

Figure 4.112 FT-IR (ATR) spectrum of **2.40** (solid).

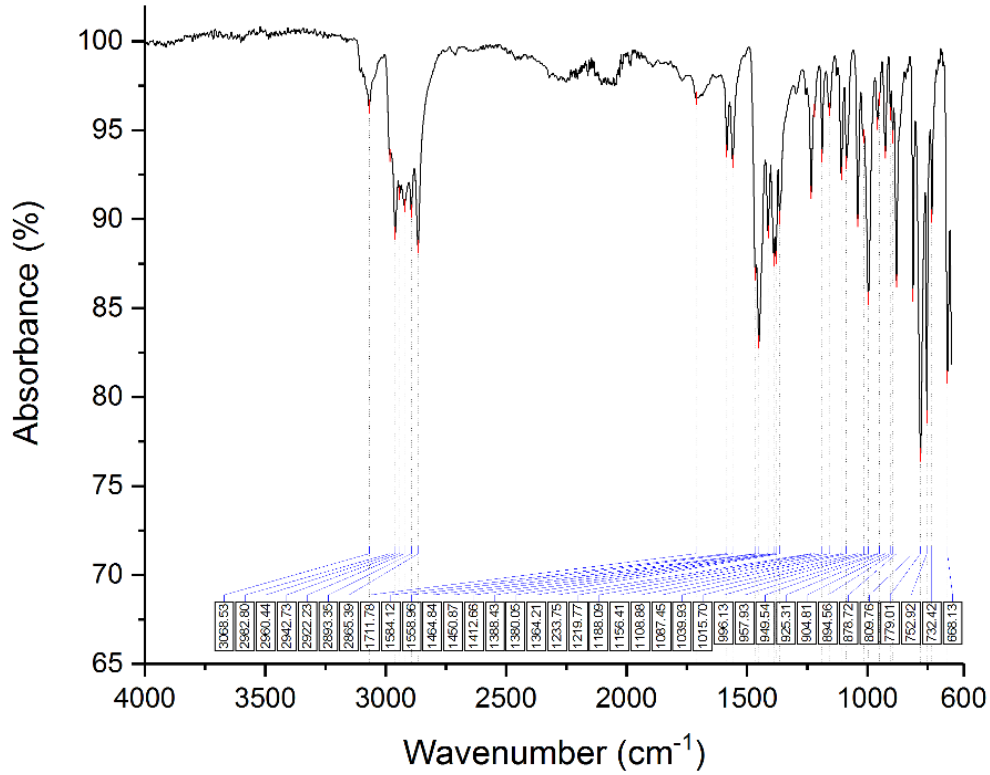

Figure 4.113 FT-IR (ATR) spectrum of **2.41** (solid).

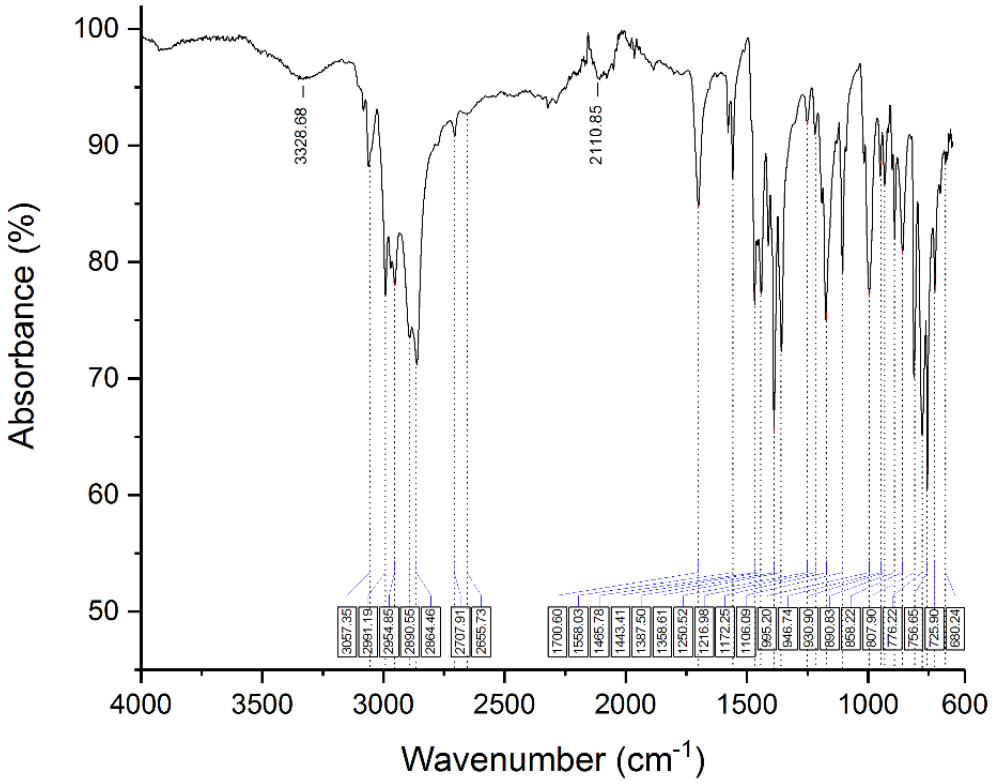

Figure 4.114 FT-IR (ATR) spectrum of **2.42** (solid).

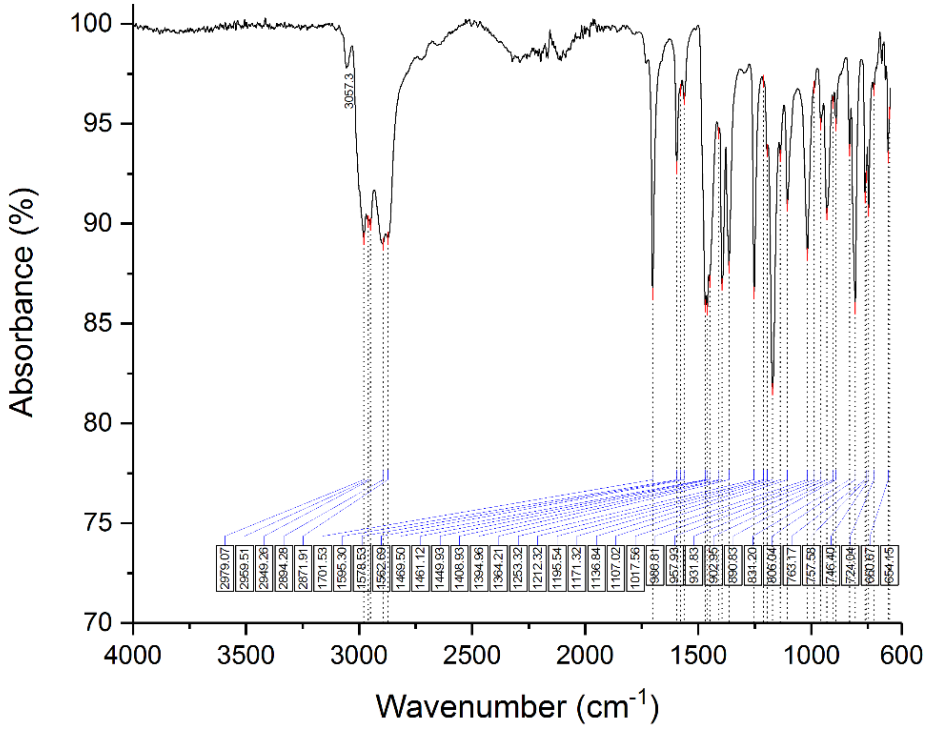

Figure 4.115 FT-IR (ATR) spectrum of **2.43** (solid).

4.6 EPR experiments

Table 4.7 Parameters used for EPR experiments.

Complexes	Temperature (K)	Solvent	Frequency (MHz)
2.36 obtained by electroreduction[a]	83.5	CH_3CN	9076.247
2.40	84	acetone	9076.602
2.41	92	MeTHF	9078.033
2.42	84	20% acetone : MeTHF	9082.155
2.43	92	35% acetone : MeTHF	9076.789

[a] This is the measurement from the *in situ* electrolysis experiment, where an aliquot of the acetonitrile solution after electrolysis was measured.

4.7 Computational data

71

Complex 5 iPrPNPMe4NiBr ub3lyp/6-311++g(d,p) PCHN Lanl2dz NiBr

Br	-0.00000	-2.51036	-1.67077
Ni	-0.00000	-0.57200	-0.00959
P	2.22610	-0.17906	0.48566
P	-2.22610	-0.17906	0.48566
N	-0.00000	1.38150	-0.75027
C	1.17664	2.03274	-0.88268
C	-1.17664	2.03274	-0.88268
C	1.19979	3.41034	-1.11080
H	2.13715	3.93838	-1.20691
C	2.92715	0.60865	2.05453
H	3.94849	0.93746	1.83713
C	-1.19979	3.41034	-1.11080
H	-2.13715	3.93838	-1.20691
C	-0.00000	4.10146	-1.21482
H	-0.00000	5.17255	-1.38518
C	3.00236	-2.87930	0.73340
H	3.18253	-2.85502	1.81011
H	3.58870	-3.70679	0.32100
H	1.95021	-3.10150	0.55268
C	2.46213	1.19114	-0.86320
C	-2.55120	0.50252	-2.25344
H	-1.74969	-0.22209	-2.40708
H	-2.48665	1.26504	-3.03639
H	-3.50897	-0.00854	-2.37131
C	-2.46213	1.19114	-0.86320
C	3.41811	-1.57179	0.03104
H	3.19260	-1.72524	-1.02722

C	4.92279	-1.30878	0.18637
H	5.27670	-0.48682	-0.43855
H	5.48045	-2.20243	-0.11292
H	5.20125	-1.08860	1.22063
C	2.97978	-0.39987	3.21402
H	1.99968	-0.85297	3.39048
H	3.27892	0.11374	4.13367
H	3.69606	-1.20275	3.03990
C	2.55120	0.50252	-2.25344
H	3.50897	-0.00854	-2.37131
H	2.48665	1.26504	-3.03639
H	1.74969	-0.22209	-2.40708
C	2.09432	1.82742	2.47821
H	2.03562	2.59931	1.70945
H	2.53228	2.28270	3.37266
H	1.07315	1.52709	2.72292
C	-3.41811	-1.57179	0.03104
H	-3.19261	-1.72524	-1.02722
C	-3.71846	2.06149	-0.67599
H	-4.60737	1.43646	-0.60109
H	-3.86853	2.71417	-1.54210
H	-3.67646	2.69020	0.21495
C	-3.00236	-2.87930	0.73339
H	-1.95021	-3.10149	0.55267
H	-3.58870	-3.70678	0.32100
H	-3.18252	-2.85503	1.81011
C	-2.92714	0.60865	2.05453
H	-3.94849	0.93746	1.83713
C	-2.97978	-0.39987	3.21402
H	-3.69606	-1.20275	3.03990
H	-3.27891	0.11374	4.13368
H	-1.99968	-0.85297	3.39048

C	3.71846	2.06149	-0.67599
H	3.67646	2.69020	0.21495
H	3.86853	2.71418	-1.54209
H	4.60737	1.43646	-0.60109
C	-2.09432	1.82742	2.47821
H	-1.07315	1.52709	2.72292
H	-2.53228	2.28270	3.37265
H	-2.03562	2.59931	1.70945
C	-4.92279	-1.30877	0.18638
H	-5.20125	-1.08860	1.22063
H	-5.48045	-2.20243	-0.11292
H	-5.27670	-0.48681	-0.43854

71

Complex 6 iPrPNPMe4NiCl ub3lyp/6-311++g(d,p) PCHN Lanl2dz NiCl

Ni	-0.00000	-0.67774	-0.31460
Cl	-0.00000	-2.01014	-2.31975
P	2.22280	-0.43868	0.25816
P	-2.22280	-0.43868	0.25816
N	-0.00000	1.39991	-0.50678
C	1.17676	2.06067	-0.45539
C	-1.20066	3.44683	-0.28765
H	-2.13810	3.98087	-0.23309
C	-0.00000	4.13856	-0.19155
H	-0.00000	5.21423	-0.05283
C	1.20066	3.44683	-0.28765
H	2.13810	3.98087	-0.23310
C	-1.17676	2.06067	-0.45539
C	-2.45534	1.23967	-0.68078
C	-2.51234	0.93984	-2.20513
H	-1.70882	0.27317	-2.52420
H	-2.42756	1.87998	-2.75977
H	-3.46866	0.48623	-2.47378

C	2.94509	-3.10834	-0.27669
H	3.07347	-3.39047	0.77071
H	3.54477	-3.79911	-0.87856
H	1.90063	-3.24578	-0.55882
C	2.93776	-0.10782	1.97521
H	3.96409	0.25236	1.85004
C	3.40139	-1.66449	-0.56418
H	3.19772	-1.50085	-1.62498
C	4.90624	-1.48835	-0.31546
H	5.28198	-0.52094	-0.65405
H	5.45819	-2.25801	-0.86519
H	5.16836	-1.59851	0.74028
C	-3.72251	2.02255	-0.29377
H	-4.60747	1.39935	-0.41774
H	-3.85692	2.88895	-0.94971
H	-3.70813	2.38087	0.73698
C	2.51234	0.93985	-2.20513
H	3.46866	0.48623	-2.47378
H	2.42756	1.87998	-2.75977
H	1.70882	0.27317	-2.52420
C	2.97253	-1.39364	2.81782
H	1.98052	-1.85075	2.88116
H	3.29555	-1.15694	3.83697
H	3.66178	-2.13867	2.42021
C	2.45534	1.23967	-0.68078
C	-3.40139	-1.66449	-0.56418
H	-3.19772	-1.50085	-1.62498
C	2.12262	0.96303	2.71511
H	2.08397	1.91708	2.18731
H	2.56127	1.14713	3.70144
H	1.09413	0.62644	2.86491
C	-2.94509	-3.10834	-0.27670

H	-1.90063	-3.24578	-0.55882
H	-3.54477	-3.79911	-0.87857
H	-3.07347	-3.39047	0.77070
C	-2.93775	-0.10782	1.97521
H	-3.96409	0.25236	1.85004
C	3.72251	2.02256	-0.29377
H	3.70813	2.38087	0.73698
H	3.85692	2.88895	-0.94971
H	4.60747	1.39935	-0.41774
C	-2.12262	0.96304	2.71511
H	-1.09413	0.62644	2.86491
H	-2.56127	1.14713	3.70143
H	-2.08397	1.91708	2.18731
C	-2.97253	-1.39364	2.81782
H	-3.66178	-2.13867	2.42021
H	-3.29555	-1.15694	3.83698
H	-1.98051	-1.85075	2.88116
C	-4.90624	-1.48835	-0.31546
H	-5.16836	-1.59852	0.74028
H	-5.45819	-2.25801	-0.86519
H	-5.28198	-0.52095	-0.65405

83

Complex 7 tBuPNPMe4NiBr ub3lyp/6-311++g(d,p) PCHN Lanl2dz NiBr

Br	-0.00000	-3.03770	0.09897
Ni	-0.00000	-0.45085	-0.18212
P	-2.33796	-0.09571	-0.01754
P	2.33796	-0.09571	-0.01755
N	-0.00000	1.76654	-0.53229
C	-1.17085	2.42191	-0.38397
C	-2.93102	0.08192	1.82007
C	-1.19896	3.75811	0.02049
H	-2.13641	4.27779	0.15328

C	2.93102	0.08191	1.82007
C	1.17085	2.42191	-0.38397
C	-2.43995	1.67282	-0.81848
C	2.44392	-1.16906	2.58800
H	1.37936	-1.34965	2.43391
H	2.61939	-1.00899	3.65811
H	2.96839	-2.07744	2.30086
C	2.20048	1.28757	2.44681
H	2.53618	2.24729	2.05542
H	2.39438	1.28971	3.52495
H	1.11991	1.21961	2.30849
C	-2.20048	1.28757	2.44681
H	-1.11990	1.21961	2.30848
H	-2.39437	1.28972	3.52495
H	-2.53617	2.24730	2.05542
C	-3.54867	-1.27579	-0.97266
C	-2.44391	-1.16906	2.58800
H	-2.96839	-2.07743	2.30086
H	-2.61938	-1.00898	3.65811
H	-1.37935	-1.34965	2.43391
C	-3.78327	-2.54419	-0.12265
H	-2.84332	-3.00020	0.19128
H	-4.31214	-3.27266	-0.74729
H	-4.40919	-2.35772	0.75021
C	-2.29502	1.54719	-2.36113
H	-1.43902	0.93313	-2.63845
H	-2.14365	2.54678	-2.78212
H	-3.19269	1.13209	-2.81671
C	-2.82397	-1.74675	-2.25536
H	-2.65140	-0.94544	-2.97189
H	-3.45305	-2.49554	-2.75015
H	-1.86954	-2.21709	-2.01374

C	-4.44554	0.25084	2.04558
H	-4.85448	1.13278	1.55185
H	-4.63027	0.36392	3.12059
H	-5.01443	-0.61798	1.71496
C	2.43995	1.67282	-0.81848
C	1.19896	3.75811	0.02050
H	2.13641	4.27779	0.15328
C	-3.71966	2.48255	-0.54132
H	-4.60236	1.91699	-0.83238
H	-3.72213	3.40397	-1.13403
H	-3.83377	2.76166	0.50559
C	2.29503	1.54720	-2.36112
H	3.19270	1.13210	-2.81670
H	2.14366	2.54678	-2.78212
H	1.43903	0.93313	-2.63845
C	3.71966	2.48255	-0.54131
H	3.83376	2.76165	0.50561
H	3.72213	3.40397	-1.13402
H	4.60236	1.91699	-0.83236
C	2.82397	-1.74674	-2.25536
H	1.86954	-2.21709	-2.01374
H	3.45305	-2.49553	-2.75016
H	2.65139	-0.94544	-2.97189
C	3.54867	-1.27579	-0.97266
C	3.78326	-2.54419	-0.12265
H	4.40918	-2.35771	0.75022
H	4.31214	-3.27266	-0.74728
H	2.84332	-3.00020	0.19127
C	-0.00000	4.42173	0.24403
H	-0.00000	5.45642	0.56910
C	4.44554	0.25083	2.04557
H	5.01443	-0.61798	1.71494

H	4.63028	0.36391	3.12058
H	4.85448	1.13277	1.55184
C	4.92025	-0.68218	-1.34695
H	4.84819	0.13180	-2.06963
H	5.52129	-1.46951	-1.81646
H	5.47720	-0.32401	-0.47999
C	-4.92025	-0.68218	-1.34695
H	-5.47720	-0.32402	-0.47999
H	-5.52130	-1.46951	-1.81645
H	-4.84819	0.13180	-2.06963

83

Complex 8 tBuPNPMe4NiCl ub3lyp/6-311++g(d,p) PCHN Lanl2dz NiCl

Ni	0.00000	-0.62311	-0.17017
Cl	0.00000	-3.04346	0.12315
P	2.32133	-0.28203	-0.00389
P	-2.32133	-0.28203	-0.00389
N	-0.00000	1.57683	-0.55860
C	2.91322	-0.08585	1.83121
C	2.44114	1.47129	-0.83485
C	2.40223	-1.31801	2.61512
H	1.34184	-1.50053	2.43582
H	2.55006	-1.13433	3.68558
H	2.93282	-2.23307	2.36251
C	1.17176	2.23316	-0.42019
C	4.42939	0.06198	2.05850
H	4.98464	-0.81986	1.73888
H	4.61472	0.18518	3.13236
H	4.85274	0.93136	1.55434
C	-3.50193	-1.50417	-0.93711
C	3.69325	-2.76433	-0.06407
H	4.32406	-2.58272	0.80640
H	4.19878	-3.52112	-0.67430

H	2.73622	-3.18074	0.25472
C	-4.88916	-0.95302	-1.31682
H	-5.45370	-0.59830	-0.45327
H	-5.47075	-1.76086	-1.77605
H	-4.83889	-0.14537	-2.04869
C	3.72558	2.27504	-0.56352
H	3.83849	2.56769	0.47984
H	3.73930	3.18793	-1.16922
H	4.60410	1.69635	-0.84312
C	3.50193	-1.50417	-0.93711
C	1.19967	3.57640	-0.04034
H	2.13736	4.09807	0.08430
C	2.76440	-1.97833	-2.21149
H	1.79724	-2.41577	-1.95823
H	3.37181	-2.75442	-2.69120
H	2.61520	-1.18663	-2.94378
C	2.19891	1.14025	2.43677
H	2.54544	2.08847	2.02731
H	2.39444	1.15997	3.51445
H	1.11745	1.08283	2.30078
C	-1.19967	3.57639	-0.04034
H	-2.13736	4.09807	0.08431
C	-2.44115	1.47129	-0.83485
C	-2.30603	1.32085	-2.37588
H	-1.44406	0.71341	-2.64907
H	-2.17101	2.31499	-2.81504
H	-3.20166	0.88612	-2.81721
C	-1.17176	2.23316	-0.42019
C	-0.00000	4.24404	0.16976
H	-0.00000	5.28463	0.47543
C	-2.76440	-1.97833	-2.21149
H	-2.61519	-1.18663	-2.94378

H	-3.37181	-2.75442	-2.69121
H	-1.79723	-2.41577	-1.95823
C	-2.19891	1.14025	2.43677
H	-1.11744	1.08283	2.30078
H	-2.39444	1.15997	3.51444
H	-2.54543	2.08847	2.02731
C	-2.40223	-1.31801	2.61512
H	-2.93283	-2.23307	2.36251
H	-2.55006	-1.13433	3.68559
H	-1.34184	-1.50053	2.43582
C	-4.42939	0.06198	2.05850
H	-4.85274	0.93137	1.55433
H	-4.61472	0.18519	3.13236
H	-4.98464	-0.81986	1.73888
C	-3.72558	2.27504	-0.56351
H	-4.60410	1.69634	-0.84312
H	-3.73931	3.18793	-1.16921
H	-3.83849	2.56768	0.47984
C	-2.91322	-0.08585	1.83121
C	4.88916	-0.95302	-1.31681
H	4.83889	-0.14537	-2.04868
H	5.47075	-1.76086	-1.77605
H	5.45370	-0.59830	-0.45327
C	2.30602	1.32085	-2.37589
H	3.20165	0.88612	-2.81721
H	2.17100	2.31499	-2.81504
H	1.44405	0.71341	-2.64907
C	-3.69325	-2.76433	-0.06407
H	-2.73622	-3.18074	0.25472
H	-4.19877	-3.52112	-0.67431
H	-4.32406	-2.58273	0.80640

4.8 Space filling representations of DFT-optimized structures of complexes 2.40-2.43

Three orientations are shown for each structure. Nickel atom is light green, phosphine atoms are light orange, nitrogen atom is light blue and chloride atom is dark green. Atoms colored in red are carbon atoms of the methyl groups on the arm. The isopropyl C-H hydrogen is highlighted in magenta

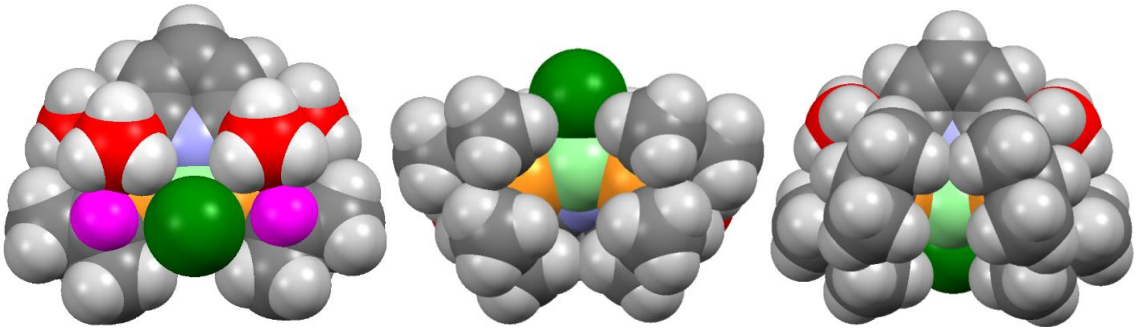

Figure 4.116 Space filling representation of DFT-optimized structure of **2.41**

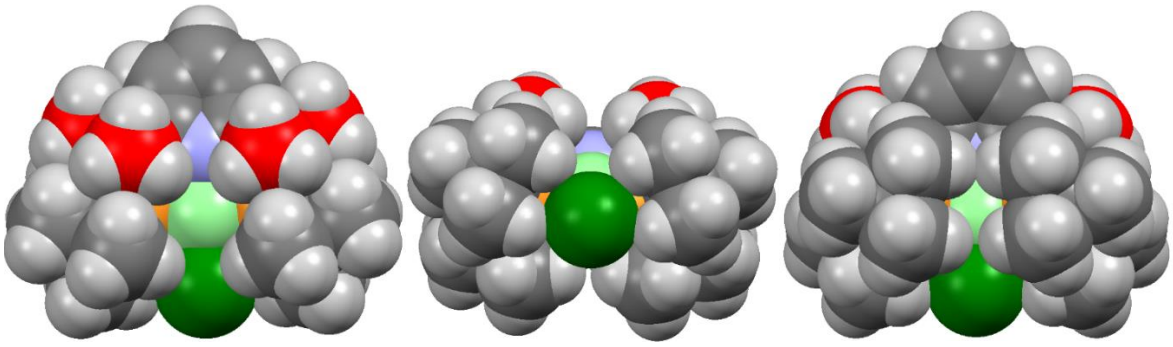

Figure 4.117 Space filling representation of DFT-optimized structure of 2.43.

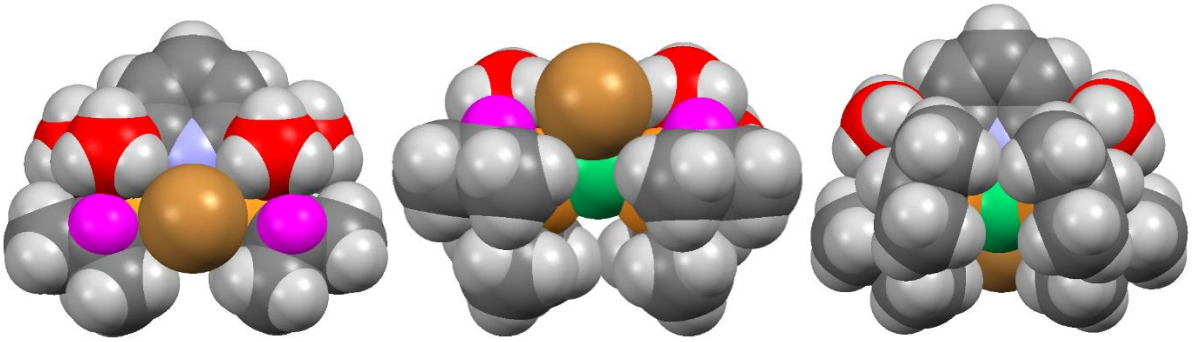

Figure 4.118 Space filling representation of the X-ray structure of **2.40**.

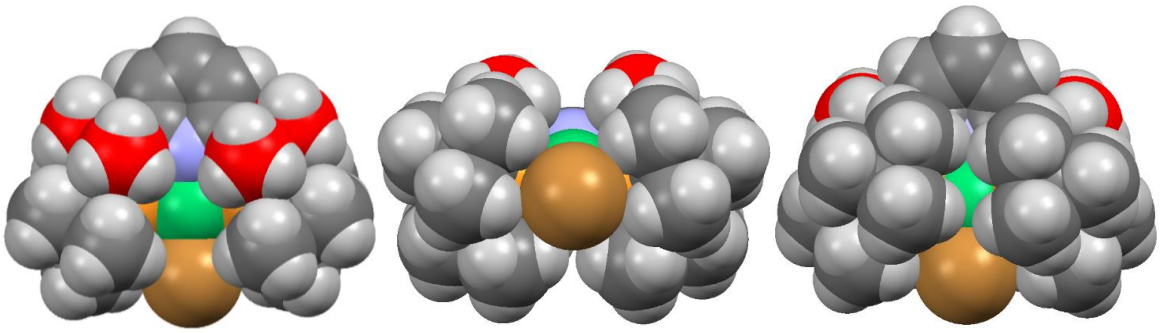

Figure 4.119 Space filling representation of the X-ray structure of **2.42.**

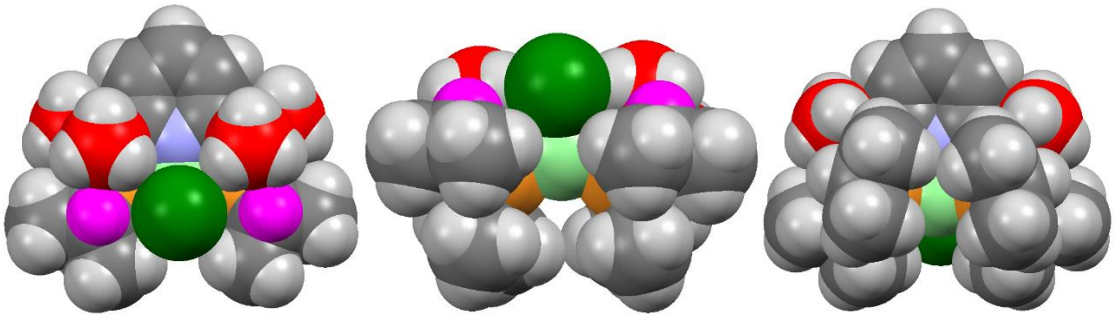

Figure 4.120 Space filling representation of the X-ray structure of **2.41.**

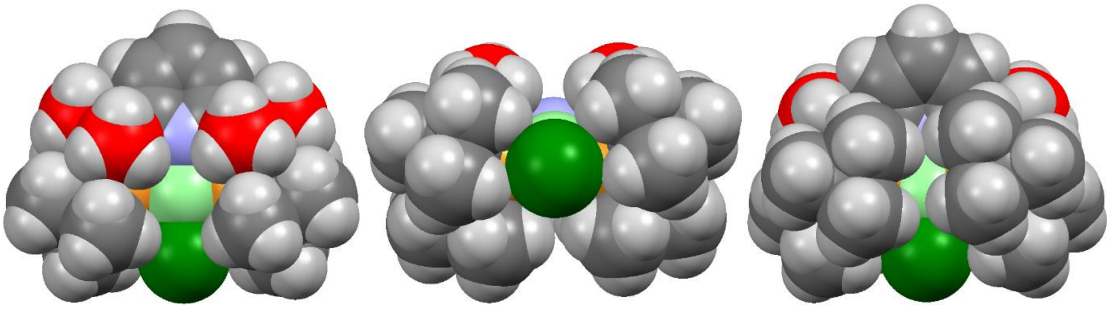

Figure 4.121 Space filling representation of the X-ray structure of **2.43**.

4.9 Exact Ligand Solid Angles

1.1.1 Calculated using zero energy point radii[18]

Nickel atom is represented in light green, phosphorous atoms in light orange, chloride atom in dark green. Atoms highlighted in red are the methyl groups on the ligand arms. This color scheme is used for all the chloride-containing complexes thereafter.

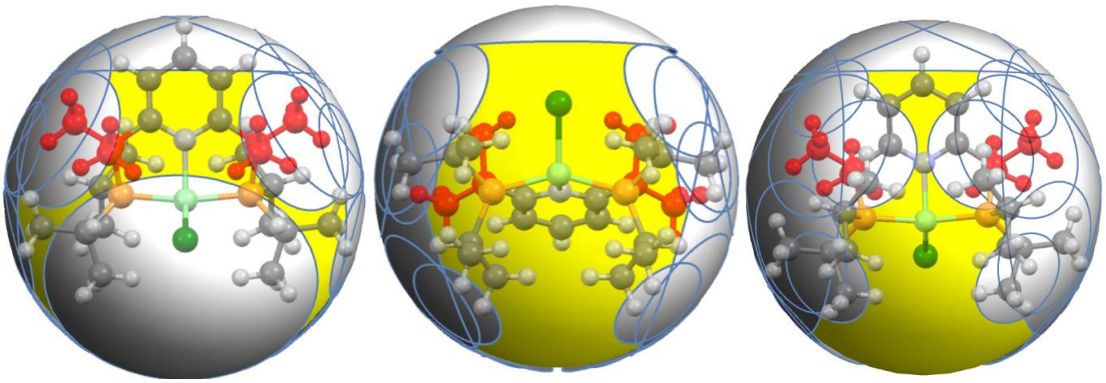

Figure 4.122 The ligand solid angle (grey area) of DFT-optimized structure of **2.41**.

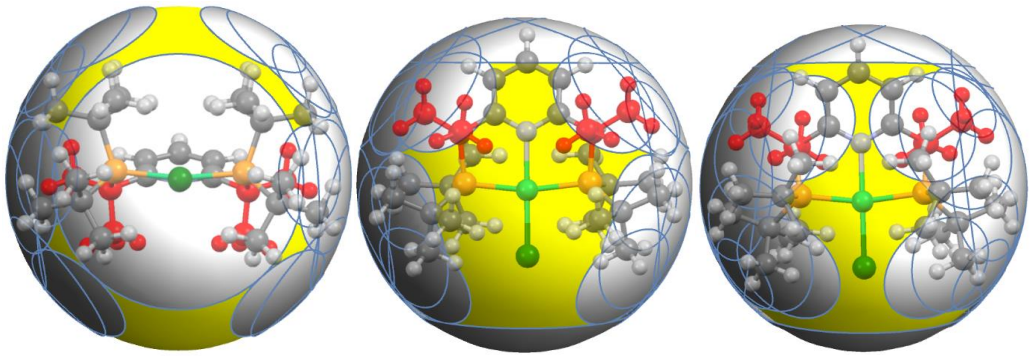

Figure 4.123 The ligand solid angle (grey area) of DFT-optimized structure of **2.43**.

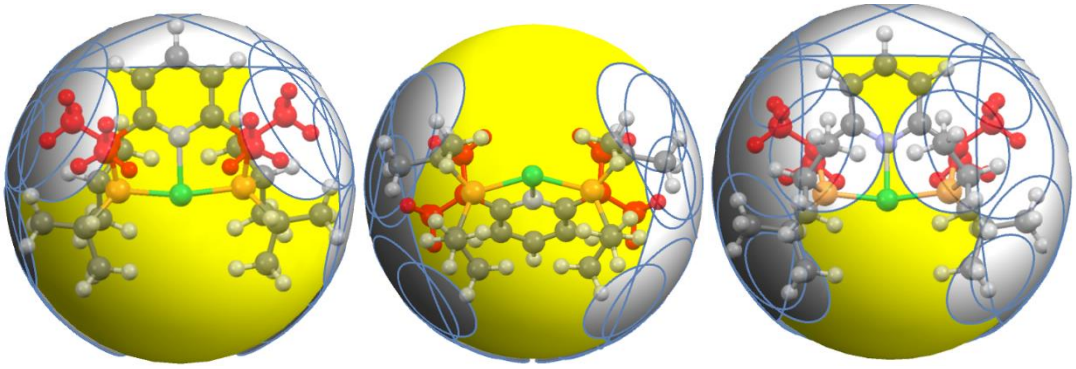

Figure 4.124 The ligand solid angle (grey area) of DFT-optimized structure of **2.40** without the bromide atom.

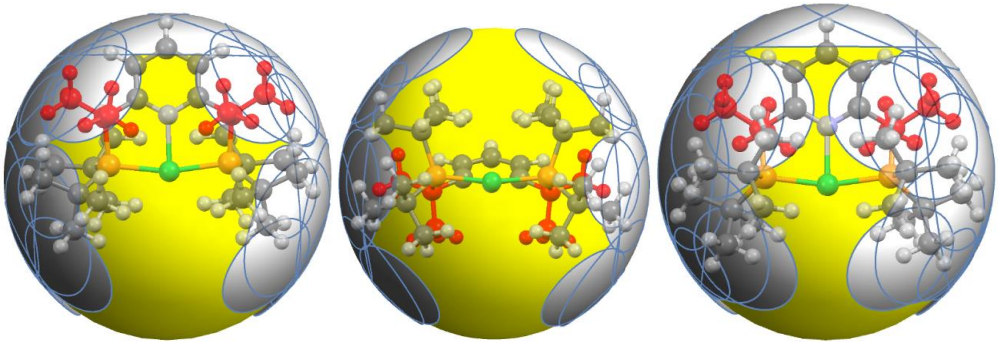

Figure 4.125 The ligand solid angle (grey area) of DFT-optimized structure of **2.42** without the bromide atom.

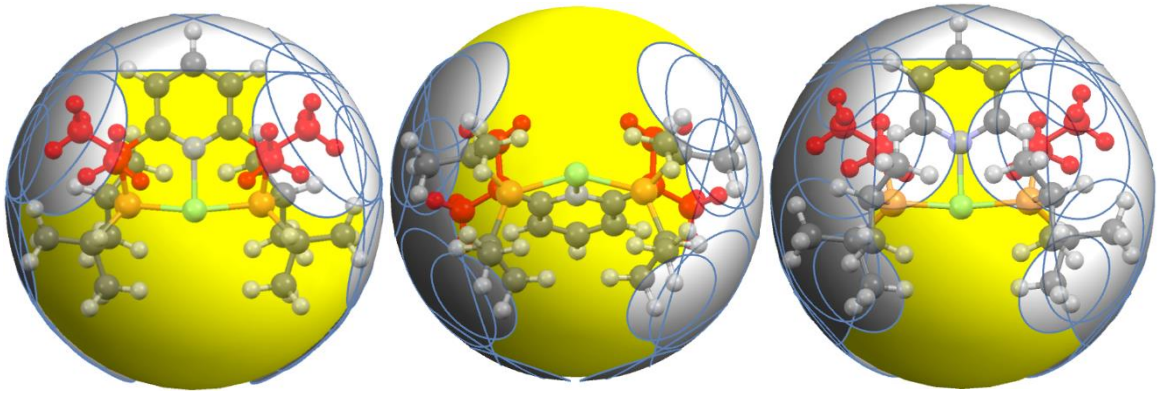

Figure 4.126 The ligand solid angle (grey area) of DFT-optimized structure of **2.41** without the chloride atom.

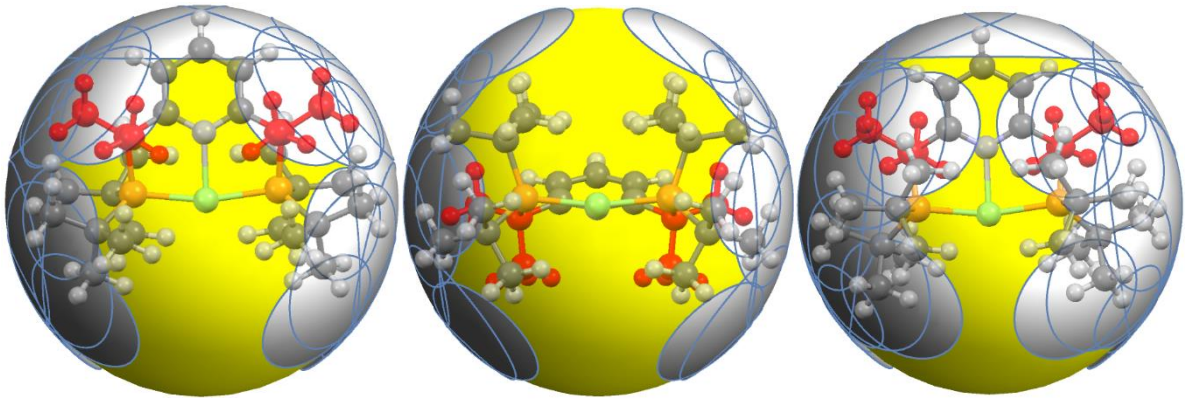

Figure 4.127 The ligand solid angle (grey area) of DFT-optimized structure of **2.43** without the chloride atom.

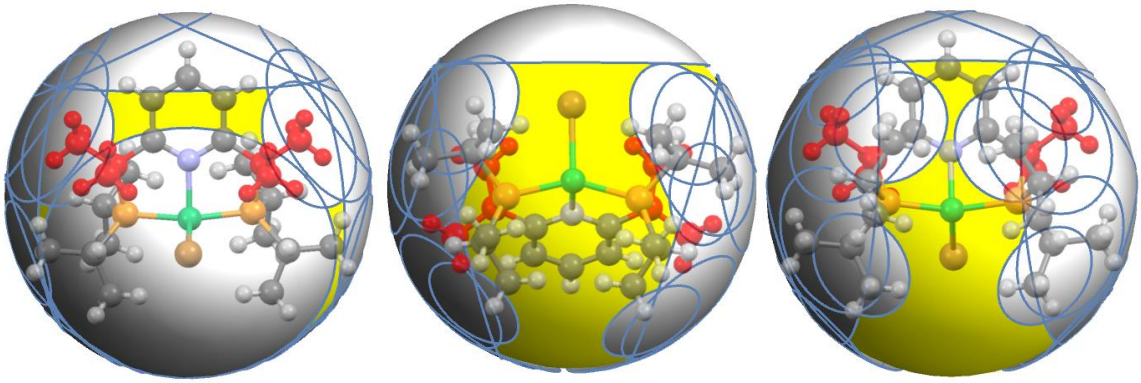

Figure 4.128 The ligand solid angle (grey area) of X-ray structure of **2.40**.

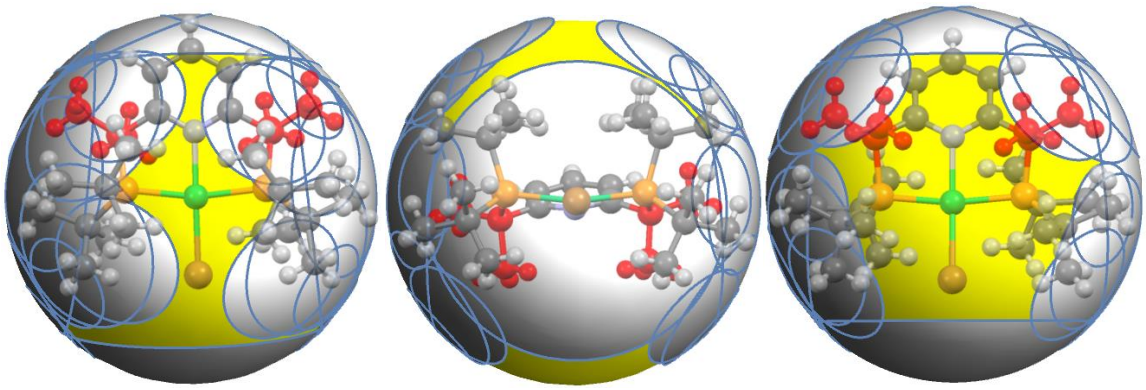

Figure 4.129 The ligand solid angle (grey area) of X-ray structure of **2.42**.

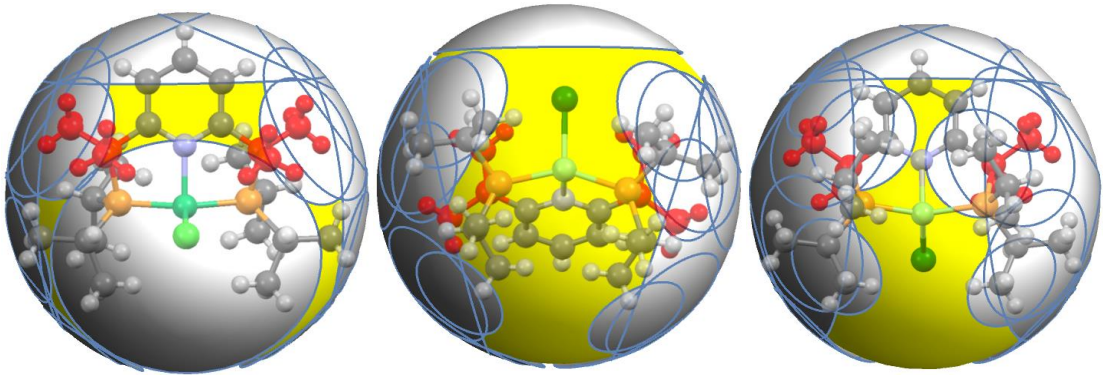

Figure 4.130 The ligand solid angle (grey area) of X-ray structure of **2.41**.

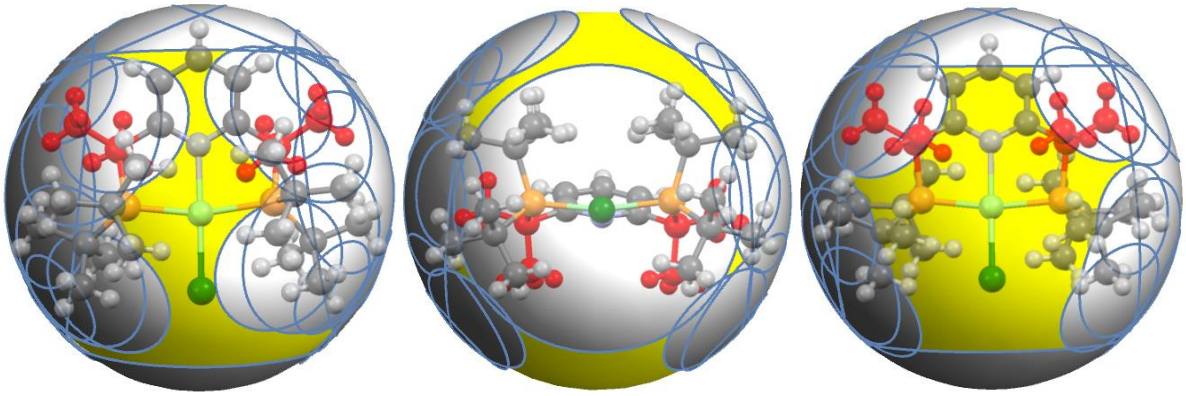

Figure 4.131 The ligand solid angle (grey area) of X-ray structure of **2.43**.

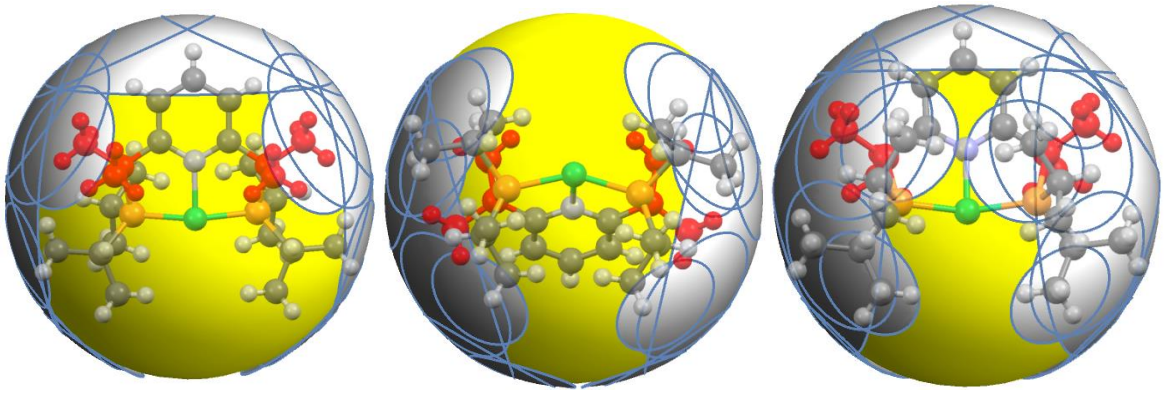

Figure 4.132 The ligand solid angle (grey area) of X-ray structure of **2.40** without the bromide atom.

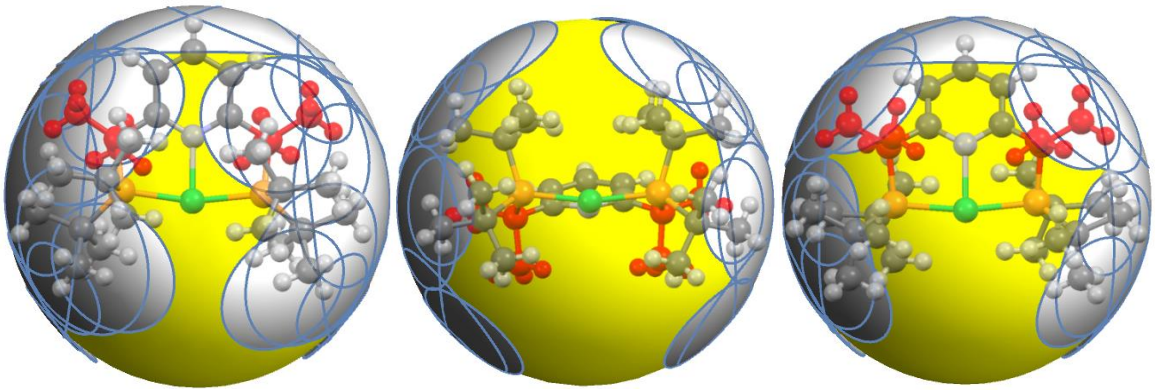

Figure 4.133 The ligand solid angle (grey area) of X-ray structure of **2.42** without the bromide atom.

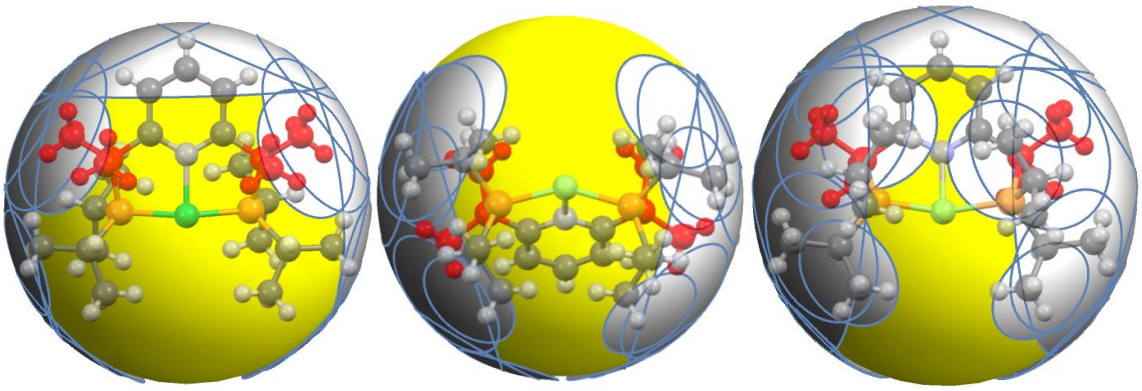

Figure 4.134 The ligand solid angle (grey area) of X-ray structure of **2.41** without the chloride atom.

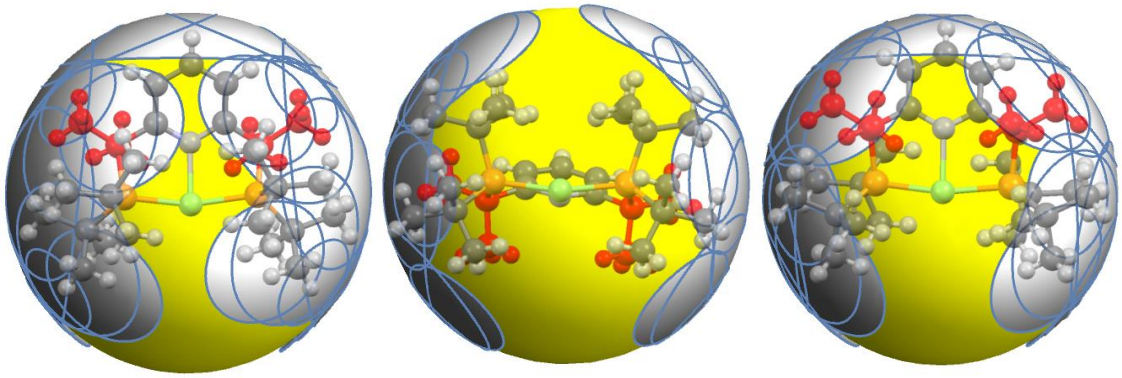

Figure 4.135 The ligand solid angle (grey area) of X-ray structure of **2.43** without the chloride atom.

1.1.2 Calculated using Bondi radii[17]

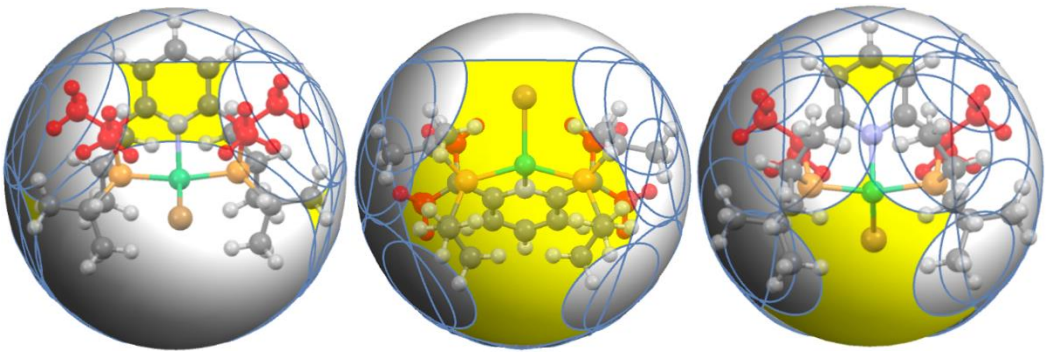

Figure 4.136 The ligand solid angle (grey area) of the DFT-optimized structure of **2.40**.

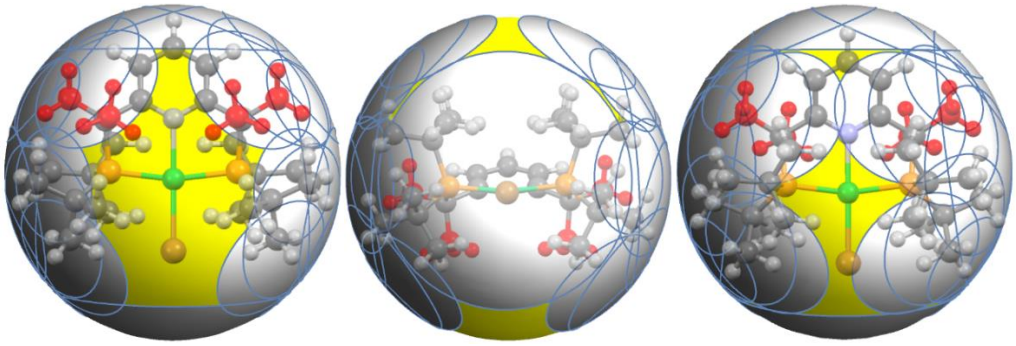

Figure 4.137 The ligand solid angle (grey area) of the DFT-optimized structure of **2.42**.

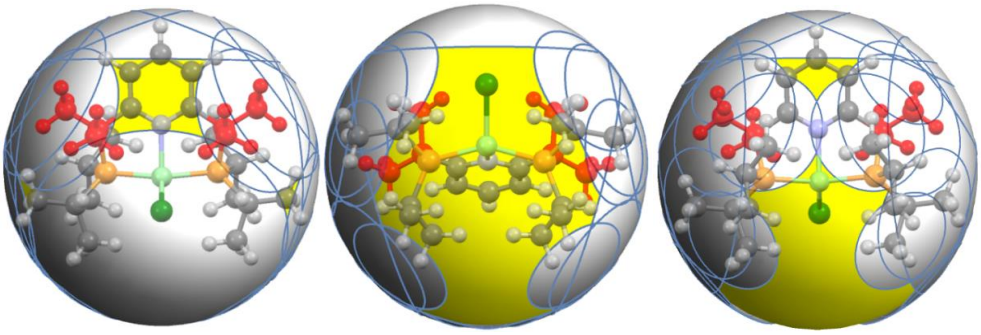

Figure 4.138 The ligand solid angle (grey area) of the DFT-optimized structure of **2.41**.

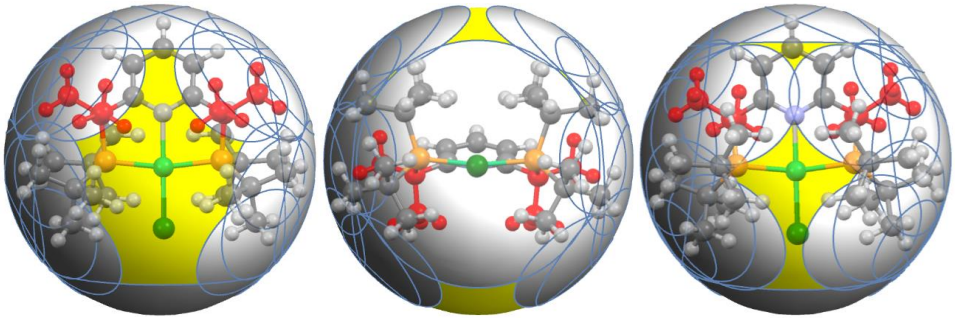

Figure 4.139 The ligand solid angle (grey area) of the DFT-optimized structure of **2.43**.

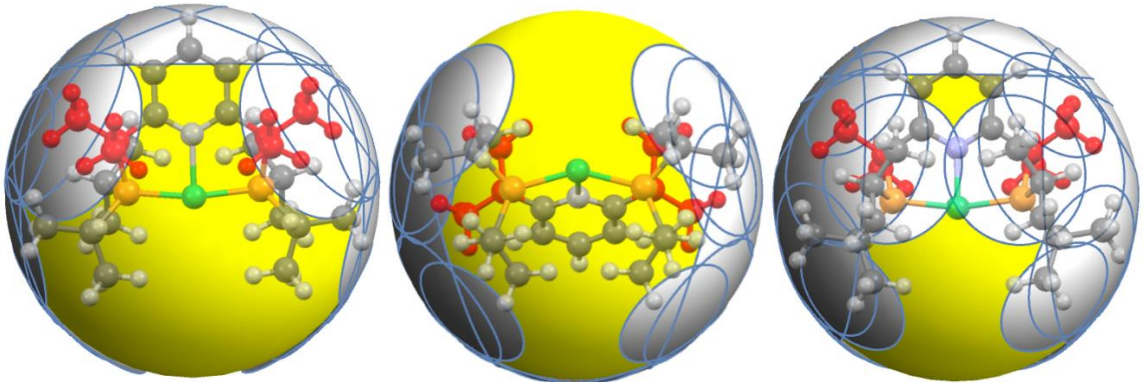

Figure 4.140 The ligand solid angle (grey area) of the DFT-optimized structure of **2.40** without the bromide atom.

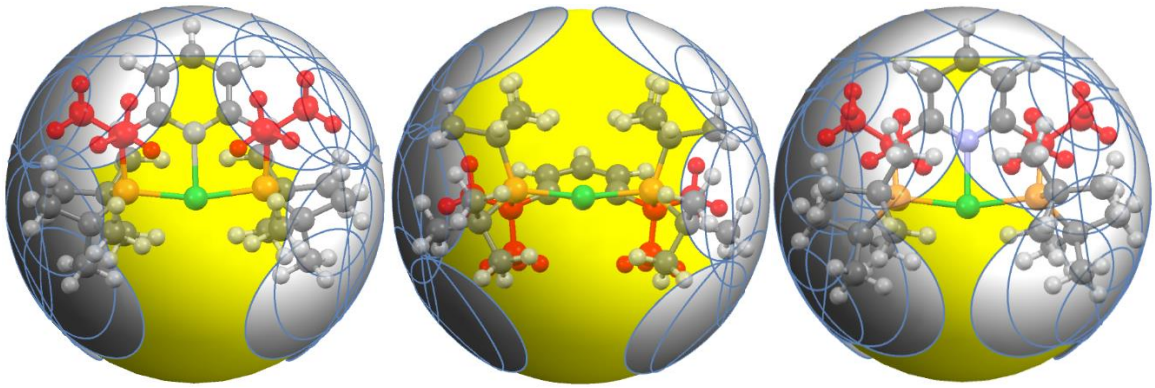

Figure 4.141 The ligand solid angle (grey area) of the DFT-optimized structure of **2.42** without the bromide atom.

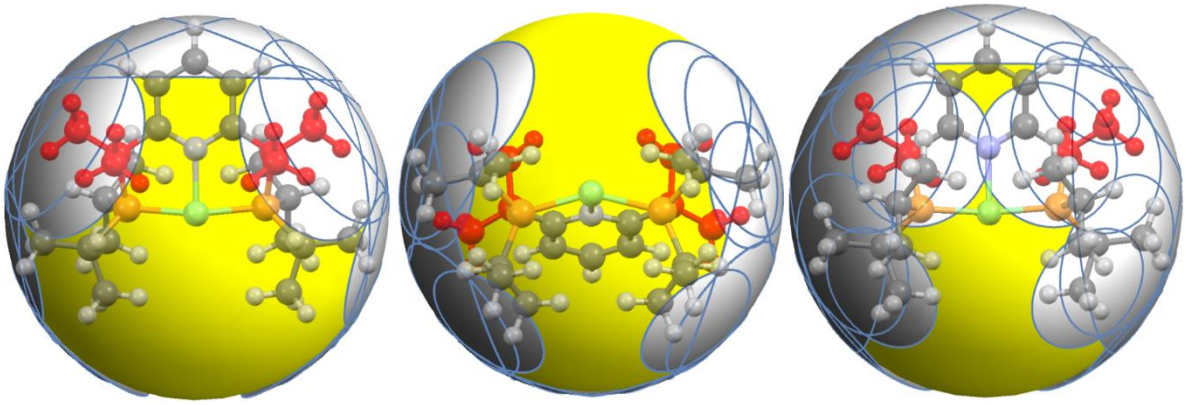

Figure 4.142 The ligand solid angle (grey area) of the DFT-optimized structure of **2.41** without the chloride atom.

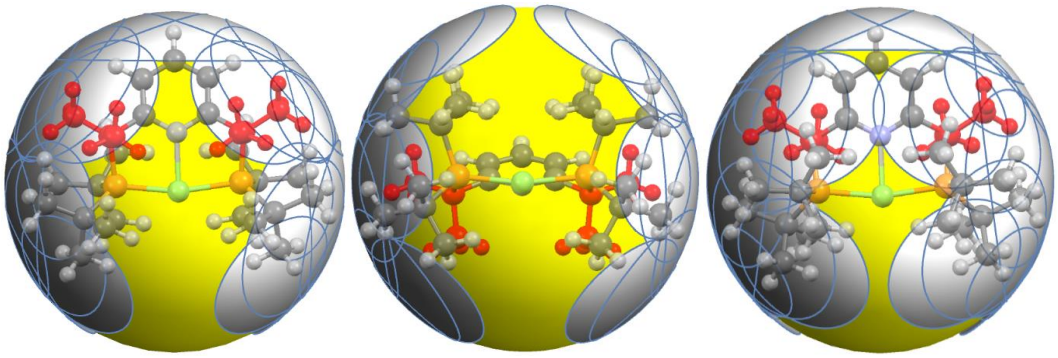

Figure 4.143 The ligand solid angle (grey area) of the DFT-optimized structure of **2.43** without the chloride atom.

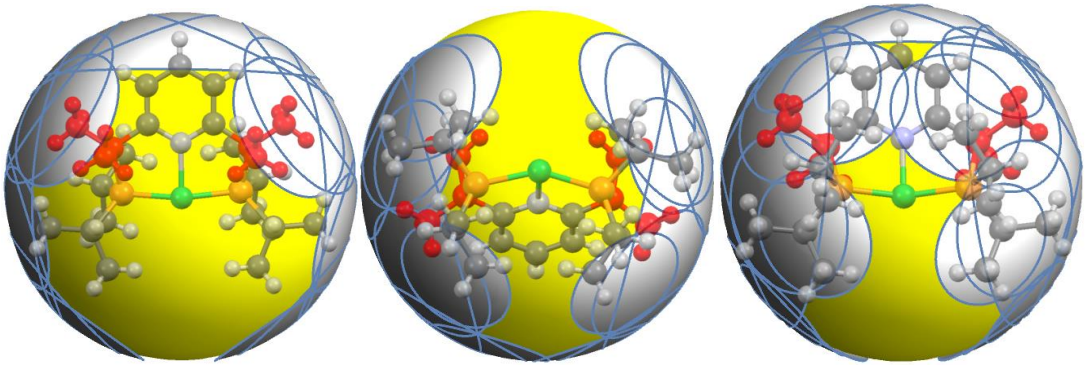

Figure 4.144 The ligand solid angle (grey area) of the X-ray structure of **2.40**.

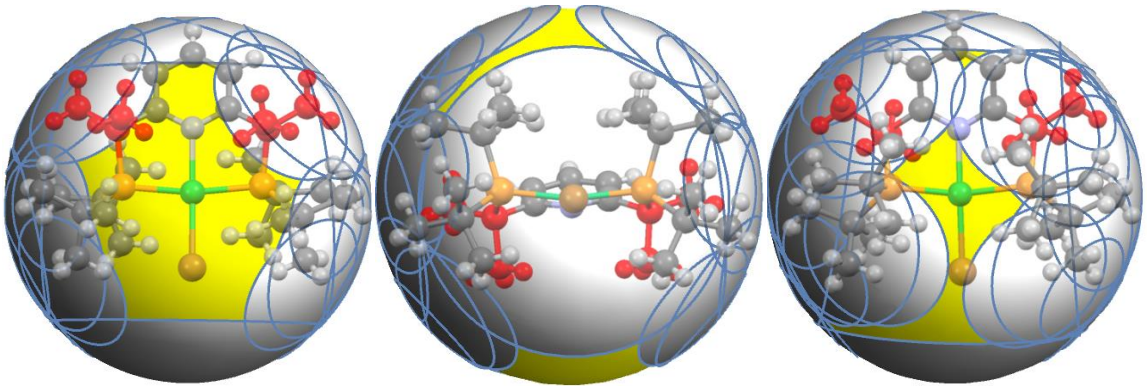

Figure 4.145 The ligand solid angle (grey area) of the X-ray structure of **2.42**.

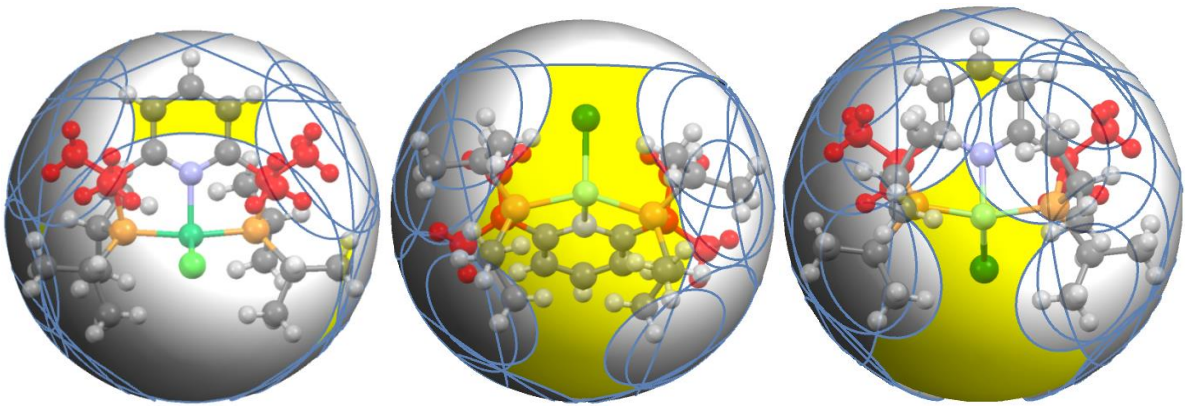

Figure 4.146 The ligand solid angle (grey area) of the X-ray structure of **2.41**.

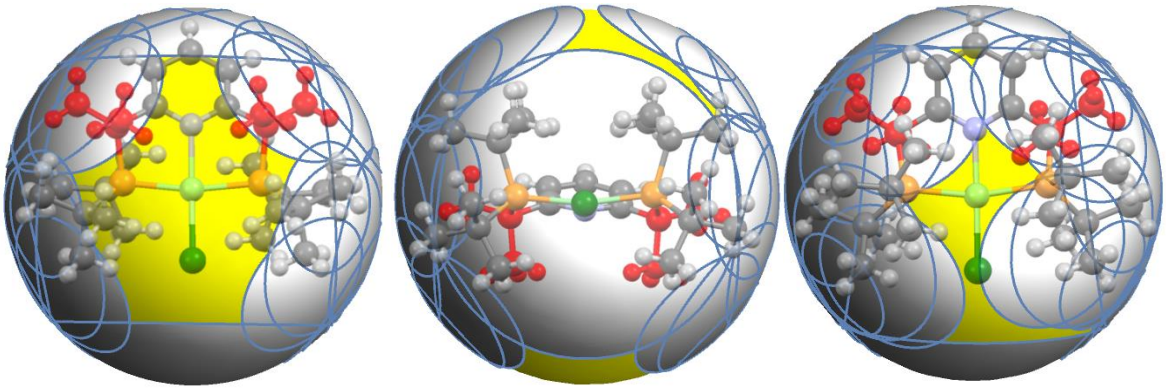

Figure 4.147 The ligand solid angle (grey area) of the X-ray structure of **2.43**.

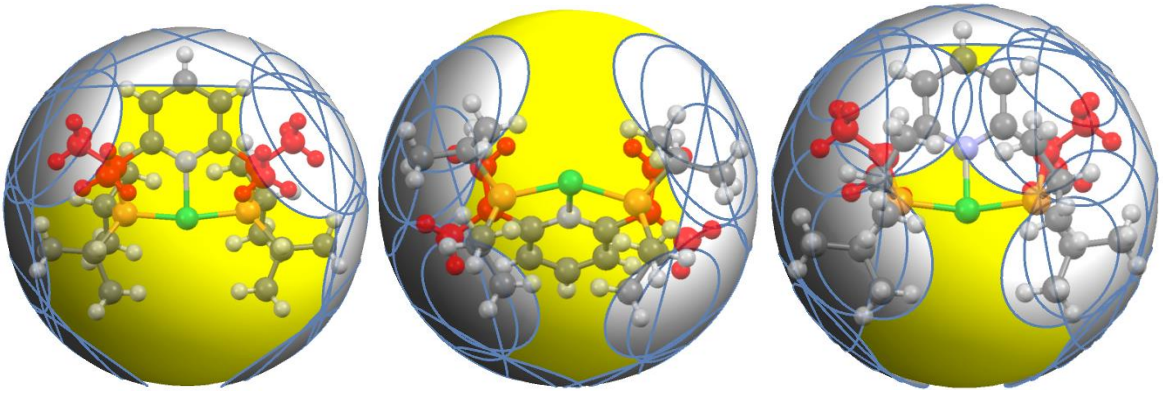

Figure 4.148 The ligand solid angle (grey area) of the X-ray structure of **2.40** without the bromide atom.

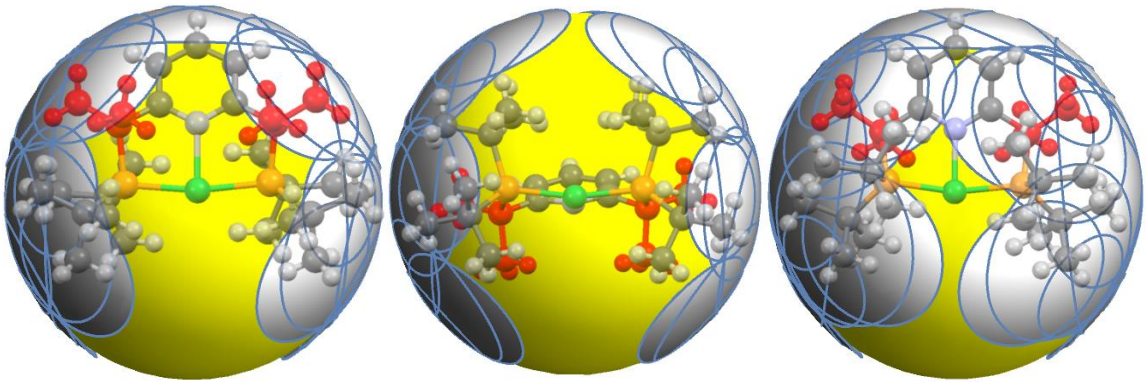

Figure 4.149 The ligand solid angle (grey area) of the X-ray structure of **2.42** without the bromide atom**.**

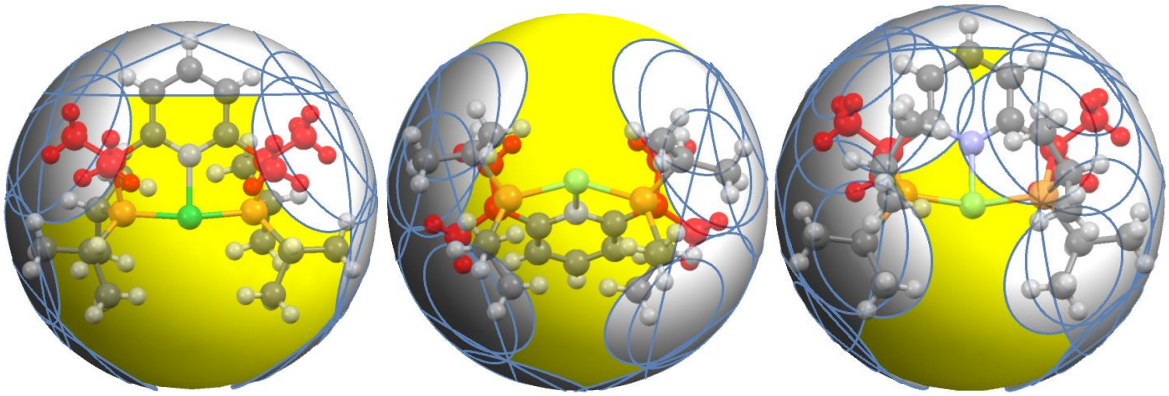

Figure 4.150 The ligand solid angle (grey area) of the X-ray structure of **2.41** without the chloride atom.

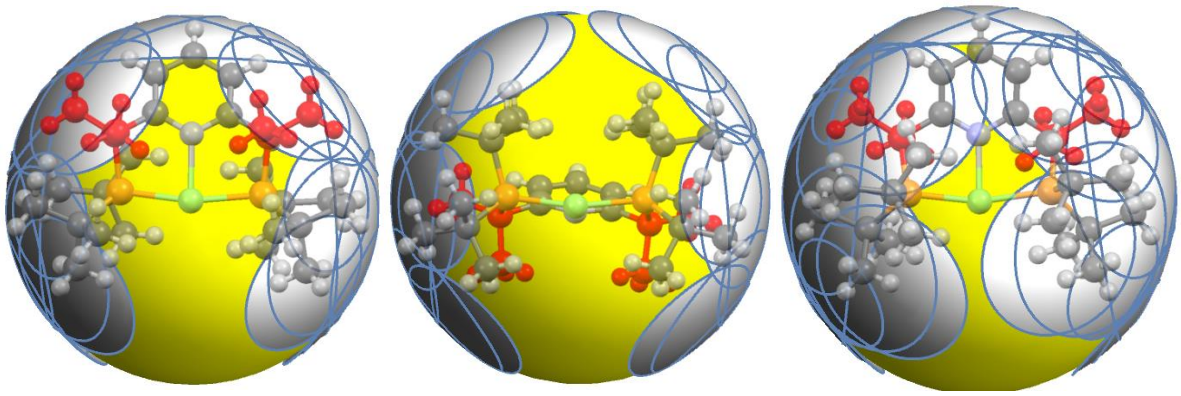

Figure 4.151 The ligand solid angle (grey area) of the X-ray structure of **2.43** without the chloride atom.

4.10 References for Appendix of Chapter 2

(1) McQuarrie, D. A.; Simon, J. D., *Physical chemistry : a molecular approach*. p xxiii, 1360 pages.

(2) De Buysser, K.; Herman, G. G.; Bruneel, E.; Hoste, S.; Van Driessche, I., Determination of the number of unpaired electrons in metal-complexes. A comparison between the Evans' method and susceptometer results. *Chem. Phys.* **2005,** *315*, 286-292.

(3) Carlin, R. L., *Magnetochemistry*. Springer-Verlag Berlin Heidelberg1986; p XI, 328.

(4) Stoll, S.; Schweiger, A., EasySpin, a comprehensive software package for spectral simulation and analysis in EPR. *J. Magn. Res.* **2006,** *178*, 42-55.

(5) MathWorks, I., *MATLAB : the language of technical computing : computation, visualization, programming : installation guide for UNIX version 5*. Natwick : Math Works Inc., 1996.1996.

(6) Neese, F., The ORCA program system. *Wiley Interdisciplinary Reviews: Computational Molecular Science* **2012,** *2*, 73-78.

(7) Sheldrick, G., SHELXT - Integrated space-group and crystal-structure determination. *Acta Crystallogr., Sect. A: Found. Adv.* **2015,** *71*, 3-8.

(8) Sheldrick, G., Crystal structure refinement with SHELXL. *Acta Crystallogr., Sect. C: Struct. Chem.* **2015,** *71*, 3-8.

(9) Dolomanov, O. V.; Bourhis, L. J.; Gildea, R. J.; Howard, J. A. K.; Puschmann, H., OLEX2: a complete structure solution, refinement and analysis program. *J. Appl. Crystallogr.* **2009,** *42*, 339-341.

(10) Farrugia, L., WinGX and ORTEP for Windows: an update. *J. Appl. Crystallogr.* **2012,** *45*, 849-854.

(11) Parsons, S.; Flack, H. D.; Wagner, T., Use of intensity quotients and differences in absolute structure refinement. *Acta Crystallogr., Sect. B* **2013,** *69*, 249-259.

(12) M. J. Frisch, G. W. T., H. B. Schlegel, G. E. Scuseria, M. A. Robb, J. R. Cheeseman, G. Scalmani, V. Barone, B. Mennucci, G. A. Petersson, H. Nakatsuji, M. Caricato, X. Li, H. P. Hratchian, A. F. Izmaylov, J. Bloino, G. Zheng, J. L. Sonnenberg, M. Hada, M. Ehara, K. Toyota, R. Fukuda, J. Hasegawa, M. Ishida, T. Nakajima, Y. Honda, O. Kitao, H. Nakai, T. Vreven, J. A. Montgomery, Jr., J. E. Peralta, F. Ogliaro, M. Bearpark, J. J. Heyd, E. Brothers, K. N. Kudin, V. N. Staroverov, T. Keith, R. Kobayashi, J. Normand, K. Raghavachari, A. Rendell, J. C. Burant, S. S. Iyengar, J. Tomasi, M. Cossi, N. Rega, J. M. Millam, M. Klene, J. E. Knox, J. B. Cross, V. Bakken, C. Adamo, J. Jaramillo, R. Gomperts, R. E. Stratmann, O. Yazyev, A. J. Austin, R. Cammi, C. Pomelli, J. W. Ochterski, R. L. Martin, K. Morokuma, V. G. Zakrzewski, G. A. Voth, P. Salvador, J. J. Dannenberg, S. Dapprich, A. D. Daniels, O. Farkas, J. B. Foresman, J. V. Ortiz, J. Cioslowski, and D. J. Fox *Gaussian, Inc.*, E.01: Wallingford CT, 2013.

(13) Lee, C. T.; Yang, W. T.; Parr, R. G., Development of the Colle-Salvetti Correlation-Energy Formula into a Functional of the Electron-Density. *Phys. Rev. B* **1988,** *37*, 785-789.

(14) Becke, A. D., Density-functional thermochemistry. III. The role of exact exchange. *J. Chem. Phys* **1993,** *98*, 5648-5652.

(15) *Mathematica*, Wolfram Research, Inc.: Champaign, IL, 2010.

(16) Bilbrey, J. A.; Kazez, A. H.; Locklin, J.; Allen, W. D., Exact Ligand Solid Angles. *J. Chem. Theory Comput.* **2013,** *9*, 5734-5744.

(17) Bondi, A., van der Waals Volumes and Radii. *J. Phys. Chem.* **1964,** *68*, 441-451.

(18) Guzei, I. A.; Wendt, M., An improved method for the computation of ligand steric effects based on solid angles. *Dalton Trans.* **2006**, 3991-3999.
(19) Leonid, S. *Chemissian*, v. 4.53; 2005-2017.